INFORMATION TO USERS

This manuscript has been reproduced from the microfilm master. UMI films the text directly from the original or copy submitted. Thus, some thesis and dissertation copies are in typewriter face, while others may be from any type of computer printer.

The quality of this reproduction is dependent upon the quality of the copy submitted. Broken or indistinct print, colored or poor quality illustrations and photographs, print bleedthrough, substandard margins, and improper alignment can adversely affect reproduction.

In the unlikely event that the author did not send UMI a complete manuscript and there are missing pages, these will be noted. Also, if unauthorized copyright material had to be removed, a note will indicate the deletion.

Oversize materials (e.g., maps, drawings, charts) are reproduced by sectioning the original, beginning at the upper left-hand corner and continuing from left to right in equal sections with small overlaps. Each original is also photographed in one exposure and is included in reduced form at the back of the book.

Photographs included in the original manuscript have been reproduced xerographically in this copy. Higher quality 6" x 9" black and white photographic prints are available for any photographs or illustrations appearing in this copy for an additional charge. Contact UMI directly to order.

UMI

A Bell & Howell Information Company
300 North Zeeb Road, Ann Arbor MI 48106-1346 USA
313/761-4700 800/521-0600

Université d'Ottawa · University of Ottawa

Study of Immiscible Oil Displacement in Unconsolidated Porous Media with and without Chemical Reaction

by

Emanoil M. Bradateanu

A thesis submitted to

the School of Graduated Studies and Research

in partial fulfillment of the requirements for the

degree of Master of Applied Science

in the

Department of Chemical Engineering

University of Ottawa

 January, 1998

To the memory of my parents

ABSTRACT

After the waterflood (secondary oil recovery) various techniques known under the generic name of Improved Oil Recovery (IOR) processes are employed to achieve the ultimate goal - increase of recovery of oil. Among IOR processes, alkaline flood is viewed as one of the most promising methods due to its ability to dramatically decrease the interfacial tension between the aqueous phase (alkaline solution) and oil which, in turn, causes a better mobilization of oil from the reservoir to be achieved.

This study was made in continuation of other studies performed in Chemical Engineering Department of University of Ottawa. Its aim was to obtain additional information regarding the process of immiscible displacement of oil by water in a cell containing an unconsolidated porous medium, namely sand. Gathering more information in this vast field of research is an important factor that leads to a better understanding of the complex phenomena involved in the process of oil recovery.

Throughout this study, distilled water and sodium hydroxide solutions with a concentration of 25 mM were used as the displacing fluids and light paraffin oil both pure and doped with 10 mM linoleic acid was used as the displaced fluid.

The cell used to perform the displacement was built from glass plates and contained 53 mesh silica sand inside, allowing pictures of the moving interface between the oil and aqueous phase to be taken during the displacements. Flow rates of displacing fluid ranging between

100 cm^3/h and 400 cm^3/h, were used covering the three domains, i.e. capillary, intermediate and viscous.

The results of the displacements showed a strong dependency of breakthrough recovery on flow rate (its decrease with the increase of the flow rate) and on interfacial tension between the two immiscible phases (decrease of recovery in order neutral oil > acidic oil > alkaline displacements).

ACKNOWLEDGMENTS

The author wishes firstly to thank the research supervisor, Dr. Hornof V., for his competent guidance, and advice as well as for always being available for useful discussions. Secondly, my thanks go to Dr. Youssef Touhami for his help with some analytical methods and fruitful talks. Thirdly, I wish to express my thanks to Messrs. L. Tremblay and F. Ziraldo of the departmental machine shop for their constant help with the equipment.

CONTENTS

List of Tables

List of Figures

NOMENCLATURE

A	cross-sectional area of flow, m^2
b	thickness of Hele-Shaw cell, m
E_D	displacement efficiency
d_p	sand grain average diameter, m
g	acceleration due to gravity, $m^2\ s^{-2}$
h	hight of the cell, m
K	proportionality constant
k	sand pack permeability(m^2)
$k_{rNW;rW}$	relative permeability of the NW/W fluid
M	viscosity ratio,
N_B	Bond number
N_{Ca}	Capillaxy number
F_r	Froude number
Re	Reynolds number
p	pressure, Pa
FR	volumetric flow rate of injected fluid, $m^3\ s^{-1}$
R_p	pore radius, m
$s_{NW,W}$	saturation of the NW/W fluid
v_i	Darcy velocity, $m\ s^{-1}$
V_s	volume of the solids (particles), m^3
V_b	bulk volume, m^3
f_l	fractional flow of water

GREEK LETTERS

γ	interfacial tension, $N\ m^{-1}$
ΔP	pressure difference, Pa
$\Delta\rho$	density difference, $kg\ m^{-3}$
Φ	porosity of the porous medium
θ	contact angle, rad
$\lambda_{NW;W}$	mobility of the NW/W fluid, $m^2\ Pa^{-1}\ s^{-1}$
μ	fluid viscosity, Pa s
$\mu_{i;d}$	viscosity of the invading/displaced fluid, Pa s
$\mu_{NW;W}$	viscosity of the NW/W fluid, Pa s
$\rho_{i;d}$	density of the invading/displaced fluid, $kg\ m^{-3}$

1. INTRODUCTION

From the earliest times in history, people have recognized that the material called petroleum comes from porous rocks. The early petroleum engineers realized that the oil must flow through very small passages between the sand grains, and that capillary forces must be involved wherever interfaces occur between two fluids. The earliest published work on the large resistance to flow caused by a series of bubbles in a capillary was that by Jamin in 1859. The first deliberate waterflood for oil recovery may have occurred in Sweden prior to 1740 when "running water was used to produce crude oil from galleries cut into the rocks bearing strata of 'tar and sand'" (Taber, 1980).

The goal of any oil exploitation method is to recover the most possible product from the reservoir. The first stage - referred to as **primary recovery** - takes place as a result of the release of internal energy of the reservoir. It has been estimated that after the completion of primary recovery, many reservoirs still contain as much as 80 - 90% of the original oil in place (Bansal and Shah, 1979). Any other recovery technique will require the use of external energy to compensate for the depleted natural energy. Waterflooding is the most common **secondary recovery** method in use. It employs the energy of water injected under pressure in the reservoir. It still leaves in the reservoir, after completion, 70 to 85% of the original oil in place. The third group of methods, referred to as **Enhanced Oil Recovery** (EOR), or, more recently as **Improved Oil Recovery** (IOR) makes use not only of pumping energy but also of various

chemicals. Thus, these methods can extract the oil from the reservoir in the range of 40-70%, and even more. Table 1.1 shows the production and consumption of petroleum in the U.S. (Lake, 1989).

Table 1.1 Production, Reserves, and Residual Oil in Place: U.S. Onshore, excluding Alaska (from Geffen, 1973)

Category	Billions of barrels*	Percent of original oil in place
Produced	100	25.2
Proved reserves**	22	5.5
EOR target	278	69.3
Total	400	100.0

* 1 bbl = 0.159 m^3

* recoverable with current technology

It is clear that only 10% out of the EOR target would constitute more than proved reserves.

Reserves are petroleum (crude and condensate) recoverable from known reservoirs under prevailing economics and technology. They are given by the following material balance equation:

$$\left[\frac{\text{Present}}{\text{reserves}}\right]=\left[\frac{\text{Past}}{\text{reserves}}\right]+\left[\frac{\text{Addition}}{\text{to reserves}}\right]-\left[\frac{\text{Production}}{\text{from reserves}}\right] \tag{1.1}$$

As one can see according to this equation, reserves can change with time because the last two terms can change with time.

Adding to reserves can be achieved in one of the following ways:

1. Discovering new fields
2. Discovering new reservoirs
3. Extending reservoirs in known fields
4. Redefining reserves because of changes in economics of extraction technology

Several methods are used for discovering new fields and reservoirs (points 1 and 2 in the above classification). Among them, a new method based on the use of fractals appears to be very promising (Barton and La Pointe, 1995). In spite of the fact that more advanced methods for the discovery of new fields are developed, the probability of success is declining.

That is why redefining reserves (4) is such an important concept and this task is accomplished mainly through the use of EOR methods.

In Canada field application of enhanced recovery dates from the North Pembina Cardium Unit hydrocarbon miscible pilot project in 1957-58. Figure 1.1 shows how the remaining supply of oil reserves in Canada has been declining in the last decades (Howes, 1988).

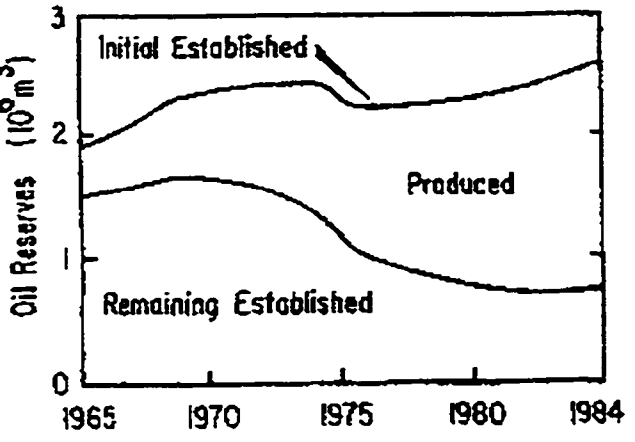

Figure 1.1 Established reserves in Canada (Howes, 1988).

Table 1.2 shows daily oil production rates for the EOR processes. One remarks the preponderance of steam flooding - about 80% of total EOR production. Of the remaining EOR production, about 80% is by solvent flooding.

Table 1.2 EOR oil rate as a percent of daily production (Lake, 1989)

	Production (bbl/day)*					
	1980	1982	1984	1986	1988	1990
Thermal methods						
Steam	243,477	288,396	358,115	468,692	455,484	444,137
In situ combustion	12,133	10,228	6,445	10,272	6,525	6,090
Hot water				705	2,896	3,985
Total thermal	255,610	298,624	364,560	479,669	464,905	454,212
Chemical						
Micellar polymer	930	902	2,832	1,403	1,509	637
Polymer	924	2,587	10,232	15,313	20,992	11,219
Alkaline	550	580	334	185		0
Total chemical	2,404	4,069	13,398	16,901	22,501	11,856
Solvent						
Hydrocarbon miscible			14,439	33,767	25,935	55,386
C02 miscible	21,532	21,953	31,300	28,440	64,192	95,591
C02 immiscible			702	1,349	420	95
Nitrogen			7,170	18,510	19,050	22,260
Flue gas (miscible and immiscible)			29,400	26,150	40,450	17,300
Total solvent	74,807**	71,915**	83,011	108,216	150,047	190,632
Grand total	332,821	374,608	460,969	604,786	637,453	656,700

* 1 bbl/day = 0. 159 m^3/day

** Other solvent methods not classified separately in these years.

A universal technical measure of the success of an EOR process is the amount of incremental oil recovered. Figure 1.2 defines incremental oil. In the course of primary oil recovery, the oil rate is declining from A to B. At B, an EOR project is initiated and, if successful, the rate should show a deviation from the projected decline at some time after B. Incremental oil is the difference between what was actually recovered, B to D, and what would have been recovered had the process not been initiated, B to C. This is the shaded region in Figure 1.2 (Lake, 1989).

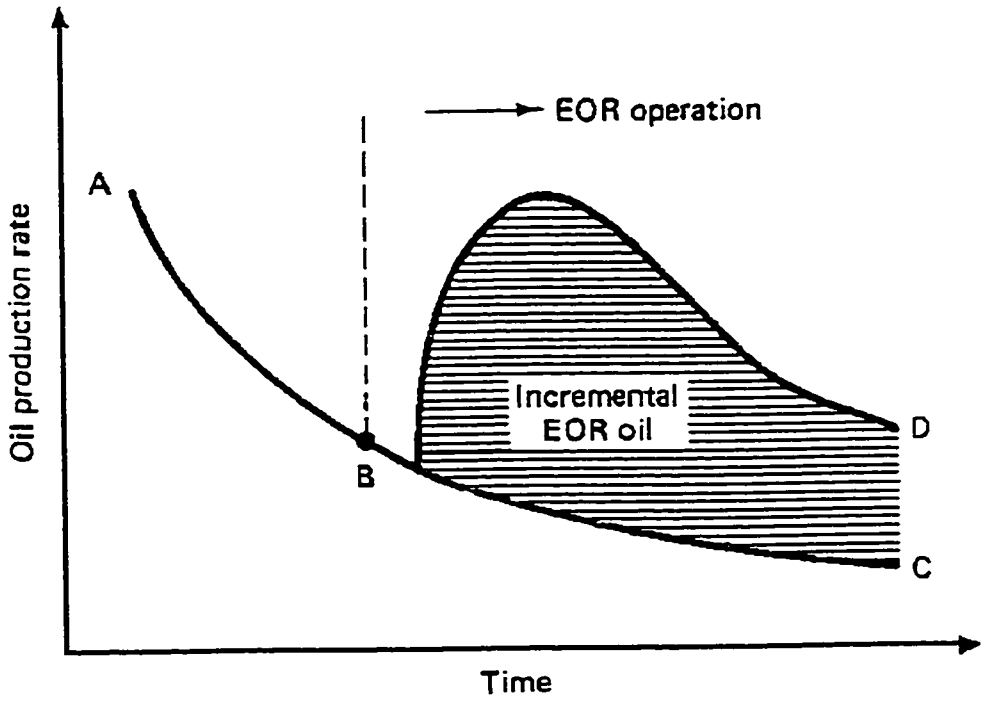

Figure 1.2 Incremental oil recovery from typical EOR response (Lake, 1989).

It is difficult however, to judge whether the EOR process is successful or only moderately successful. There are several reasons that make the judgment difficult:

1. Combined production from EOR and non-EOR wells. This makes it difficult to tell which is more efficient, the EOR well or the standard ones.
2. Oil from other sources. Usually the EOR project has experienced substantial well cleanup or other improvements. The oil produced as a result of such treatment is not easily differentiated from the EOR oil.
3. Inaccurate estimate of hypothetical decline. The curve from B to *C* in Fig. 1.2 must be accurately estimated. But since it did not occur, there is no way of assessing this accuracy. Techniques ranging from decline curve analysis to numerical simulation must still be tempered by good judgment.

The first incentive for the use of a particular EOR process is the value of the incremental oil recovered. Thus, the economics dictates ultimately whether or not that process will be applied to a given reservoir. The economics comprises, among other factors, the amount of oil that can be recovered, the cost of injection process, and the price that the producer can get for the oil. If the additional oil recovered by using a particular EOR method cannot pay back the costs associated with the project, this method is considered a failure and will not be installed.

2. LITERATURE SURVEY

Two major constituents play the key role in the process of fluid flow in porous media - the fluids and the porous solid itself, both with their intrinsic properties. When they are in contact, the interactions developed between them during the displacement of fluid phase are rather complex making the study of these systems a difficult task.

The phenomena occurring during the flow in porous media have been intensively studied. Many engineering and scientific applications and processes such as oil extraction from underground reservoirs, powder metallurgy, water purification, ground water hydrology, filtration, packed column distillation, ceramic engineering and catalysis, all deal with porous media. (Scheidegger 1974, Lake 1989, Dullien 1992). One of the most important of these processes is the multi-fluid flow in underground reservoirs.

2.1. Porous Materials; Structure and properties

A solid containing holes or voids, either connected or non-connected, dispersed within it in either a regular or random manner will be classed as a porous material provided that such holes occur relatively frequently within the solid.

Pores are either **interconnected** or **non-interconnected**. A fluid can flow through a porous material only if at least some of the pores are interconnected. The interconnected pore space is termed the **effective pore space**, while the whole of the pore space is termed the **total pore space**. Pores are of three morphological types: catenary, cul-de-sac, and closed (Figure 2.1. Selley, 1985).

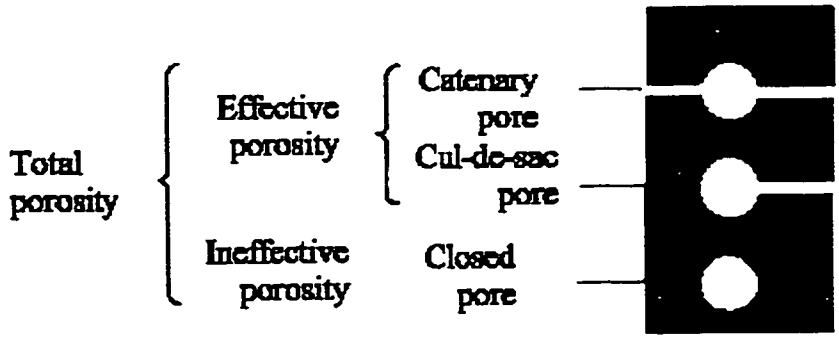

Figure 2.1. The three basic types of pores (Selley, 1985).

Catenary pores are those that communicate with others by more than one throat passage. Cul-de-sac, or dead-end, pores have only one throat passage connecting with another pore. Closed pores have no communication with other pores.

According to their size the voids within a porous material can be classified in three categories: **interstices** - the tiniest void spaces, **pores** - the spaces with an intermediate size, and **caverns** - those with the largest void spaces.

An additional classification of porous materials divides them into two groups, ordered or random. A regular packing of uniform spheres is ordered while the reservoir rocks have a random porous structure.

2.1.1 Packing of particles

Figure 2.1.1 shows two of the most common packing systems. along with spatial placement of pores.

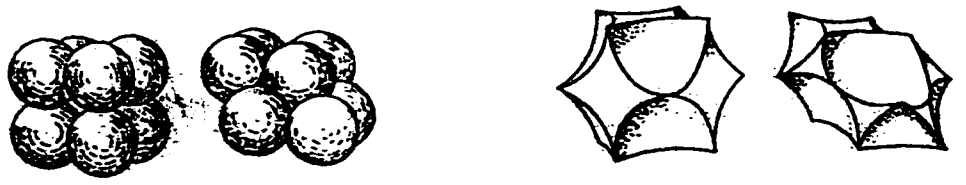

Cubic Rhombohedral Cubic Rhombohedral

a b

Figure 2.1.1. Packing of uniform spheres (a), and pore space in packing of uniform spheres (After Graton and Fraser, 1935) (Collins, 1961)

The easiest approach in studying the packing of particles is the analysis of random packing of mono-size spheres. The regular close packed hexagon array has the minimum porosity of 0.26 compared_with the simple cubic array with the maximum porosity of 0.48. Typically a random pack will have a porosity in the vicinity of 0.40, which is not that much greater than the average of close packed hexagon and simple cubic packing. It has been demonstrated that the density of packed mono-sized spheres cannot exceed

$$\frac{\pi}{\sqrt{18}} = 0.7404$$ (Cumberland and Crawford, 1987)

The **co-ordination** number is defined as the number of spheres in contact with any given sphere. Table 2.1.1.1 below lists the co-ordination number and its associated porosity.

Table 2.1.1.1 The co-ordination number for the most regular packing possible, with its associated porosity (Cumberland and Crawford, 1987)

Co-ordination number	Porosity	Density
3	0.7766	0.2234
4	0.6599	0.3401
5	0.5969	0.4031
6	0.4764	0.5236
7	0.4388	0.5612
8	0.3955	0.6045
9	0.3866	0.6134
10	0.3019	0.6981
11	0.2817	0.7183
12	0.2595	0.7405

The quality of packing has a great influence on the results of the experiments of displacement in unconsolidated porous media.

It is very difficult to obtain a regular packing by pouring a container full of spheres. "Bridging" invariably occurs and very high porosities result. Sand packs of uniform grain size usually consist of small regions of more or less regular packing separated by regions of irregular packing in which "bridging" has occurred. In the bridged regions, the porosity is invariably greater than that corresponding to the "loosest" regular packing.

The quality of a packed bed of spheres or irregular-shaped particles depends on a variety of factors, such as: the intensity of effect of deposition (mode of filling) - defined as the number of spheres falling per unit time per unit area, particle friction, deformability of particles, container shape, etc. The most important variables are summarized in the table 2.1.1.2. (Cumberland and Crawford, 1987).

Table 2.1.1.2 The variables which control the packing of particles

Variable	Experimental observation	Theory
1. *Particle*		
Shape	*	**
Absolute size	*	*
Size distribution	**	**
Mass	*	*
Elasticity	**	*
Resilience	**	*
Surface properties (friction)	*	*
2. *Container*		
Shape	*	*
Size	**	*
Elasticity	·	·
Surface properties (friction)	·	·
3. *Deposition*		
Intensity of deposition	**	*
Velocity of depositing particles	**	*
Method	*	·
4. *Treatment after deposition*		
Vibratory compaction	**	*
Pressure compaction	**	*

· no evidence
* qualitative evidence
** quantitative evidence

Theoretically, the porosity of a packing of uniform spheres should be independent of the size of the spheres, but for natural materials this proves not to be the case. Actual measurements show that, for sands of essentially uniform grain size, the porosity increases as the grain size decreases. As a general rule, the smaller the grains the greater will be the porosity in any naturally unconsolidated material of uniform grain size.

2.1.2 Porosity

The **porosity** (ϕ) of a porous material is defined as the fraction of the bulk volume of the material occupied by voids.

$$\phi = \frac{V_p}{V_b} = \frac{\text{Volume of pores}}{\text{Bulk Volume}} \qquad (2.1.2.1)$$

which is a dimensionless quantity. Since that portion of the bulk volume not occupied by pores is occupied by the solid grains or matrix of the material, it follows that

$$1 - \phi = \frac{V_s}{V_b} = \frac{\text{Volume of solids}}{\text{Bulk Volume}} \qquad (2.1.2.2)$$

Two classes of porosity can be defined, namely, **absolute or total**, and **effective porosity**. **Absolute porosity** is the fractional void space with respect to bulk volume regardless of pore connections. **Effective porosity** is that fraction of the bulk volume constituted by interconnecting pores. Of course this classification is the same as for pore space (page 8). Many naturally occurring rocks, such as lava and other igneous rocks, have a high total porosity but essentially no effective porosity. Effective porosity is an indication of

permeability but not a measure of it. Both types of porosity can be naturally altered through compaction and consolidation.

2.1.3 Permeability

Permeability is that property of a porous material that characterizes the ease with which a fluid may be made to flow through the material by an applied pressure gradient. Permeability is the ***fluid conductivity*** of the porous material.

The mathematical expression was developed by Darcy in 1856. If an incompressible fluid flows horizontally and linearly with a volumetric flow rate of q through a porous material of length L in the direction of flow, and cross-sectional area A, and ΔP is the applied pressure difference across the length of the sample.

The permeability k, of the material is defined as (Collins, 1961)

$$k = \frac{q\mu}{A(\Delta P/L)} \qquad (2.1.3.1)$$

The value of the permeability k, is determined by the structure of the porous material. The theory of Kozeny treats the porous medium as a bundle of capillary tubes of equal length and relates permeability to porosity (Lake,1989).

For an assemblage of uniform spheres, k is

$$k = \frac{1}{72\tau}\frac{\phi^3 D_p^2}{(1-\phi)^2} \qquad (2.1.3.2)$$

where τ, is the tortuosity, and D_p is the sphere or particle diameter.

The experimental best fit tortuosity for an assemblage of regularly packed spheres is a $\frac{25}{12}$ ratio

2.2 *Properties related to both, porous media and fluids*

2.2.1 Fluid Saturations

The void space of a porous material may be jointly filled with two or more immiscible fluids. The **saturation** of a porous medium with respect to a particular fluid is defined as the fraction of the void volume of the medium filled by the fluid in question. Thus, denoting the saturation with respect to fluid i by S_i, the definition of saturation is

$$S_i = \frac{\text{Volume of fluid i in the medium}}{\text{Total void volume of the medium}} \qquad (2.2.1.1)$$

For two fluids, w (wetting) and nw (non-wetting), jointly filling the void space, it follows that

$$S_w + S_{nw} = 1 \qquad (2.2.1.2)$$

with a similar relation holding for three immiscible fluids.

Saturation is dimensionless and a bulk property which ignores the relative distributions of the fluids within the porous structure of the material.

2.2.1.1 Measurement of Fluid Saturations

Several methods have been used for measuring fluid saturations.

Volumetric Balance Method. If a sample of porous material whose porosity is known is initially devoid of a fluid w and then a volume of the fluid, V_w, is introduced into the material, the saturation is calculated directly by conservation of volume. Thus

$$S_w = \frac{V_w}{\phi V_B} \tag{2.2.1.3}$$

A similar procedure applies if the sample of porous material is initially saturated with the fluid and a volume is withdrawn.

Direct Weighing. In the case of two immiscible fluids jointly saturating a porous medium the respective saturations can be determined by direct weighing. Thus, for example, if the weight of the porous material is determined in an evacuated (or gas-filled) state and again when partially saturated with a liquid of density ρ_l, the saturation with respect to the liquid is given by

$$S_l = \frac{W_2 - W_1}{\phi \rho_l V_B} \tag{2.2.1.4}$$

Here W_2 is the weight at liquid saturation S_l, and W_1 is the weight when no liquid is present.

Electrical Resistivity Method. If a porous material is a poor conductor of electrical current then when the void space of the material is partially filled with a fluid which is a good

conductor, such as a sodium chloride solution, the saturation with respect to this fluid can be determined by electrical resistivity measurements.

X-Ray Absorption Method. When x-rays traverse any material the intensity of the rays is attenuated in accordance with the exponential equation:

$$I = I_o e^{-\beta x} \qquad (2.2.1.5)$$

where I is the intensity, I_o the intensity of the beam for zero penetration distance. x is the thickness of material traversed and β is the absorption coefficient for x-rays in the material in question. If, in a porous material jointly saturated by two immiscible fluids, one of the fluids contains a dissolved salt which is a good absorber of x-rays, then variations in the saturation of this fluid will be reflected in significant changes in the over-all x-ray absorption coefficient of the sample. Consequently, x-ray absorption can be used as a measure of saturations.

Figure 2.2.1 Emphasizes a comparison between the porosity, permeability and saturation.

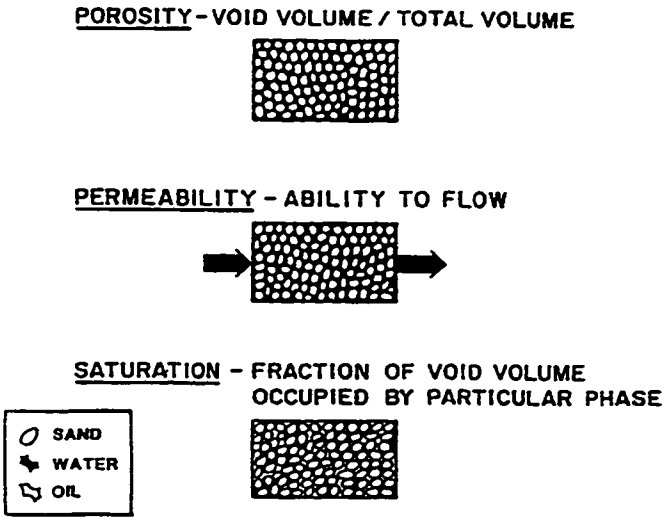

Figure 2.2.1 Visual comparison between porosity, permeability and saturation.

2.2.2 Capillary Pressure

Capillary pressure represents the pressure difference, which develops across the interface separating two immiscible fluids when they come in contact.

Capillary pressure is the most basic rock-fluid characteristic in multiphase flows, just as porosity and permeability are the most basic properties in single-phase flow.

If we consider the capillary tube (shown in Figure 2.2.2.1 containing two phases, a nonwetting phase on the left and a wetting phase on the right, phase I wets the tube surface because the contact angle θ, measured through this phase, is less than 90'. The boundary between the two phases is a phase boundary or interface across which one or more of the intensive fluid properties change discontinuously (Lake, 1989).

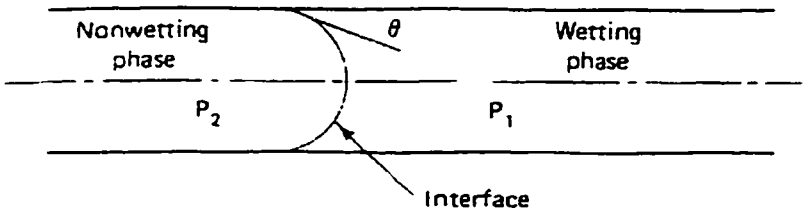

Figure 2.2.2.1 Configuration of an interface between two phases.

If the phases and the interface in the tube are not flowing, a higher pressure is required in the nonwetting phase than in the wetting phase to keep the interface from moving. A static force balance across the interface in the direction parallel to the tube axis yields an expression for the nonwetting-wetting phase pressure difference.

$$P_2 - P_1 = \frac{2\gamma\cos\theta}{R} \equiv P_c \qquad (2.2.2.1)$$

Equation (2.2.2.1) defines **capillary pressure**. It is a simple form of Laplace's equation and relates the capillary pressure across an interface to the curvature of the interface R, the interfacial tension γ, and the contact angle θ. If either the interfacial tension is zero or the interface is perpendicular to the tube wall, the capillary pressure will be zero. The first condition is satisfied when the absence of interfacial tension (and, hence, the interface) renders the two adjoining phases miscible. The second condition holds only for the simple uniform tube geometry because only in a simple shape – such a cylinder – the two radiuses of curvature are constant. The contact angle can take on all values between 0° and 180°. If it is greater than 90°, the wetting pattern of the two fluids is reversed, and the capillary pressure, as defined by Eq. (2.2.2.1), becomes negative. In more complicated geometries, the form of the 1/R term in Eq. (2.2.2.1) is replaced with the mean curvature, a more general expression. In this case, the capillary pressure is inversely proportional to a generalized interfacial curvature. To force the interface into the pore, it must be compressed through the pore neck radius R_n, causing a decrease in the interface curvature and an increase in the capillary pressure. When the forces acting on the interface become too high, it can collapse and create a disconnected globule of

the nonwetting phase within the pores. The globule conforms to the pore body to minimize its energy, and the curvature again increases, causing an abrupt decrease in the capillary pressure. When this happens the wetting phase changes from a continuous funicular (two positive curvatures) configuration to a discontinuous pendular (one positive and one negative curvature) configuration (Stegemeier, 1976), as pictured in Figure 2.2.2.2.

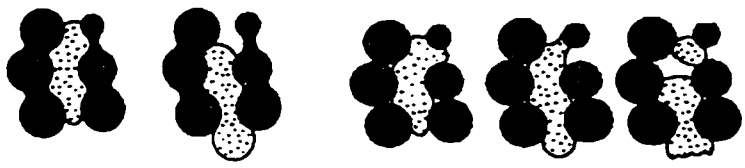

a b

Figure 2.2.2.2 Mechanisms of residual oil mobilization; (a) continuous oil droplets; (b) smaller discontinuous oil droplets.

If the nonwetting phase saturation is again increased, the blob is forced farther into the rock-rock contacts, which manifests itself in large capillary pressure increases. The wetting phase at this point retreats to saturations approximated by monolayer coverage of the rock surfaces. Though this would seem to result in quite a small saturation. Melrose (1982) has shown that wetting phase saturations above 10% are possible at this limit.

2.3 Physical and mathematical theory of flow

The ***dimensionality*** of a flow is the number of independent space coordinates necessary to specify the velocity. From another point of view, dimensionality is the number of directions in which the velocity can vary. Dimensionality can vary from zero to three. A flow with **zero dimensionality** is called a ***uniform flow***.

The ***directionality*** of a flow field is the number of nonzero velocity components present in the field, that is, the number of nonzero dependent variables in the velocity function. Directionality can vary from one to three. (Gerhard *et al.*,1992)

Among the parameters employed in studies on fluid flow, four are the most important (Constantinescu, 1995):

- Sherwood number: $$Sh = \frac{l_o}{v_o t_o} \qquad (2.3.1)$$

- Froude number: $$Fr = \frac{v_o^2}{g t_o} \qquad (2.3.2)$$

- Euler number: $$Eu = \frac{P}{\rho v_o^2} \qquad (2.3.3)$$

- Reynolds number: $$Re = \frac{\rho v_o l_o}{\mu} \qquad (2.3.4)$$

Thus, **Sherwood** number controls the order of magnitude of unsteady effects. Unsteady motions with $Sh << 1$ will behave like quasi-steady ones since the influence of the respective term may be neglected.

The **Froude** number gives an idea of the importance of gravity effects. Such effects may be neglected when $Fr >> 1$. It is seen that most flows around bodies satisfy this condition. Indeed, if $Vo \sim 10$ m/s, $l_o \sim 10^{-1}$m, $g \sim 10$ m/s^2 then $Fr \sim 100$. Gravity effects are even smaller at higher speeds.

The **Euler** number is the only parameter occurring in steady inviscid flow; it is widely used under the form of the pressure coefficient, with the only difference being that dynamic pressure $\rho V^2/2$ is used instead of ρV^2.

Finally, the **Reynolds** number represents the ratio between convective inertia forces and viscous ones. Inviscid fluids will thus correspond to $Re \rightarrow \infty$ while, at the other extreme, slow viscous flow will correspond to $Re \rightarrow 0$ when inertia forces become negligible. As stated several times, the Reynolds number plays a fundamental role in viscous fluid flow.

The above parameters are the basic ones derived from the Navier-Stokes equations. The parameters v_o, l_o and t_o in these equations are reference values for velocity, length and time respectively.

2.3.1 Categories of flow

Besides classification as steady or unsteady, uniform or one-, two-, or three-dimensional, and one-, two-, or three-directional, flows are divided into three flow regimes to describe the state of fluid motion. The three regimes are:

1. irrotational/inviscid flow (often called *ideal flow);*
2. laminar flow; and
3. turbulent flow.

Mathematical models of these regions neglect the effects of shear stress.. Regions of flow (close to the axis of the channel or pipe) with small velocity gradients and negligible shear stress, are called ***irrotational*** (to reflect the negligible particle spin), or ***inviscid***, flow regions. Irrotational/inviscid flow is characterized by smooth streamlines and orderly fluid motion. Because the top and bottom of the particle are moving in the same direction at the same speed, the particle is not being sheared or deformed, nor is it rotating (spinning) about its center.

A fluid particle in a region near the channel or pipe walls is moving faster with the edge nearer the center of the channel than the edge nearer the wall. That is why the particle is being deformed or sheared, and shear stress is significant in the particle's dynamics. Regions of flow where shear deformation is significant are called ***shear flow*** regions. In some flows, shear flow occurs in thin regions near walls or other surfaces of discontinuity, while the remainder of the flow is nearly irrotational/inviscid. When this type of flow occurs, the thin region of shear flow is called a ***boundary layer***.

An ideal fluid must satisfy the following requirements:

1. The continuity equation: $\text{div } q = 0$, or $\frac{\partial u}{\partial x} + \frac{\partial v}{\partial y} + \frac{\partial w}{\partial z} = 0$ (2.3.1.1)

2. Newton's second law of motion at every point at every instant

3. Neither penetration of fluid into, nor gaps between, fluid and boundary at any solid boundary

If, in addition to requirements 1, 2, and 3, the assumption of irrotational flow is made, the resulting fluid motion closely resembles real-fluid motion for fluids of low viscosity outside boundary layers.

2.3.1.1. Viscous Flow Pattern

Viscous flow represents a rather intricate problem due to the character of the basic equations, nonlinearity, and the multitude of effects occurring either directly in the differential equations or indirectly through the intermediary of boundary conditions. Therefore, any successful approach, mainly leading to analytical solutions, has to be done by making rational simplifications. Such results are usually valid for certain types of flow and for a certain range of Reynolds numbers.

2.3.1.2. Influence of Porous Surfaces

All applications of fluid flows examined so far assumed boundary conditions for a solid surface. That is the **no-slip** condition stating that at a solid wall the velocity of fluid equals the velocity of the solid. The same no-slip condition applies on a fluid boundary (the boundary

between two immiscible liquids). Another condition is that the velocity profile remains linear but exhibits a slip δu at the wall. In the case of a porous (or permeable) surface one should accept a nonzero normal component of the fluid velocity at the wall.

The hydrodynamics of porous media - slow (or creeping) flow - is based on Darcy's equation (2.1.3.1). By analogy to slow laminar flow through ducts, one assumes a linear pressure loss due to viscous drag. Darcy's equation for a single-phase flow and in the absence of gravity, is valid provided that Reynolds number is very small.

The movement of a fluid through a porous medium, such as sandstone or through a material composed of solid grains or fibers is called **percolation**. Axially symmetric Poiseuille flow and percolation flow through a porous solid (Darcy flow) are fundamentally similar. Each of the two equations expresses the velocity of the fluid as a function of the force per unit volume acting on the fluid and of the inverse of dynamic viscosity. Because this similarity it is assumed that flow in the void spaces of the porous material is laminar. This assumption is supported by the fact that for a given combination of porous material and flowing fluid. Darcy's law ceases to be valid for fluid velocities higher than a particular limiting value. In general the unity is accepted as a limiting value for Reynolds number. Flows at $Re < 1$ are laminar. In addition, Darcy's law is limited at the situation when only one fluid phase flows in porous solid. For the more general case of two or more fluids flowing simultaneously through the porous medium, this law has been generalized.

2.3.2 Multiphase flow of immiscible fluids in porous media

For two-phase flow, a generalized form of Darcy's equation is applied (Lake 1989, Dullien 1992)

$$v_i = \frac{k\ k_{ri}}{\mu_i} \nabla P_i \qquad (2.3.2.1)$$

$$v_d = \frac{k\ k_{rd}}{\mu_d} \nabla P_d \qquad (2.3.2.2)$$

where the subscripts i and d signify the injected and displaced fluids, respectively. The volume, is a small section of a larger displacement, but is still of macroscopic size. P_i and P_d denote the pressures in the injected and displaced fluids, k_r is the relative permeability for the particular fluid and k is the absolute permeability.

An empirical approach to determining how the oil recovery is affected is made through study of capillary number relationships. Capillary number is a generic term for the ratio of viscous-to capillary forces. The numerous forms of capillary number used in the past were reviewed by Taber (1981). A common form of capillary number is

$$N_{Ca} = \frac{v\ \mu}{\gamma} \qquad (2.3.2.3)$$

From Darcy's law, the capillary number $v\mu/\gamma$ can be expressed as

$$\frac{v\mu}{\gamma} = \frac{k_{rw}\ k}{\mu} \frac{\Delta P}{L} \qquad (2.3.2.4)$$

where k_{rw} is the relative permeability of the medium to water.

The mobility of a fluid in a porous medium is a measure of the ease with which fluid flows through the medium, and is defined as the permeability of the formation to that fluid divided by the viscosity of the fluid, as shown in Eq. 2.3.2.5.

$$\lambda = \frac{k}{\mu} \tag{2.3.2.5}$$

Mobility ratio, in the case of water (w) displacing oil (o), can be defined as :

$$M = \frac{\frac{k_w}{\mu_w}}{\frac{k_o}{\mu_o}} \tag{2.3.2.6}$$

where k represents the permeability of each fluid and μ is the viscosity of each fluid.

2.3.3 Relative Permeability

Relative permeability curves and their associated parameters are relevant petrophysical relations for EOR. If the flow of several incompressible, single-component phases in a one-dimensional, linear permeable medium, is steady-state (that is, the saturation of all the phases does not vary with time and position), Darcy's equation may be integrated over a finite distance Δx to give

$$v_j = -\lambda_j \Delta \phi_j / \Delta x \tag{2.3.3.1.}$$

where λ_j is the mobility of phase j. The mobility is the "constant" of proportionality between the flux of phase velocity v_j and the potential difference, $\Delta\Phi$

$$\Delta \Phi_j = \Delta(P_j - \rho_j g h_j) \tag{2.3.3.2}$$

λ_j can be decomposed into a rock property, the absolute permeability k, a fluid property, the phase j viscosity μ_j, and a rock-fluid property, the relative permeability k_{rj}. The elevation of the particular point in the fluid is h_j .

The relative permeability is a strong function of the saturation of phase j (S_j). Since the functionality between k_{rj} *and* S_j is a rock-fluid property, it is also a function of rock properties (pore size distribution, for example) and wettability. It is not, in general, a strong function of fluid properties, although when certain properties (interfacial tension, for example) change drastically, relative permeability can be affected.

Alternate definitions involving the mobility and relative permeability are the relative mobility λ_j

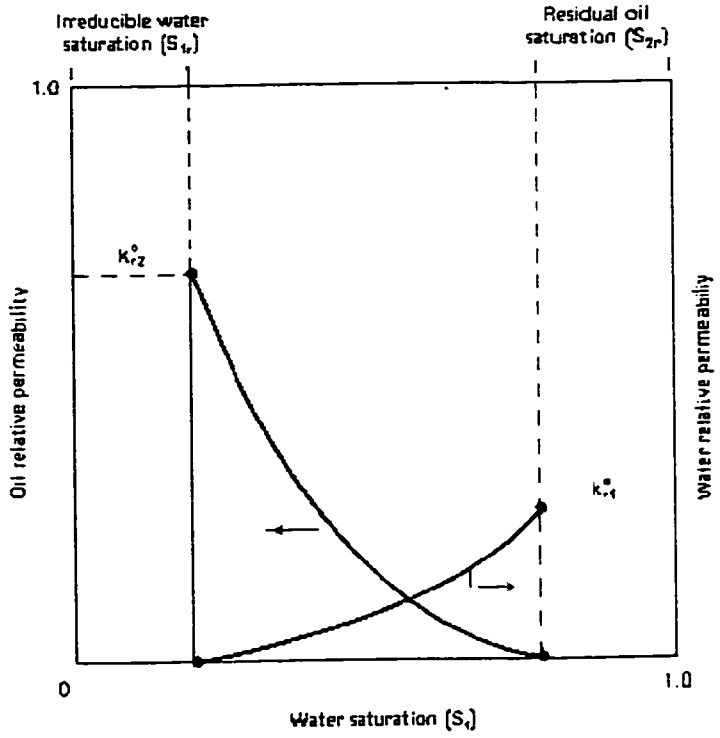

Figure 2.3.3.1 Typical water-oil relative permeabilities (Lake 1989)

Figure 2.3.3.1 shows oil-water relative permeability curves. The relative permeability (k_r) to a phase decreases as the saturation of that phase (S) also decreases. If the relative permeability of a phase is zero, it can no longer flow, and the saturation at this point cannot be lowered any further. Reducing the "trapped" oil saturation is one of the most important objectives of EOR The trapped oil saturation is called the residual oil saturation and given the symbol S_{2r} or S_{OR}. The end-point relative permeability to water (k_r^o), corresponds to S_{2r}.

2.3.4 Displacement efficiency

If we assume constant oil density, the definition of displacement efficiency for oil becomes

$$E_D = \frac{\text{Amount of oil displaced}}{\text{Amount of oil contacted by displacing agent}} \qquad (2.3.4.1)$$

E_D is bounded between 0 and 1. The rate at which E_D approaches 1 is affected by the initial conditions, the displacing agent, the amount of displacing agent, fluid, rock, and fluid-rock properties. If the displacement is such that the displacing agent will contact all of the oil initially present in the medium, the volumetric sweep efficiency will be unity, and E_D becomes the recovery efficiency E_R.

2.3.5 Immiscible Displacement

In order to understand the phenomena involved in EOR displacements it is very important to understand the displacement of one fluid by an immiscible second fluid. The specific case of water displacing oil was first solved by Buckley and Leverett (1942) and later broadened by Welge (1952), Collins (1976), Craig (1971), Dake 1(978), and Lake (1989).

For the isothermal flow of oil and water in two immiscible, incompressible phases in a one-dimensional permeable medium, the mass conservation equation (1.1) reduces to

$$\Phi \frac{\partial S_1}{\partial t} + v \frac{\partial f_1}{\partial x} = 0 \qquad (2.3.5.1)$$

for flow in the positive x direction. In this equation, f_1, is the fractional flow of water,

$$f_1 = \frac{v_1}{v} = \frac{\lambda_{r1}}{\lambda_{r1} + \lambda_{r2}} \left(1 - \frac{k \lambda_{r2} \Delta\rho g \sin \alpha}{u} \right) \qquad (2.3.5.2)$$

in the absence of capillary pressure. In Eq. (2.3.5.2), α is the dip angle defined to be positive when measured in the counterclockwise direction from the horizontal, and $\Delta\rho = \rho_1 - \rho_2$ is the density difference between the water and oil phases.

Either S_1 or S_2 can be chosen as the dependent variable in Eq. (2.3.5.1) since both $S_2 - S_1 = 1$, and $f_2 + f_1 = 1$. It is important that in the absence of capillary pressure, f_1 is uniquely determined as a function of S_1 only through the relative permeability relations $\lambda_{r1} = k_{r1}/\mu_1$ and $\lambda_{r2} = k_{r2}/\mu_2$.

2.3.6 *Fractional Flow Curves, Buckley-Leverett Solution*

Substituting the exponential form of the oil-water relative permeability curves into Eqn. (2.3.5.2), one gets:

$$f_1 = \frac{1 - N_g^o (1-S)^{n2} \sin\alpha}{1 + \frac{(1-S)^{n2}}{M^o S^{n1}}} \qquad (2.3.6.1)$$

where

$$S = \frac{S_1 - S_{1r}}{1 - S_{2r} - S_{1r}} = \text{ Reduced water saturation} \qquad (2.3.6.2)$$

and

$$M^o = \frac{k_{r1}^o \mu_2}{\mu_1 k_{r2}^o} = \text{ Endpoint water-oil mobility ratio} \qquad (2.3.6.3)$$

$$N_g^o = \frac{k k_{r2}^0 \Delta\rho g}{\mu_2 v} = \text{Gravity number} \qquad (2.3.6.4)$$

N_g^o is the ratio of gravity to viscous pressure gradients based on the endpoint oil relative permeability.

2.3.7 Volumetric Sweep Efficiency

Typical values of residual oil and connate water saturations indicate that ultimate displacement efficiency should normally be between 50% and 80% of the contacted oil in a waterflood. This range is substantially higher than the 30% average recovery efficiency observed in waterfloods; it is also higher than recovery efficiency in most EOR projects (see Sec. 1 - introduction). Of course, the reason displacement efficiency is higher than the recovery efficiency is that not all of the oil is contacted by the displacing agent.

E_v, the volumetric sweep efficiency is defined as

$$Ev = \frac{\text{Volumes of oil contacted by displacing agent}}{\text{Volumes of oil originally in place}} \qquad (2.3.7.1)$$

The volumetric sweep efficiency can be decomposed into the product of an areal sweep efficiency E_A and a vertical sweep efficiency E_I:

$$Ev = E_A E_I \qquad (2.3.7.2)$$

The definition of the areal sweep efficiency is

$$E_A = \frac{\text{Area contacted by displacing agent}}{\text{Total area}} \qquad (2.3.7.3)$$

The total area denotes the area of the reservoir.

The vertical sweep efficiency is

$$E_I = \frac{\text{Cross - sectional area contacted by displacing agent}}{\text{Total cross - sectional area}} \qquad (2.3.7.4)$$

2.3.8 Instability phenomena - hydrodynamical fingering

Practically every EOR process is associated with some sort of instability. Engelberts and Klinkenberg (1951) coined the expression "viscous fingering" to characterize the instability that occurs when a fluid of relatively low viscosity is injected into a medium of higher viscosity, contained between parallel plates, or in a porous medium. Finger-like instabilities are formed at the interface, branched to a grater or lesser extent. The early occurrence of fingers is one of the main problems that causes low oil recoveries and the knowledge of the ways that allow to diminish the effects this adverse phenomenon leads to more successful operation of these processes. This phenomenon will be analyzed in more detail in the section 2.5.

2.4 *Commercial processes using EOR techniques.*

The three natural oil recovery mechanisms in oil reservoirs are solution gas drive, gas cap expansion drive, and water drive. The first group of methods - called primary recovery - is based on the three natural mechanisms mentioned above. Water or gas injection drives are known as secondary recovery methods.

In a solution gas drive reservoir, the gases dissolved in the crude oil expand and come out of solution as the pressure in the reservoir drops. This expansion of gases causes the oil to be driven towards the wellbore. As production continues, the pressure in the expanding gas is no longer sufficient to cause the oil to flow to the surface, and pumping is required for further oil production. In a solution gas drive reservoir, the primary recovery is usually quite low, on the average 5 to 25% of the original oil-in-place (Prince, 1978). Another recovery technique (source of energy) for the production of oil is water encroachment from an adjoining aquifer, as a result of the lower pressure at the wellbore. The aquifer associated with a water drive reservoir is often much larger than the reservoir itself, and thus the energy supplied by the aquifer results in continued oil production over a long period of time. An effective water drive reservoir is characterized by a slow and gradual drop in reservoir pressure with time, and thereby a high recovery efficiency.

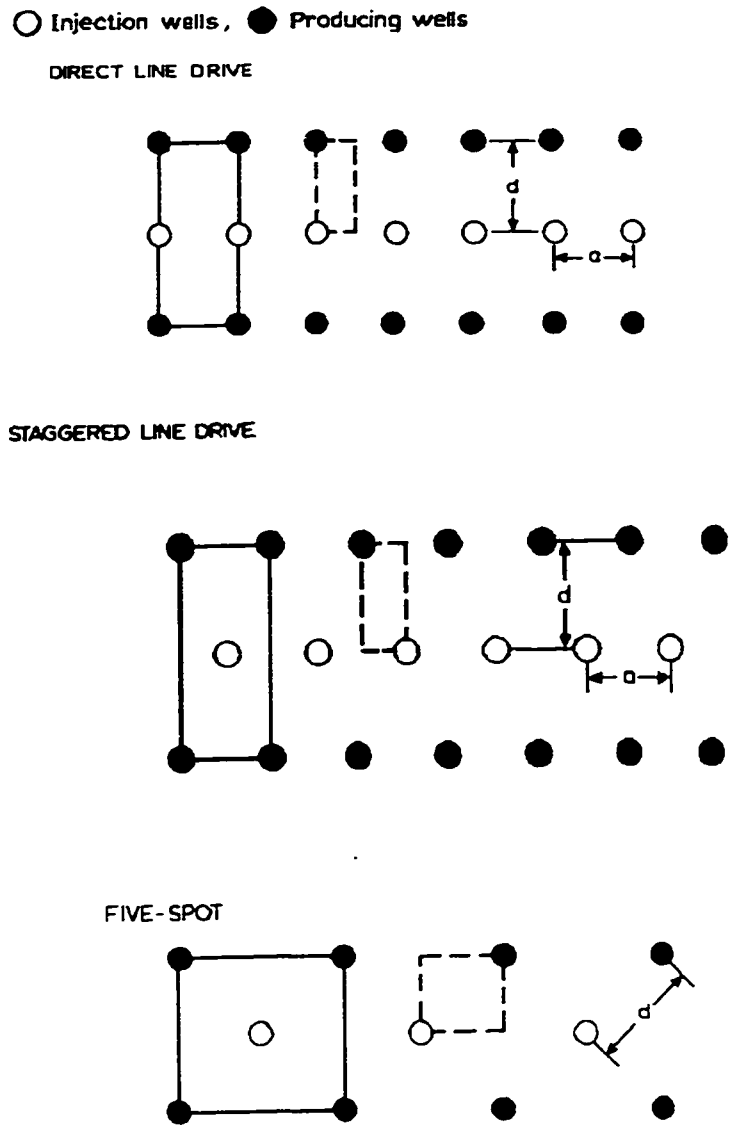

Figure 2.4.1 Some examples of the most common flood patterns (Donaldson. 1985) Solid line indicates symmetry pattern of infinite well network. Dashed line indicates symmetry element of infinite well network.

Figure 2.4.1 shows the most common schemes of well placement in the field used in waterfloods. For the case of five-spot pattern the shape of the flood fronts is presented in Figure 2.4.2

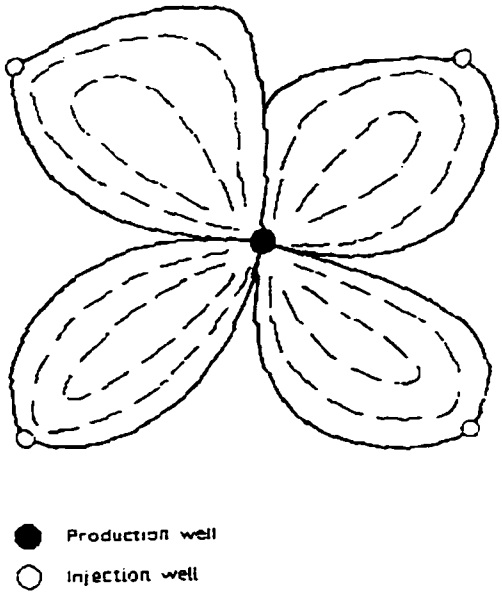

Figure 2.4.2 Five-spot well pattern illustrating enhanced recovery flood pattern (Donaldson, 1985).

Enhanced Oil Recovery (EOR) usually encompasses tertiary recovery-the third group of methods employed with various degree of success to recover additional oil not economically recoverable by secondary methods. They must provide energy to compensate for the loss of natural energy of the reservoir during the exploitation following the drilling of the well. The natural energy of the reservoir gradually depletes and a new stage begins when the oil is no longer able to come out naturally.

All processes are strongly affected by reservoir description. Recovery process effectiveness depends so heavily on reservoir fluid flow and phase behavior that thorough knowledge of these factors is essential. Accurate reservoir description is particularly critical in determining the applicability of any enhanced recovery process. Information on reservoir properties comes from a combination of sources that include geologic studies, core analyses, logging, and pressure transient testing, as well as analysis of reservoir behavior and production history.

As mentioned in earlier, (page 4) basically there are three groups of EOR methods

1. Chemical
2. Solvent (miscible)
3. Thermal

A brief description is given below.

2.4.1 Chemical methods

2.4.1.1 Alkaline flooding

This method is based on the chemical reaction that occurs between acidic oils and alkaline solutions (for example: sodium hydroxide, sodium silicate, sodium carbonate). As a result of neutralization of organic acids present in the majority of crude oils, the corresponding sodium salts of these acids are produced. These organic salts have tensioactive properties and can dramatically lower the interfacial tension between the two phases - aqueous and organic. A water flood may be converted to an alkaline flood by adding one to five weight percent of sodium hydroxide to the injected water. The pH of the injected solution can vary between 11

and 13. Occasionally polymers are added to increase viscosity. Other processes that could contribute to oil recovery include emulsification and entrapment of oil in the water phase, and changes in rock wettability (Gilbert et.al.,1986).

Acidity of oil is usually characterized by the "acid number", defined as the number of milligram of potassium hydroxide required to neutralize one gram of oil. Alkaline flooding can mobilize more residual crude oil than any other method of enhanced oil recovery.

Table 2.4.1.1 shows sensitivity to high saltiness is common to all chemical flooding EOR. Total dissolved solids should be less than 100,000 g/m^3, and hardness should be less than 2,000 g/m^3. Chemical agents are also susceptible to loss through rock-fluid interactions.

Table 2.4.1.1 Chemical EOR Processes (adapted from Taber and Martin, 1983)

Process	Recovery mechanism	Issues	Typical recovery (%)	Typical agent utilization*
Polymer	Improves volumetric sweep by mobility reduction	Injectivity Stability High salinity	5	0.3-0.5 lb polymer per bbl oil produced
Micellar polymer	Same as polymer plus reduces capillary forces	Same as polymer plus chemical availability, retention, and high salinity	15	15-25 lb surfactant per bbl oil produced
Alkaline polymer	Same as micellar polymer plus oil solubilization and wettability alteration	Same as micellar polymer plus oil composition	5	35-45 lb chemical per bbl oil produced

*1 lb/bbl $\approx$ 2.86 kg/m^3

Maintaining adequate injectivity is a persistent problem. Their history shows that these processes ranged from small to moderately large. Chemical utilization factors have meaning only when compared to the costs of the individual agents; polymer, for example, is usually three to four times as expensive (per unit mass) as surfactants.

Alkali when injected can also reduce concern over calcium and magnesium ion interactions with the anionic surfactant. Sodium silicate keeps both calcium and magnesium out of solution better than sodium hydroxide or sodium carbonate does, but sodium silicate and sodium hydroxide are consumed in the reservoir by reaction with kaolinite clay much more than sodium carbonate.

With proper attention to important formulating considerations and adequate characterization of the prices of the crude oil at that particular moment.
Progress is being made on lowering the cost of alkaline flooding. Surfactant loss to the reservoir is substantially lower under alkaline conditions.

Figure 2.4.1.1 illustrates how oil is emulsified inside the pores by the alkaline solution. transformed in smaller droplets that are easily displaced through the pore network. The photograph has been taken from a videotaped sequence of an oil-in-water emulsion flowing through a curved pore channel network (Bear 1987).

Figure 2.4.1.1 Oil in water emulsion flowing (left to right) within a curved pore channel.

2.4.1.2 Polymer Flooding

Polymer solutions have been used in three ways to increase oil production:

1. Near-well polymer treatment has been performed in production wells and water injection wells. Production well treatments are designed to reduce fluid flow from zones producing excessive amounts of water. Injection well treatments are designed to reduce the volume of water that enters high permeability zones.

2. Polymer solutions which can be cross-linked within the formation have been used to plug high permeability zones at a substantial distance from the wellbore. The technique involves the injection of the polymer solution with an inorganic metal cation which will cross-link subsequently injected polymer molecules with the molecules already bound to the rock surface.

3. Polymer solutions may be injected for the purpose of reducing the mobility of the displacing fluid, thus improving the efficiency with which the reservoir crude oil is displaced.

2.4.1.3 Surfactant Flooding

Also known by the names: micellar-polymer flooding, low tension water flooding, and microemulsion flooding, this method typically involves the injection of a slug of surfactant containing fluid, followed by polymer-thickened water, and finally ordinary brine. Despite the very high displacement efficiency of the micellar solution, micellar/polymer flooding is not profitable today because of the high cost of chemicals (George and Marvin, 1990).

2.4.2 Solvent methods

One of the earliest methods for producing additional oil is through the use of solvents to extract the oil from the permeable media. In the early 1960s, interest centered on injecting liquefied petroleum gas (LPG) in small "slugs" and then displacing the LPG by a dry "chase" gas. This process became economically less attractive as the value of the solvent increased. In the late 1970s, interest in solvent methods restarted because of an increased oil price and more confidence in the ability to estimate oil recovery. During this period, carbon dioxide became the most used solvent (Stalkup, 1985).

Two fluids that mix together in all proportions within a single-fluid phase are ***miscible***. Therefore, miscible agents would mix in all proportions with the oil to be displaced. But most practical miscible agents exhibit only partial miscibility toward the crude oil itself, so it is more appropriate to use the term ***solvent flooding***. Many solvents, of course, will become miscible with crude under the right conditions, but all solvents of commercial interest are immiscible to an aqueous phase.

Solvent flooding refers to those EOR techniques whose main oil recovering function is because of extraction, dissolution, vaporization, solubilization, condensation, or some other phase behavior change involving the crude. These methods have other, sometimes very important, oil recovery mechanisms (viscosity reduction, oil swelling, and solution gas drive), but the primary mechanism must be extraction.

This oil extraction can be brought about by many fluids: CO_2, alcohols, ketones, refined hydrocarbons, condensed petroleum gas (LPG), and natural gas. Injection of CO_2 into the oil reservoirs may initiate oil displacement by a number of mechanisms. Although not usually miscible with reservoir oil upon contact, CO_2 creates a miscible front and miscibility is initiated by extraction of significant amounts of heavier hydrocarbon (C5 to C30) by CO_2. Carbon dioxide may also be useful in heavy oil reservoirs where thermal methods may not be applied.

If the solvent is completely (first contact) miscible with the oil, the process has a very high ultimate displacement efficiency since there can be no residual phases. If the solvent is only partially miscible with the crude, the total composition in the mixing zone between the solvent and the oil can change to generate or develop miscibility in situ. Regardless of whether the displacement is developed or first contact miscible, the solvent must immiscibly displace any mobile water present with the resident fluids.

The economics of the process usually dictates that the solvent cannot be injected indefinitely. Therefore, a finite amount or *slug* of solvent is usually followed by a *chase* fluid whose function is to drive the solvent toward the production wells.

2.4.3 Thermal methods

Most successful commercial applications of EOR up to the present have involved thermal processes. As of 1986, about 78% of all EOR oil production in the United States has resulted from thermal projects (Boberg, 1989)

2.4.3.1 Steam stimulation

This process is also called cyclic steam injection, steam soak, or huff and puff. Steam is injected into the reservoir through a production well (huff) for a period of several weeks to heat up the reservoir. The well is then shut-in for several days or weeks before production is resumed. During the shut-in period, the heat from the steam increases the reservoir temperature, which decreases the oil viscosity and makes the mobility ratio more favorable. The oil is then produced (puff) until economic factors necessitate another steam injection. The production period is often up to one year in length, and is often followed by steam flooding.

2.4.3.2 Steam Flooding

In this process steam is injected into the reservoir through injection wells laid out in a pattern around the producing well. The steam mobilizes the oil and drives it towards the production wells. At the steam front, condensation occurs and a hot water bank is formed. The hot water causes thermal expansion of the crude oil and brings about a decrease in oil

viscosity. Behind the steam front, oil is displaced by the vaporization of the lighter hydrocarbons and the resultant gas drive.

2.4.3.3. In-Situ Combustion

In the in-situ combustion process, also known as fire flooding, air is injected into the oil reservoir through an injection, and the crude oil ignites either spontaneously or with the aid of a gas burner or resistance heater. As air injection continues, the combustion front moves away from the injection well, heating and displacing oil and water to the surrounding wells. At the combustion front, the connate (interstitial) water is vaporized and the oil is cracked leaving a residue of coke on the rock to maintain combustion. The steam produced in this manner moves ahead of the combustion front, condenses and mobilizes the oil into an oil bank, which is pushed towards the production well. The portion of the reservoir swept by the front is then burned clean. Often water is injected along with the air, a process known as wet combustion. The advantage of this is that the amount of heat transported to the region ahead of the combustion front is significantly increased (Gangoli and Thados, 1977). As a result of this, the oil viscosity is greatly reduced, improving oil recovery.

2.5 *Laboratory experimental techniques.*

2.5.1 Hele-Shaw model

For studying viscous fingering problems, a Hele-Shaw (1898) cell has been used as an analog of two-dimensional isotropic homogeneous porous media (Saffman & Taylor 1958; Chuoke et al. 1959; Stalkup 1984). Flow in a Hele-Shaw is described by the equation 2.5.1.1 which is similar to Darcy's equation,

$$V = -\frac{b^2}{12\mu}\nabla P \qquad (2.5.1.1)$$

since the term $b^2/12$ can be replaced by an effective permeability.

In this equation this the gap between the two glass plates from which the cell is constructed. ∇P is the pressure gradient across he cell and μ is the viscosity of the fluid.

Single-phase Hele-Shaw flow is considered an analogous to two-dimensional incompressible flow in porous media. However, the flow of two immiscible fluids in porous media is more complex and this analogy fails.

Figure 2.5.1.1 depicts the schematic of a longitudinal Hele-Shaw cell along with the representation of some fingers that occur during a displacement of a more viscous liquid by a less viscous liquid.

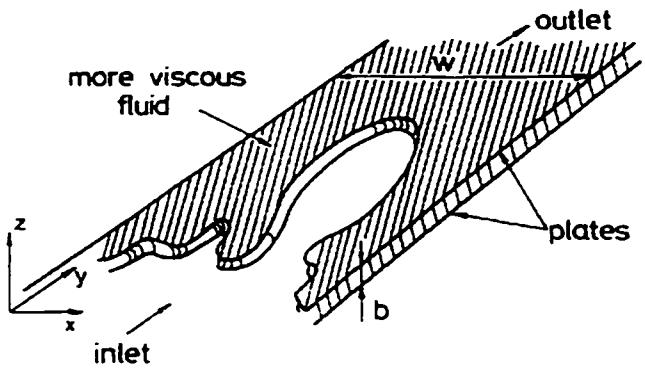

Figure 2.5.1.1 Schematic representation of a Hele-Shaw cell, along with finger-like patterns (Vicsek, 1988)

Paterson (1981) analyzed the linear instability of an expanding circular interface when an inviscid fluid is displacing an immiscible viscous fluid at a constant volumetric flow rate q in a Hele-Shaw cell.

Howison (1986) in his paper gave some explicit solutions for finger development in one-phase flow in a Hele-Shaw cell (that is. a flow in which the viscosity of the less-viscous fluid is so small that it may be ignored).

Chen (1987) performed viscous fingering experiments in radial Hele-Shaw cells consisting of both smooth and etched plates. He studied the influence of plate roughness. flow rate and interfacial tension on the fingering mechanism.. The results show that symmetric dendritic finger patterns can form in the presence of anisotropy provided by an etched square network. in both miscible and immiscible displacements.

Coskuner (1985) modified a new approach to stability theory developed by Bentsen (1985) to predict the behavior of fingers once they are formed. The experiments were undertaken in a Hele-Shaw cell because in this model the assumption of a sharp front between the two fluids is satisfied exactly.

Hornof and Bernard (1992) studied the displacement in a Hele-Shaw of a heavy crude oil by both water and alkaline solutions. The experimental results showed a decrease of the recovery at breakthrough in the case of alkaline flooding compared with water flooding, while in the case of total recovery the situation was reversed, waterflood being the process associated with highest recovery.

Other studies performed by Hornof and Baig (1995) showed a higher recovery in the case of reactive systems.

2.5.2 Displacements in porous media

Both unconsolidated and consolidated porous media are used in experimental works, specially when flow of two immiscible fluids is investigated.

Warren (1954) used fritted glass as a porous medium and found a correlation between breakthrough recovery and several variables including interfacial tension, contact angle and porosity.

Flock et al. (1977) found an increase of breakthrough recovery with the increase of flow rates for the small values range. In the medium value range of the flow rates, however, the breakthrough recovery stayed constant, and for high flow rates, the recovery decreased. The explanation was that there are three domains: the low flow rate range where the capillary forces are dominant, the medium range where the recovery is stabilized, and the high flow rate range where the viscous forces dominate.

Pavone (1992) studied viscous fingering in 3D consolidated porous media and remarked the occurrence of stable displacements behind the unstable front. The shape of the fingers was different than that of the fingers developed in Hele-Shaw cell.

Porous media can be also modeled by etching polymer plates, (Lenormand, Zarcone (1985), Lenormand (1990)).

As in the case of Hele-Shaw cells, studies regarding immiscible displacement using reactive systems, have been conducted in porous media. Using cells made from sintered glass beads for the displacement of acidic oils by the sodium hydroxide solutions, Nasr-El-Din et al. (1990) got higher recoveries in the case of non-reacting systems than for the reacting ones.

Unconsolidated porous media were also used by Hornof et.al. (1994) to study the flooding of acidic oils by alkaline solutions. The results showed a decrease of recovery with the increase of the concentration of alkaline solution. The porous media they employed were prepared using a method described by Polikar et al. (1988). They reported a reproducible packing technique for clean, unconsolidated sand cores, using natural sand of a specific size range, for the simulation of enhanced recovery processes in the laboratory. They employed both dry and wet packing techniques under a constant sand fall rate and continuous vibration and foun that dry packing gave better results. Wet packing caused the formation of distinct layers in the presence of a slight excess of water. The influence and importance of several factors used in the process of packing is again emphasized (see Table 2.2.1.2 on page 11)

3. EXPERIMENTAL WORK

The aim of this work was to obtain both qualitative and quantitative information about the process of immiscible displacement in unconsolidated porous media, along with a better understanding of the instability phenomena occurring during the flow using non - reactive as well as reactive systems. The quantitative information consists of recovery data and qualitative information consists of pictures taken in order to visualize the pattern of moving front and its instabilities (finger formation) during the flow. The unconsolidated porous medium is more difficult to handle than consolidated porous media for a number of reasons, mainly because of care that must be taken to avoid the modification of its porosity in the process of performing displacement experiments. This research follows up and extends the work previously done in this laboratory by Hornof and Chen (1992) and Hornof et al. (1994).

Obtaining additional information for these systems is important, since their occurrence in natural reservoirs is rather frequent.

The experiments were divided in three groups. The first group consists of the displacements of neutral oil by distilled water. It was followed by the displacements of acidic oil by distilled water (see table 3.1.1). The last group of experiments consisted of alkaline displacement of acidic oil (same composition as in previous group of experiments) by a sodium hydroxide solution (solution d in table 3.1.1). The experiments were performed in this order to minimize the possible influence of the wettability change (occurring during alkaline displacement) on the first and the second group of experiments. Downward displacements of

neutral and acidic oil were also performed in order to study the influence of gravity on the breakthrough recovery.

3.1 The equipment and materials.

The cell that was used to perform the displacement experiments is the two-spot cell, analogous to one-quarter of the inverted five-spot pattern. This design was chosen for flow visualization because of its simple geometry and construction. Since the displacing fluid was going to be water or an aqueous solution, transparent glass plates were used because glass is preferentially water-wet and is also inert to organic phase (oil). The use of silica beads was selected for the same reasons. The choice of a homogeneous packing over a non-homogeneous one reduces the likelihood of channeling through the grains of different sizes. Finally the two liquids (i.e. water and paraffin oil) were used to simulate the conditions prevailing in a reservoir in terms of viscosity ratio, interfacial tension, and immiscibility.

3.1.1 Cell construction.

A schematic of the experimental setup is shown in Figure 3.1.1.

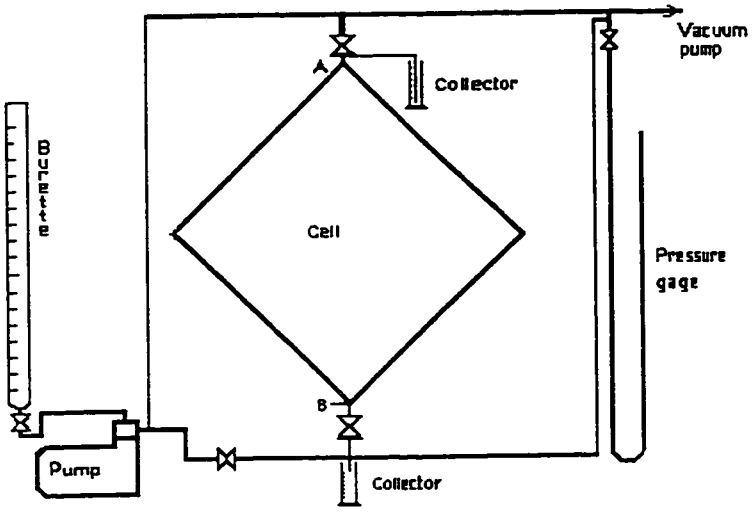

Figure 3.1.1 Schematic of the experimental setup

The cell was built out of two square glass plates having a thickness of 10 mm and side length of 451 mm. Four aluminum strips, placed along the edges of the plates were used as spacers between the glass plates. They created a 6.2 mm gap between the plates. Stainless steel tubing with external diameter of 6 mm and internal diameter of 5 mm was inserted at two opposite corners of the cell to be used as injector (inlet) and producer (outlet). Through one of these tubes the cell was filled with silica sand. This packing in the cell constituted the unconsolidated porous media in which the displacement experiments were performed. In order to prevent leakage, the glass plates were glued to the spacers using silicone sealant. A system of valves connected to both ends of the cell allowed feeding the cell upwards as well as downwards. Also this system was used to make measurements of the pressure drop across the

cell during the displacements using a pressure gage filled with a fluid immiscible with water and much denser (tetrabromoethane). This fluid (with a specific gravity of 3 g/cm^3) allowed pressure drop being measured when the height of water in the gage would have been too high to measure.

The specifications for the experimental setup and materials that were used are given in Table 3.1.1.

Table 3.1.1 Specifications for the setup parts and other materials

Setup - parts/material	Specifications
Cell	
internal volume	0.001207 m^3
glass plate size	0.451 x 0.451 x 0.01m
aluminum spacers	
width	0.0082 m
thickness	0.006 m
metal tubing (external diameter)	0.006 m
Packing	Homogeneous bed silica sand
average grain diameter	35 mesh = $5x10^{-4}$ m
apparent sand density	1691 kg/m^3
porosity(ϕ)	35% (average of three measurements)
Pump	2 piston (duplex) with adjustable flow rate
Fluids	
a. distilled water	
viscosity	0.982 cp (at 21°C)
density	998.0 kg/m^3
interfacial tension water-paraffin oil	43.5 dynes/cm
b. light paraffin oil	
viscosity	25.84 cp (at 21 °C)
density	847 kg/m^3 (at 21 °C)
c. Solution of linoleic acid in light paraffin oil	10 mmoles/l
d. Aqueous solution of NaOH	25 mmoles/l

3.1.2 Cell preparation and testing.

The preparation of the cell for the experiments consisted of two steps:

a. filling the cell with sand to obtain the unconsolidated medium

b. checking the cell for leaks.

Filling the cell has been the most difficult operation, requiring special care and a large amount of time for completion. Two techniques have been tried for this purpose:

i. dry packing

ii. wet packing

The first method did not give good results, the end result being a loose packing that negatively affected the reproducibility of displacement experiments, in spite of the intense vibration to which the cell was subjected during the packing operation. The main problem seemed to be static electricity which was accumulating while the grains of sand poured into the cell. The electrostatic forces kept the grains apart, making possible the formation of channels inside the sand bed. Even after flooding the cell with water, oil and brine, this inconvenience did not go away, rendering the cell useless. All attempts to carry out a waterflood in such a cell have been a failure because the only pattern that could be observed during the experiment was a Christmas tree-like layers of red oil alternating with layers of sand, inclined at about 45°, while the exact placement of the sand remained unchanged after the packing operation.

The second approach proved itself much better, giving - upon completion - a more homogeneous sand pack. The operation consisted of filling the cell (kept in vertical position)

with distilled water, about three quarters of its volume, having the bottom valve closed. The pouring of the sand through the upper metal tube was then performed. The cell was subjected to intense vibration using an electrical vibrator. The rate with which the grains of sand were added was kept as constant as possible. Every time when the level of water in the cell reached the outlet, some water was allowed to flow out of the cell through the bottom valve. After all the sand was added (about four hours) the cell was continuously vibrated. As the sand settled down and its level decreased, a new portion of sand vas added, to maintain the cell full. The process of settling is lengthy: it took a few days alternatively vibrating the cell and pumping distilled water through it in order to achieve a stable sand bed. After the level of the sand ceased to decrease, a vacuum of about 20 torr was applied at the outlet (the upper tube) in order to remove the small amount of air trapped into the sand pack. This operation was also a check for leaks, because any hole in the layer of silicone that was used to seal the sides of the cell allowed the air to enter the cell, the bubbles of air being visible. If that was the case a new layer of silicone was applied over that region. In the end the cell was full of sand and water and free of air. It was finally ready for the experiments.

Compared to the data reported by other authors (Polikar et al., 1988) it can be said that the conditions of packing were almost the same: room temperature, and sand fall rate of 600 g per hour. The grain size of the sand used in the present work was 0.5 mm, greater than their values (0.14 - 0.21mm). Also the container that they packed with sand was a cylinder, totally different than the narrow cell used in this work. This might explain the totally different results reported in the article, namely the dry packs did not display layering, while wet packing did. According to the data presented in the work published by Cumberland and Crawford (1987),

and assuming a spherical shape of particles, a value of 8 for the co-oordination number would result for the porosity determined for the pack used in the present work (see Table 2.1.1.1, page 10).

In order to evaluate the homogeneity of the sandpack a run has been conducted for displacing water by dyed water. In this case due to unity value for the mobility ratio, flow instabilities should not occur, and the shape of the moving front should be symmetrical in the cell. A flow rate of 250 cm^3/h was used for this run because it represents the average of the values for the flow rates used throughout this study (many runs have been conducted at flow rates around this value). The displacing fluid was distilled water dyed with methylene blue, whereas the displaced fluid was distilled water by itself. Pictures of the cell were taken at several periods of time during the displacement, as this method has been extensively used throughout this work to monitor the development of the flow patterns. The results are presented in Figures 3.1.2.1 and 3.1.2.2.

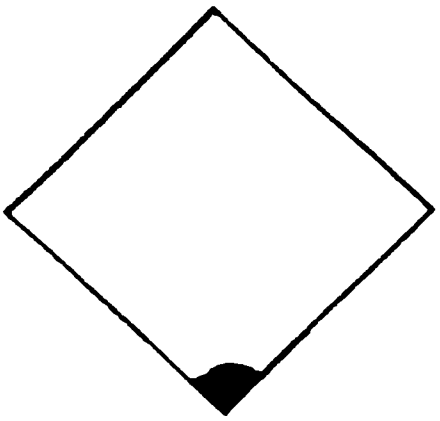

a) at 0.05 PV

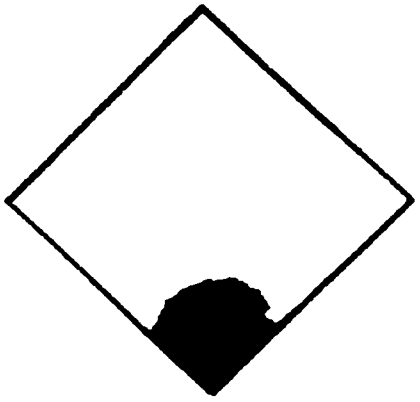

b) at 0.175 PV

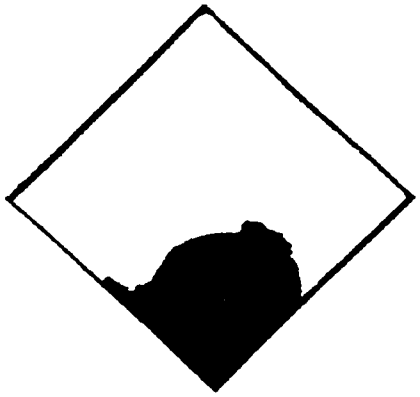

c) at 0.327 PV

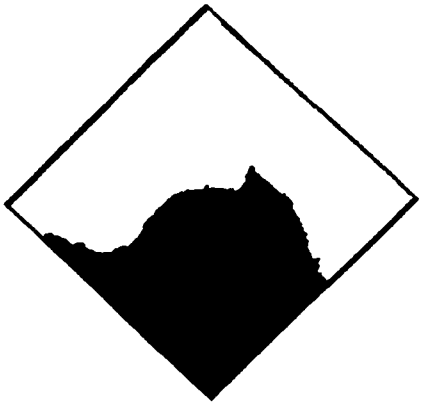

d) at 0.482 PV

Figure 3.1.2.1 The evolution of the moving front with time for water displacing water.

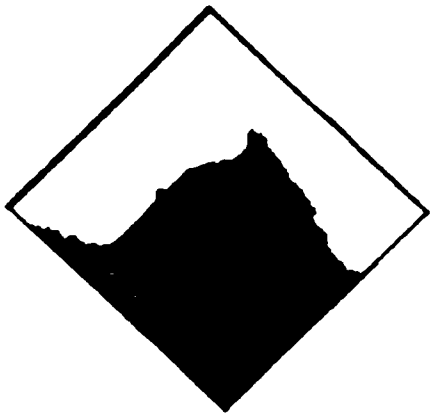

e) at 0.634 PV

f) at 0.855 PV (breakthrough)

g) at 1.0 PV

h) at 1.472 PV

Figure 3.1.2.2 The evolution of moving front with time for water displacing water. (Figure 3.1.2.1 continued)

3.1.2.1 Measurement of permeability of the cell

In order to determine the permeability of the sand pack, the pressure drop across the cell was measured at four different flow rates of water injected at the bottom of the cell. Using the the density and viscosity of water at 21°C, the sand grain diameter $D_p=5x10^{-4}$ m and the porosity of the sand pack ϕ = 0.35 (see data from Table 3.1.1), an average value of the experimental permeability of the sand pack of $1.66x10^{-10}$ was obtained, as seen in Table 3.1.2.1.

Table 3.1.2.1 Pressure drop across the cell versus flow rate of the injected water

F.R., cm^3/h	ΔP, N/m^2	$k_{exp.}$ m^2
115	$55 x10^4$	1.72E-10
169	$85 x10^4$	1.64E-10
236	$120 x10^4$	1.62E-10
290	$145 x10^4$	1.65E-10
		1.66E-10

The value k_{Koz} = 3.52E-10 obtained for permeability of the sand pack using Kozeny's equation (eqn. 2.1.3.2, page 13), is in relatively good agreement with the experimental value of average permeability $k_{exp.}$, given in the Table 3.1.2.1. Its calculation was based on Darcy's equation.

The relative permeabilities ratio versus water saturation was ploted using the Welge technique described in the literature (Collins (1961), Marle (1981)). Using data from the displacement of neutral oil by distilled water, at 200 cm^3/h flow rate and the equations:

$$S(h) = S_{1r} + \frac{Q_o}{Ah\phi} - \frac{Q_w}{Ah\phi}\left(\frac{dQ_o}{dQ_w}\right) \qquad (3.1.2.1)$$

and

$$\frac{k_w}{k_o} = \frac{\mu_w}{\mu_o}\left(\frac{dQ_i}{dQ_w} - 1\right) \qquad (3.1.2.2)$$

where:

S(h) is the water saturation along the height of the cell (h)

S_{1r} is the connate water saturation

S_{2r} is the residual oil saturation

Q_o , Q_w , Q_i are the flow rates of produced oil, produced water and injected water respectively

$Ah\phi$ = PV pore volumes of water injected up to time t

k_w, k_o, μ_w, μ_o are the relative permeabilities of water, oil, and the viscosities of water and oil, respectively

The figure 3.1.2.1 shows the plot for the values of S_{1r} = 0.12, and S_{2r} = 0.08 that have kept constant throughout the experiments and determined by mass balance.

Using equations 3.1.2.2 and 2.3.2.6, the mobility ratio M can also be calculated. The M values vary from 0.1 at the inlet to 2.5 to the outlet of the cell.

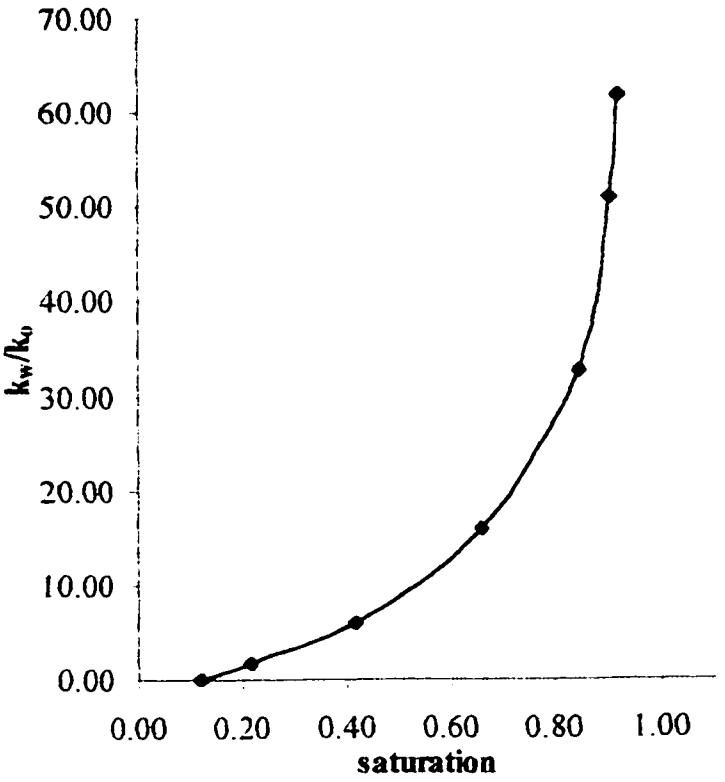

Figure 3.1.2.3 The relative permeabilities ratio versus water saturation

3.2 Experimental procedure

The experimental procedure used in all the experiments is as follows:

1. the cell, totally saturated with water (for the first experiment) or at residual oil saturation, (in the subsequent experiments), was filled with oil through the top port, while the water was allowed to exit from the cell through the bottom port.
2. at the end of the first step, the connection between the bottom of the cell and the pressure gage was established by opening the valve between them.

3. the pump, preset to the proper flow rate, was started at the same time as the stop watch.
4. the displaced oil coming out from the cell through the upper port was collected in a graduated cylinder. This has allowed the monitoring of the process (the volume of oil displaced as a function of time).
5. pictures were taken at the designated times in order to monitor the evolution of the moving front (the interface between the two liquids).
6. at the end of the experiment, the pump was kept running for a sufficient period of time to remove the remaining oil from the cell until the residual oil saturation has been reached (7-9% for all experiments). In this way every experiment could be started with the cell in the same state as far as the fluid saturations are concerned.

The time required to perform a displacement run was between six hours, for low flow rates - under 100 cm^3/h - and two hours for the upper limit of the range of flow rates - about 400 cm^3/h . Referring to the whole time, including the cell preparation for the particular run, the value is considerably larger - 6 to 12 hours - even more for the case of alkaline displacements.

The range of flow rates at which the displacement experiments were performed was chosen according to the results of previous work performed in this laboratory (Chen, 1992), as well as our preliminary experiments. Flow rates lower than 100 cm^3/h led to extended periods of time required to perform the displacements without showing a significant increase of breakthrough. The upper limit of the flow rates range was imposed by the characteristics of the cell employed to perform the displacements. Because the displacements were performed using an unconsolidated porous medium on one hand, and due to the geometry of the cell on the other hand, when flow rates higher than 400 cm^3/h were employed, the occurrence of cracks

within the sand pack - due the lifting of the grains by the moving front of water and/or oil - was frequent, causing the creation of channels inside the sand pack. The channels, once formed, led to preferential paths for the moving fluids, which, in turn, caused a drastic decrease of the breakthrough recovery.

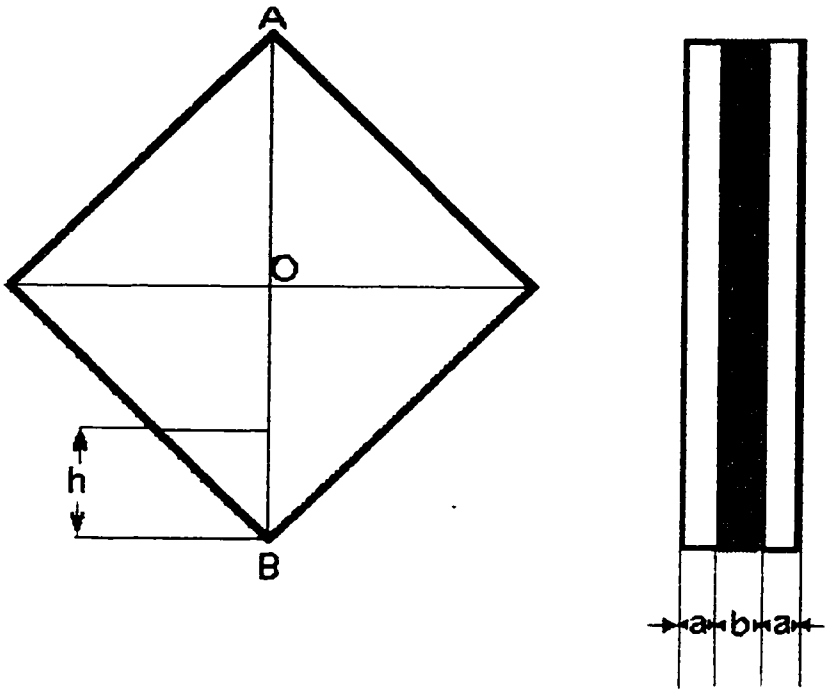

i) ii)

Figure 3.2.1 The schematic of the cell: i: frontal view; ii: cross-sectional cutoff
AB - height of the cell; h - instantaneous height of moving front;
a - glass plate thickness; b - sand pack thickness;

Due to the particular geometry of the cell, it was expected that the velocity of fluid flow along the axis of the cell would not be constant. Likewise, the Reynolds number would not be constant. In order to have a reasonable characterization of the cell, as far as the flow regime is concerned, the variation of the cross-sectional area of the cell and the Reynolds number for the displacement of neutral oil by distilled water at a flow rate of 240 cm^3/h, were plotted in figure 3.2.2 versus the height of the cell.

The instantaneous liniar fluid velocity was calculated with the formulas:

$$V_{BO} = \frac{F.R.}{2bh} \tag{3.2.1}$$

$$V_{OA} = \frac{F.R}{b(y - 2h)} \tag{3.2.2}$$

for the lower half of the cell (BO) and for the upper half of the cell (OA) respectively. In these equations F.R. represents the flow rate in cm^3/h while dimensions b, h and y = AB are defined in Figure 3.2.1.

The values for Reynolds number were calculated with the equation:

$$Re = \frac{\sqrt{2} D_p \phi \rho F.R.}{3\mu by(1 - \phi)} \tag{3.2.3}$$

deduced by using the hydraulic radius equation (Lake, 1989) and the equation for the Reynolds number (2.3.4). The meaning of the terms is:

D_p - sand grain average diameter;

ϕ - porosity of the sand pack;

ρ, μ - density and viscosity of the injecting fluid (water);

all other terms having the meaning already stated above.

The cross-sectional area of the cell varies (increases linearly) between a minimum value, at the bottom of the cell, and a maximum value, at the middle of the cell. As the middle of the cell is reached (point O in Figure 3.2.1), the situation is reversed and the cross-sectional area starts decreasing in a symmetrical manner from the middle of the cell to its top (point A in Figure 3.2.1). The results of the calculations for the Reynolds number are depicted in Figure 3.2.2.

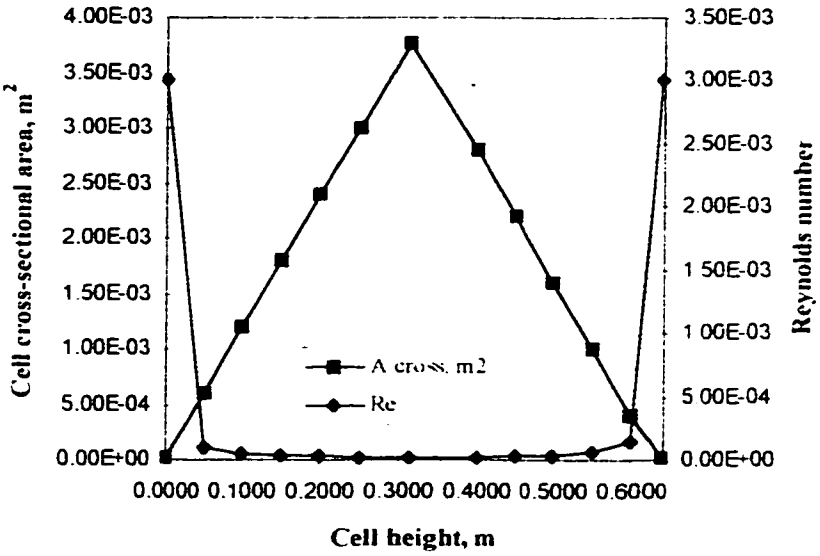

Figure 3.2.2. Variation of cross-sectional area of the cell and the Reynolds number from the bottom to the top of the cell for neutral oil displaced by distilled water, at a flow rate of 240 cm^3/h.

As it can be seen from the above picture, the Reynolds number decreases sharply as the fluid moves upward in the cell, until a height of about 10 cm is reached (above point B). After that, the variation of the Reynolds number is much less visible, practically the curve levels off at a value of it of about 10^{-5}. For the upper half of the cell the variation of the Reynolds number is reversed, the curve being symmetric with the one for the lower half of the cell. Even the maximum value of Reynolds number, at the bottom and top of the cell($\sim 10^{-3}$), is well below the range of the Reynolds numbers where the flow becomes turbulent. The flow rate used to illustrate the nature of flow in the cell (240 cm^3/h), represents a mean flow rate of the displacement experiments, performed throughout this work.

The variation of the Reynolds number, linear velocity of the injecting fluid and capillary number, versus flow rate, for some displacements of neutral oil by distilled water is illustrated in figure 3.2.3. The curve representing the recoveries at breakthrough versus flow rate is also shown to allow a better comparison. The calculations of velocities, Reynolds and capillary numbers were done using the average value for the cross-sectional area of the cell. All these three variables show a linear increase when the flow rate increases. Both Reynolds number and capillary number exhibit values in the range 10^{-4} -10^{-5}. The variation of the breakthrough recovery versus flow rate is discussed in the next chapter (4).

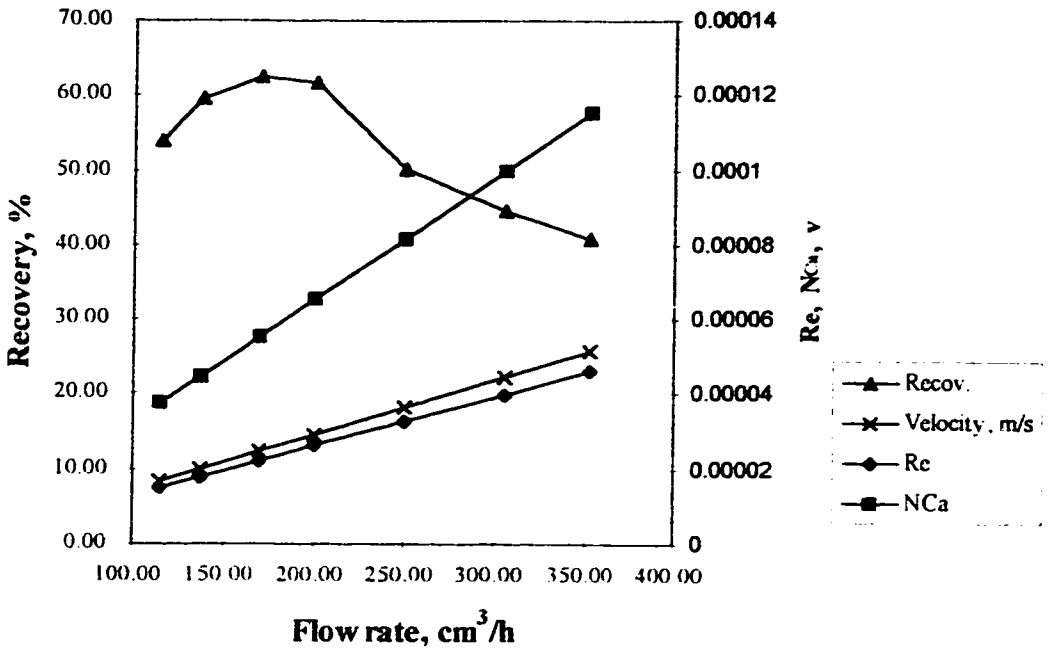

Fig 3.2.3 Breakthrough recovery, linear velocity, Reynolds and capillary numbers, versus flow rate of water in the displacements of neutral oil by water.

A similar plot, for the displacement of acidic oil by water, is shown in Figure 3.2.4. One can see that Reynolds numbers in this case are close to corresponding Reynolds numbers for the displacement of neutral oil. Capillary numbers, however, are about half of the ones calculated for the neutral oil displacements.

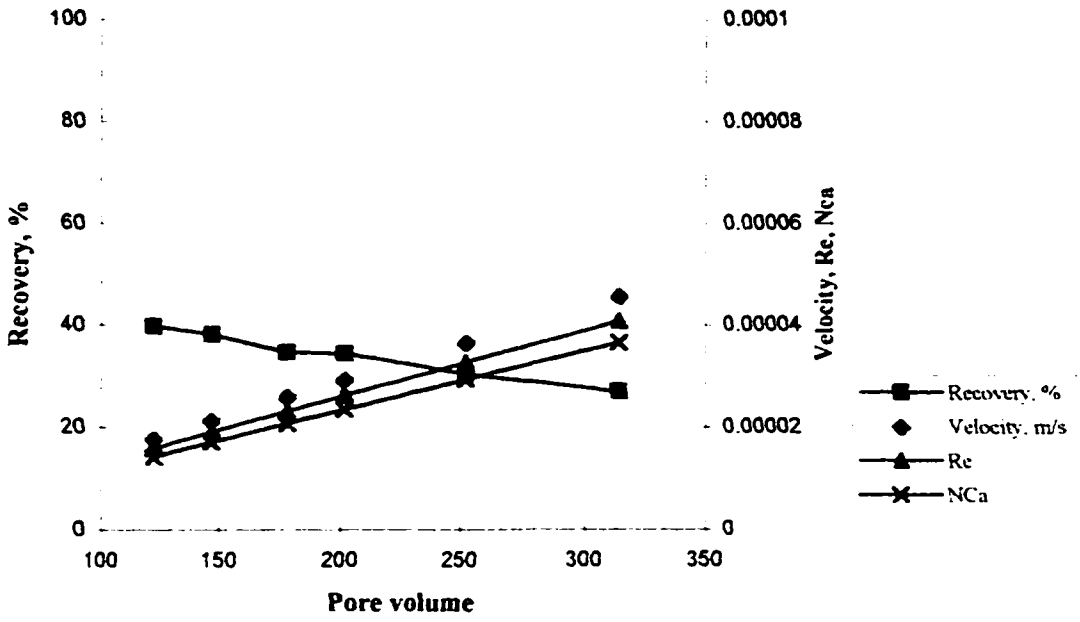

Fig 3.2.4 Breakthrough recovery, linear velocity, Reynolds and capillary numbers, versus flow rate of water in the displacements of acidic oil by water.

4. RESULTS AND DISCUSSION

The outline of the experiments was done at the beginning of the last chapter. As stated there, three sets of experiments were performed.

For all displacement experiments the recovery was calculated using the formula:

$$R = \frac{V_o}{\phi V_c} x100 \qquad (4.1)$$

where

R - recovery at time t

V_o - oil volume collected up until time t

V_c - internal cell volume

ϕ - porosity of the sand pack

4.1 Upward displacement of neutral oil by water.

The results of the displacement experiments of neutral oil by water in upward direction are shown below, in the Figures 4.1.1 through 4.1.7.

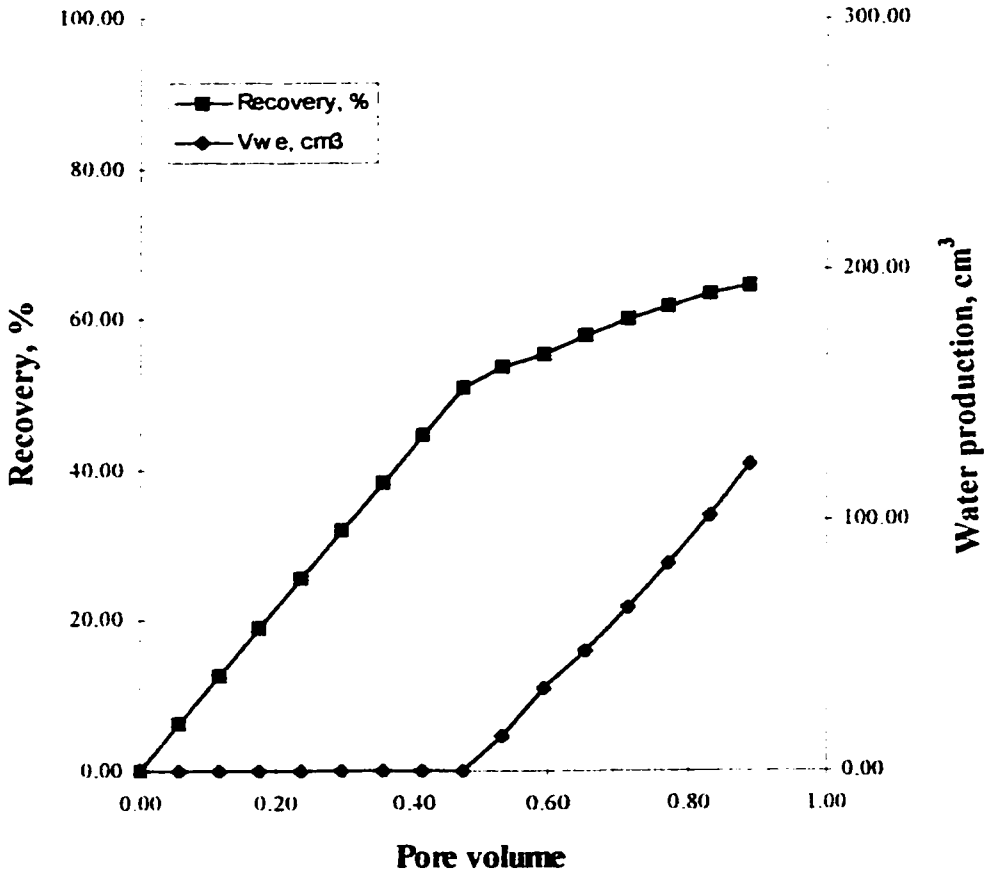

Figure 4.1.1 Upward displacement of neutral oil by distilled water at 115 cm^3/h flow rate

Figure 4.1.1 shows the plot of the oil recovery and cumulative water production versus pore volume of water at the flow rate of 115 cm^3/h. One can see that after the breakthrough (which occurred at about 0.47 pore volume injected) the recovery curve levels off relatively early.

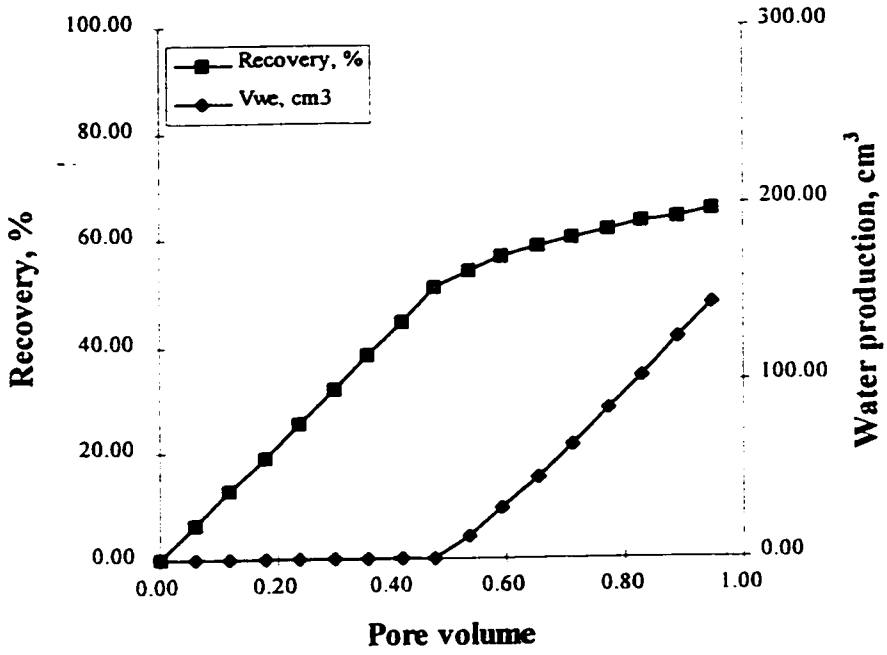

Figure 4.1.2 Upward displacement of neutral oil by distilled water at 136 cm^3/h flow rate

Figure 4.1.2 shows the plot of the recovery and the volume of water collected after breakthrough versus pore volume of water injected, in the case of the 136 cm^3/h flow rate. In this run the breakthrough occurred at about 0.5 pore volume injected, close to the corresponding value of the previous displacement. The breakthrough recovery was slightly larger (51%) than in the previous case (49%).

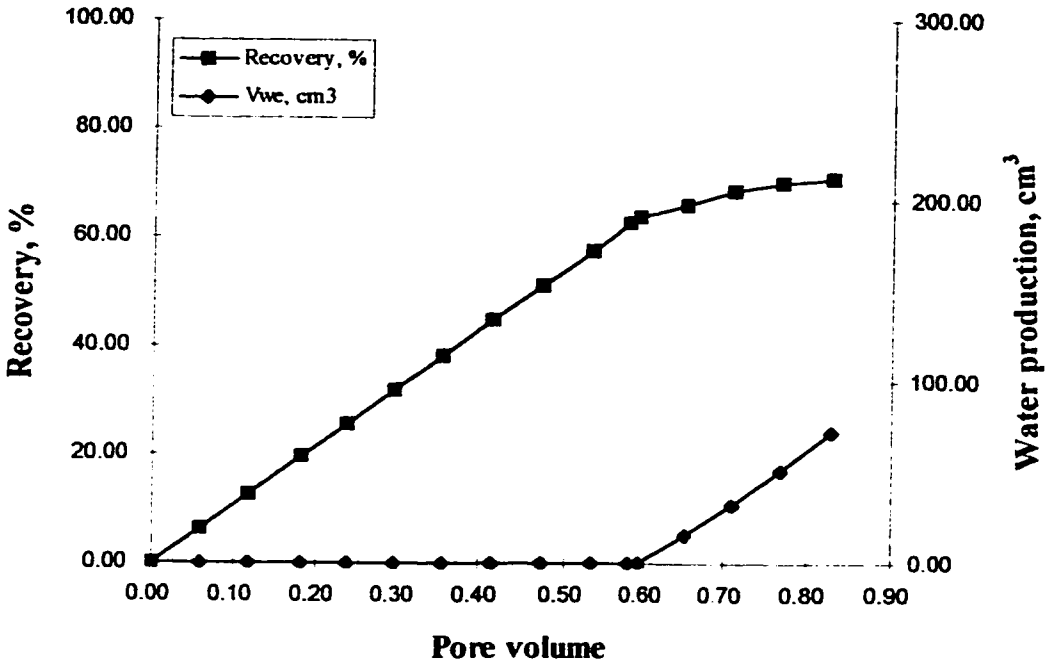

Figure 4.1.3 Upward displacement of neutral oil by distilled water at 169 cm^3/h flow rate

Figure 4.1.3 shows the plot of the recovery and the volume of water collected after breakthrough in the case of the 169 cm^3/h flow rate. In this displacement the greatest breakthrough recovery was achieved (62%).

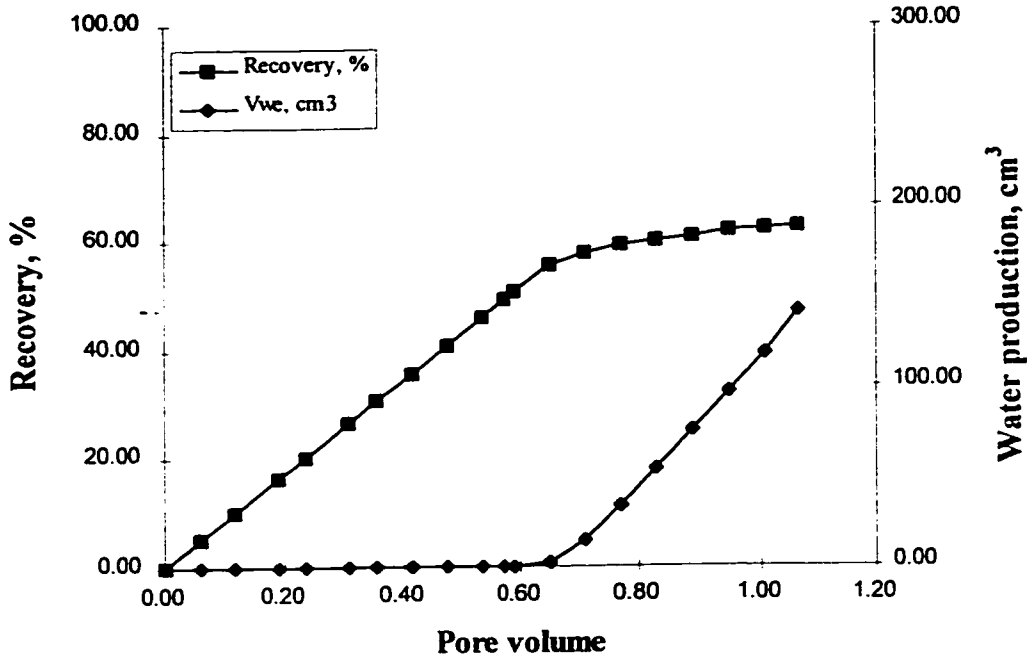

Figure 4.1.4 Upward displacement of neutral oil by distilled water at 200 cm^3/h flow rate

Figure 4.1.4 shows the evolution of the recovery and the volume of water collected after breakthrough in the case of the 200 cm^3/h flow rate. In this run the breakthrough occurred at about 0.6 pore volume injected. One can see that the breakthrough recovery is lower (52%) than that in the previous case, at the flow rate of 169 cm^3/h.

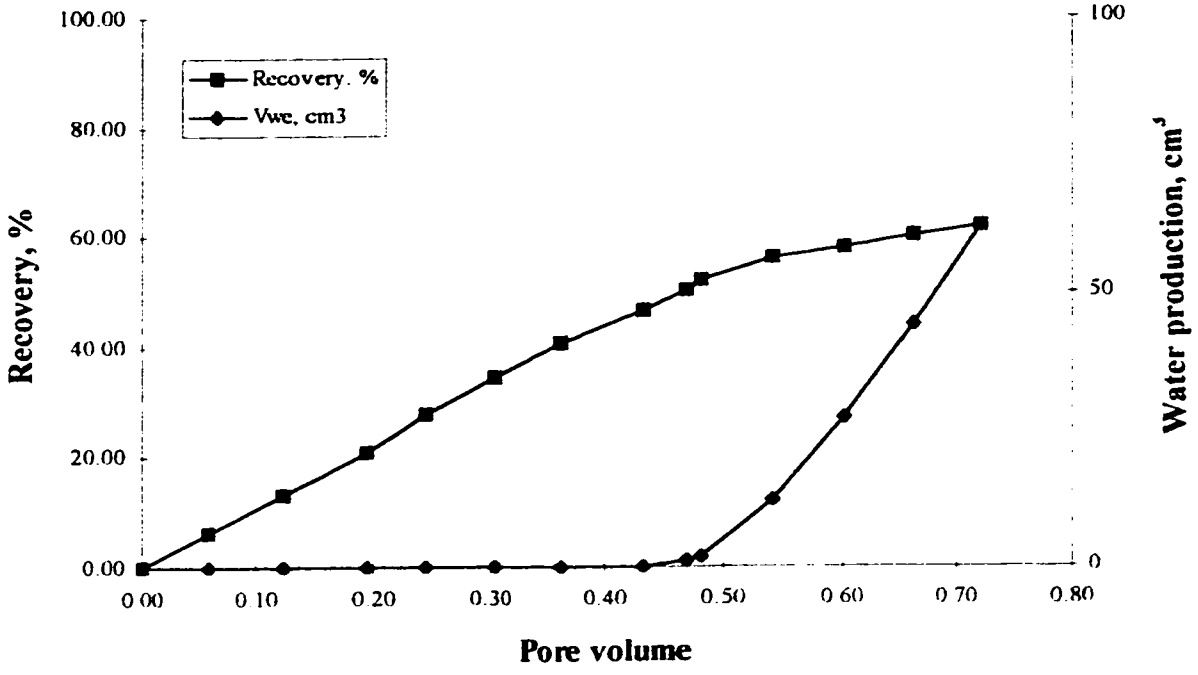

Figure 4.1.5 Upward displacement of neutral oil by distilled water at 250 cm^3/h flow rate

The results of the displacement at the flow rate of 250 cm^3/h depicted in figure 4.1.5. show that both the breakthrough recovery (50%) and the pore volume at breakthrough became smaller than for the displacement at 200 cm^3/h.

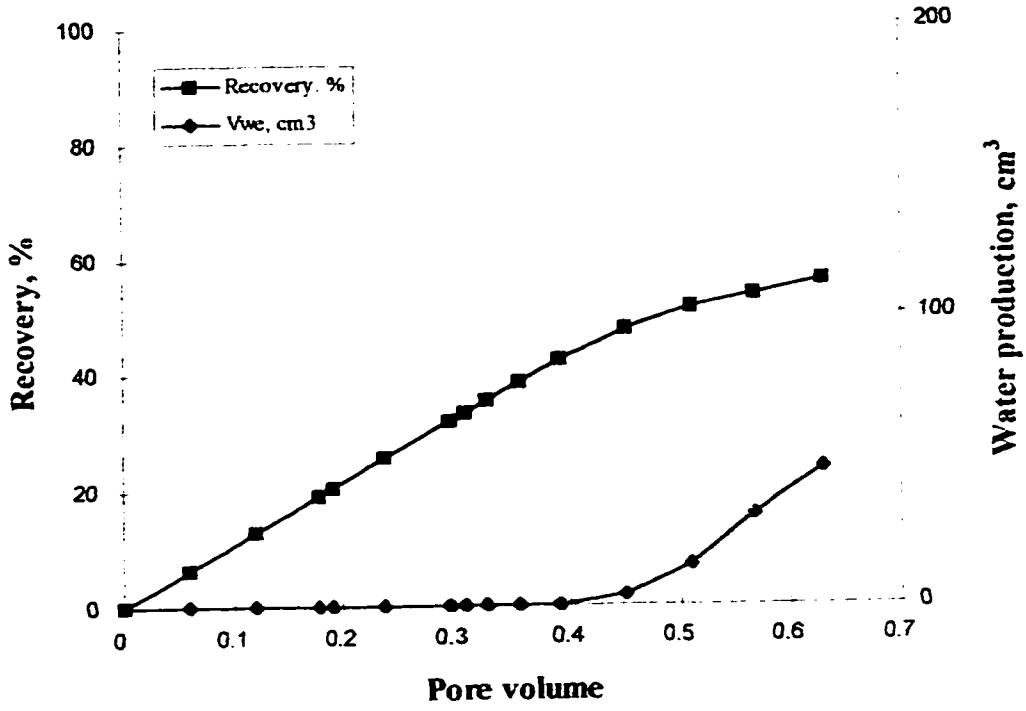

Figure 4.1.6 Upward displacement of neutral oil by distilled water at 300 cm^3/h flow rate.

The breakthrough recovery and pore volume injected at breakthrough, continue to decrease (43%) for this displacement at the flow rate at 300 cm^3/h.

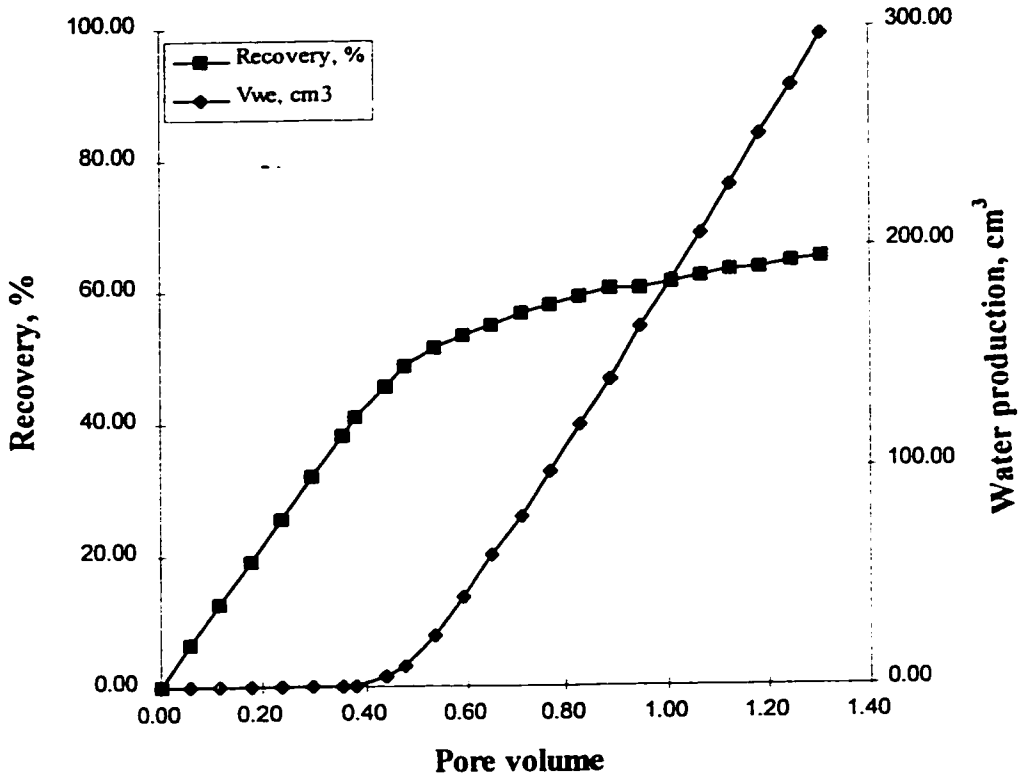

Figure 4.1.7 Upward displacement of neutral oil by distilled water at 353 cm^3/h flow rate.

The last experiment (4.1.7) of this first set was run at the flow rate of 353 cm^3/h. The breakthrough recovery is the lowest (41%) of all in this set.

4.2. Downward displacement of neutral oil by water.

In this section, the results of the displacement of neutral oil by water in downward direction are presented. For these experiments, the injection and collector ports were reversed.

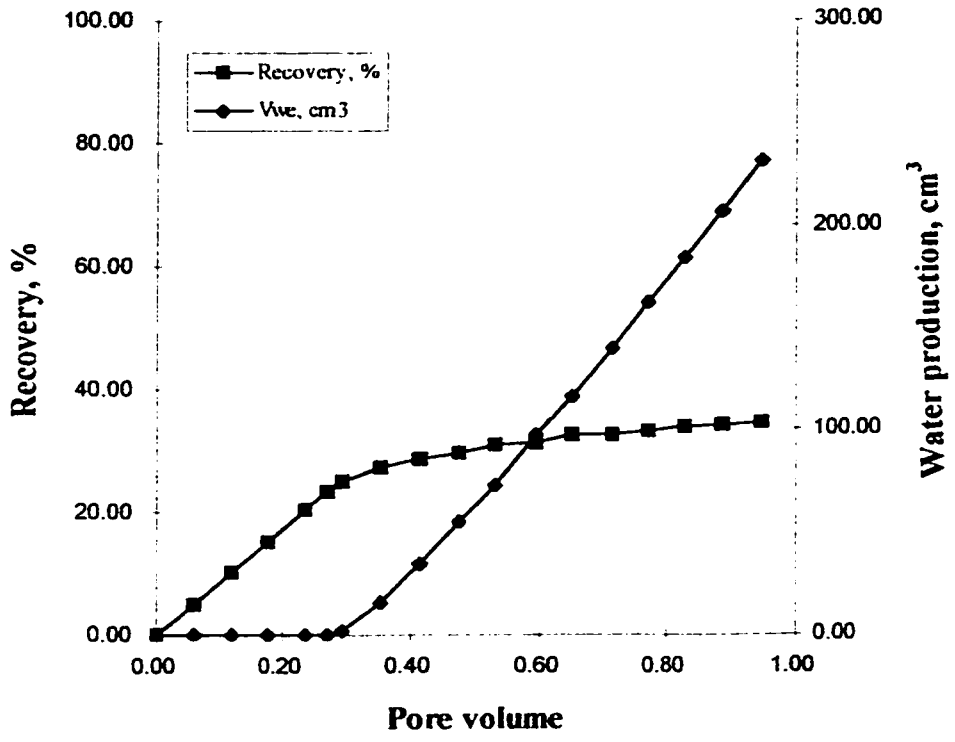

Figure 4.2.1 Downward displacement of neutral oil by distilled water at 115 cm^3/h flow rate.

One remarks the much smaller value for breakthrough recovery (28%) than in the case of upward displacement at the same flow rate (4.1.1).

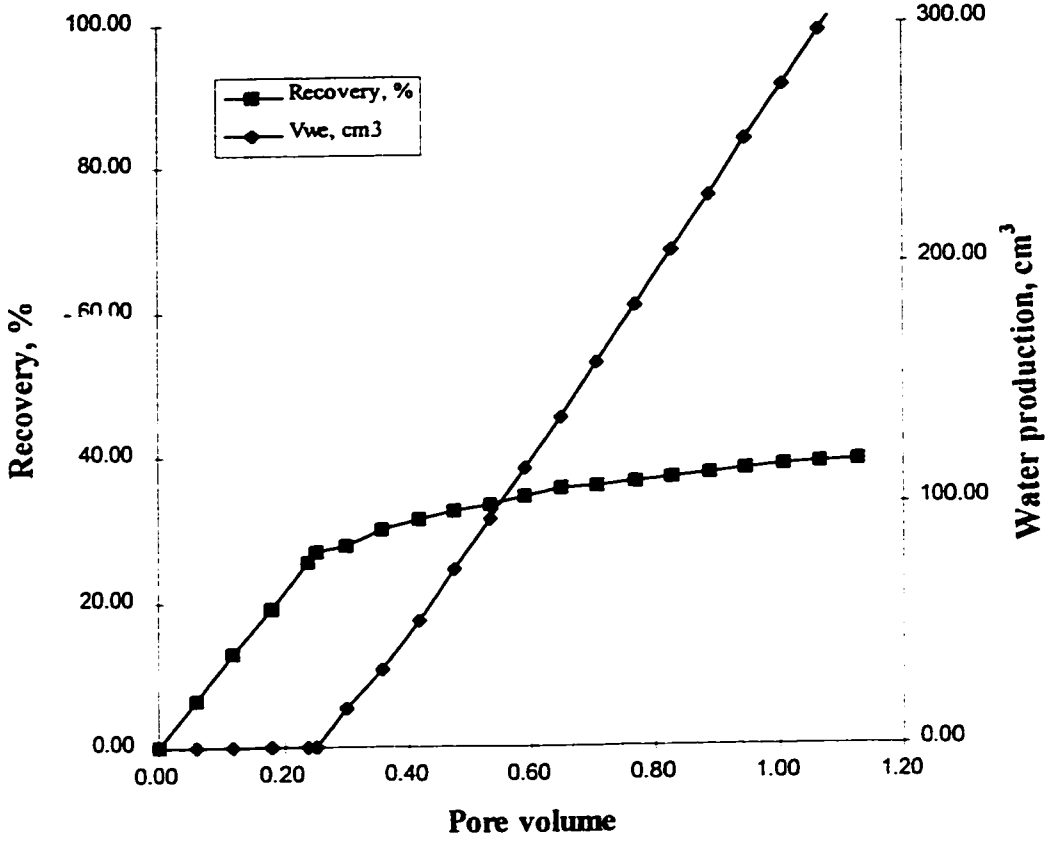

Figure 4.2.2 Downward displacement of neutral oil by distilled water at 151 cm^3/h flow rate.

The breakthrough recovery decreases as the flow rate increases (26%) (compared to previous displacement).

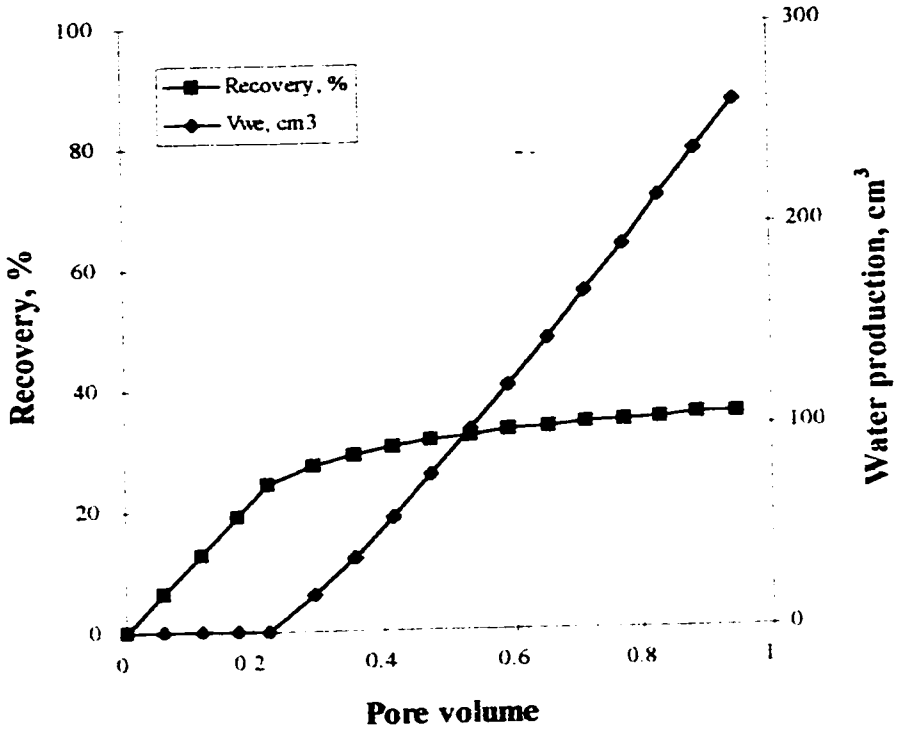

Figure 4.2.3 Downward displacement of neutral oil by distilled water at 200 cm^3/h flow rate.

The trend - decrease of breakthrough recovery - is the same in this displacement experiment.(breakthrough recovery ~ 24%).

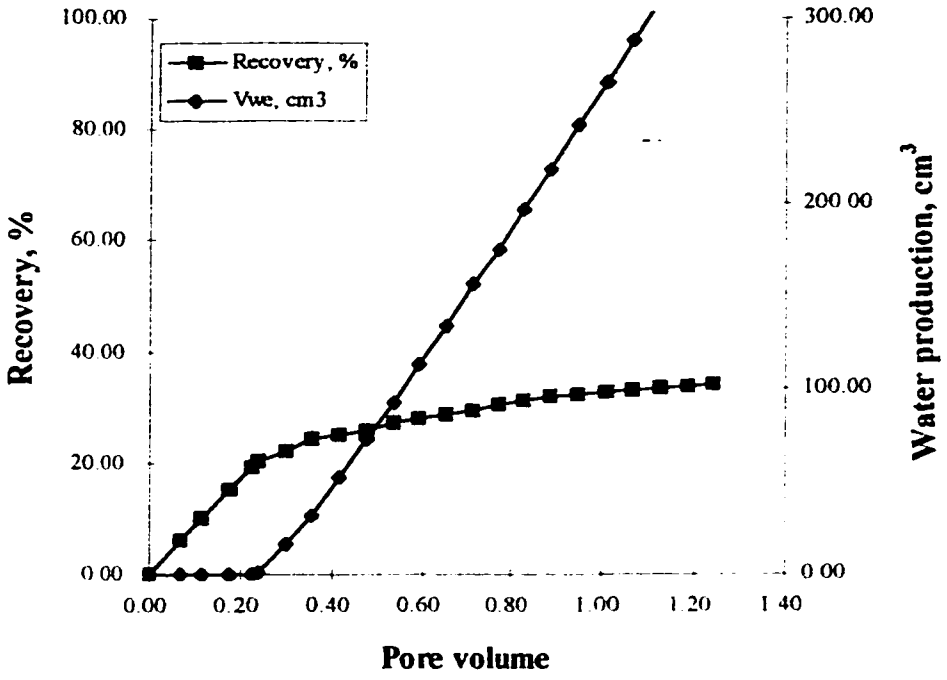

Figure 4.2.4 Downward displacement of neutral oil by distilled water at 301 cm^3/h flow rate.

This is the last experiment from the set of downward displacements of neutral oil by water, featuring the smallest recovery of all experiments so far.

The range of flow rates employed in the displacements covered both the domain where capillary forces dominate (low flow rates) and the domain where viscous forces dominate (high flow rates). The variation of breakthrough recovery versus flow rate for upward neutral oil displacements summarized in Figure 4.2.5 below, is consistent with other workers' findings , for instance Flock et al (1977).

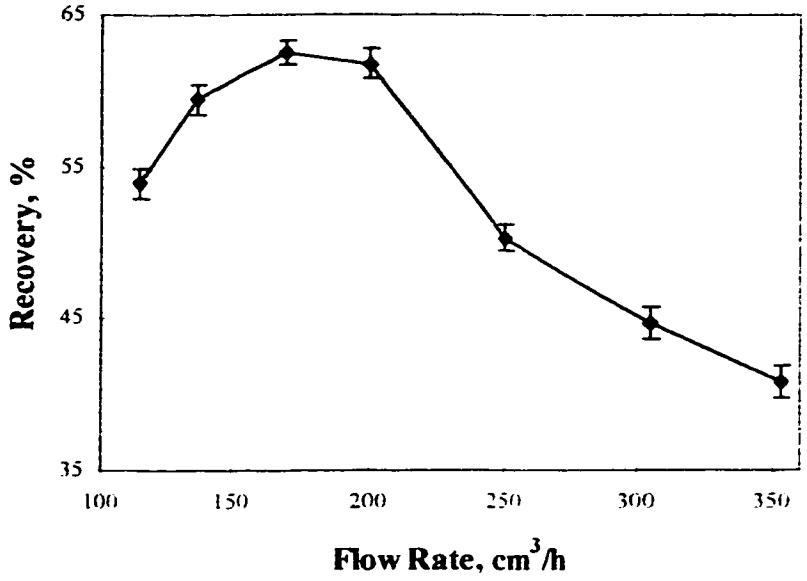

Figure 4.2.5 Breakthrough recovery versus flow rate for upward displacements of neutral oil by distilled water.

What differentiates the process of upward displacement of neutral oil is the fact that it is the only one featuring a variation of breakthrough recovery versus flow rate that displays a maximum value, as seen in figure 4.2.5. This behavior can be explained by the dominating effect of capillary forces in the domain of small flow rates. Capillary forces play a stabilizing role on the interface between the two immiscible fluids. As flow rate increases, the viscous forces become predominant, and the instabilities (viscous fingers) occur. Thus, for this case of the cell with the sand pack having the characteristics shown in table 3.1.1, the capillary, viscous and transitional domains could be observed over the range of flow rates employed in the displacements. Figure 4.2.5 features error bars that indicate a margin of error in the range

of 1-3%, when the two – four replicates of the experiments are taken into account. This fact shows o good reproducibility of the experiments.

Figure 4.2.6 summarizes the results obtained for the downward displacements of neutral oil by pure water. One observes that it lacks the characteristics of the previous set of displacements, namely a curve featuring a maximum. In this case the general tendency is a continuous decrease of breakthrough recovery with the increase of the flow rate. Moreover the values for the breakthrough recoveries are much smaller than in the case of upward displacements.

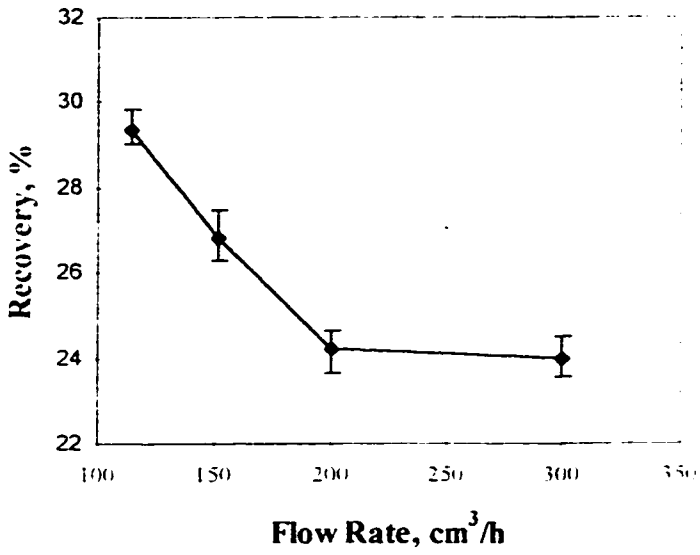

Figure 4.2.6 Breakthrough recovery versus flow rate for downward displacements of neutral oil by distilled water.

As in the previous case, the error bars show good reproducibility of the experiments, in the same range as the one for upward displacements.

Some of the pictures taken with the camera during the upward displacements, are presented in figures 4.2.7 through 4.2.10. One remarks that the moving interface between the two immiscible fluids is rather diffuse, the instabilities (fingers) are hard to define. Even for the displacement that gave the highest breakthrough recovery, - namely at the flow rate of 169 cm^3/h - one observes the increase of flooded area (yellowish in the pictures), but the breakthrough is hard to tell from the picture 4.2.7.d. Only the appearance of water in the collected oil signals with accuracy the occurrence of the breakthrough. The swept area is even more difficult to observe in the next sets of photographs, presented in figures 4.2.8 - 4.2.10 for the displacements at the flow rates of 200 cm^3/h , 300 cm^3/h, and 353 cm^3/h, respectively. This behavior may be caused by the fact that silica sand used as porous medium is highly water wet. Because of that, the capillary forces push the water into small channels causing an increase in water velocity in the areas with a higher permeability. However, low values of linear velocity with which the fluids move in the cell, associated with gravity effects do not allow these small instabilities to develop. As a result the fingers are small, not well defined.

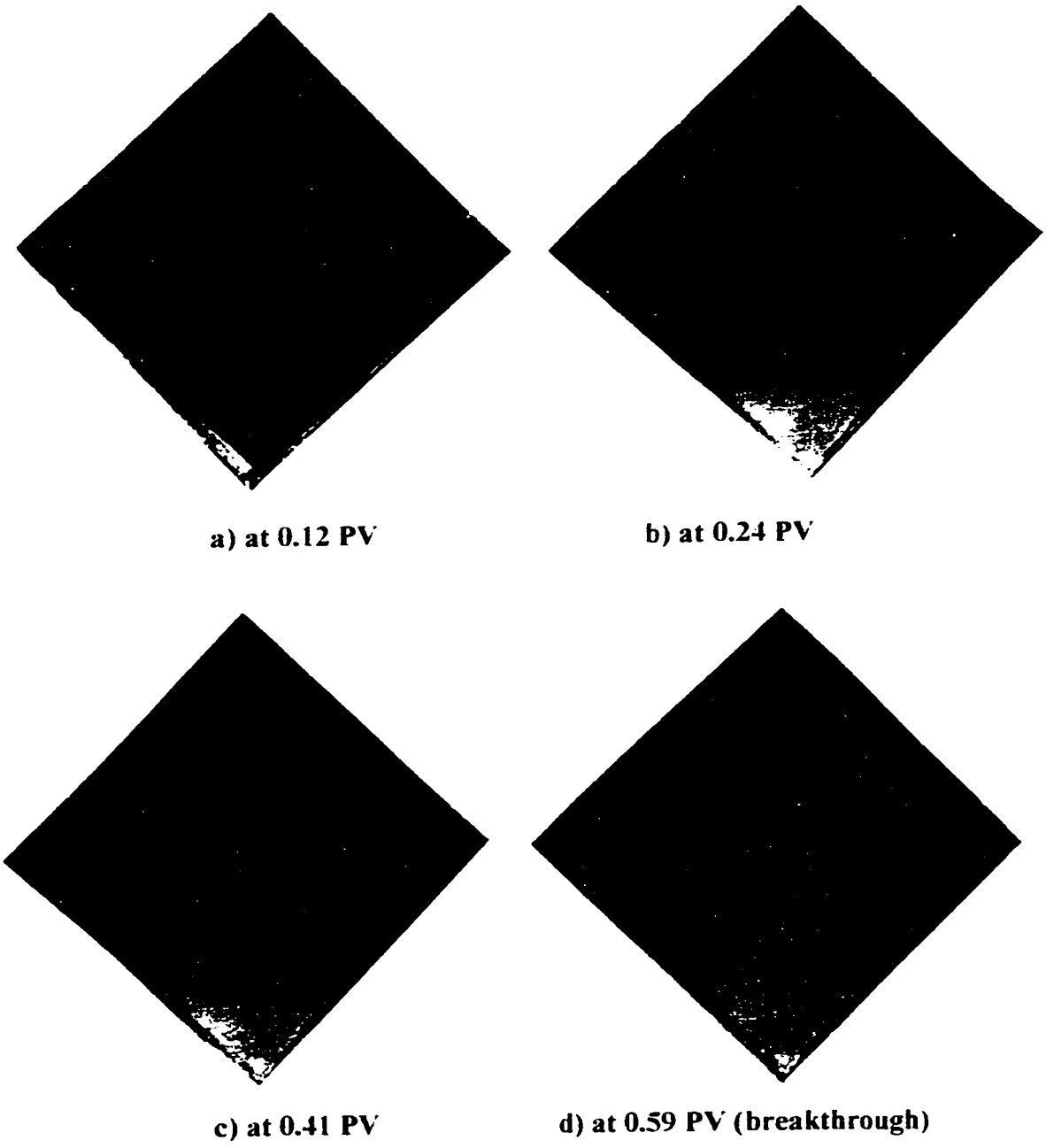

a) at 0.12 PV **b) at 0.24 PV**

c) at 0.41 PV **d) at 0.59 PV (breakthrough)**

Fig 4.2.7 Upward displacement of the neutral oil by distilled water at 169 cm^3/h flow rate.

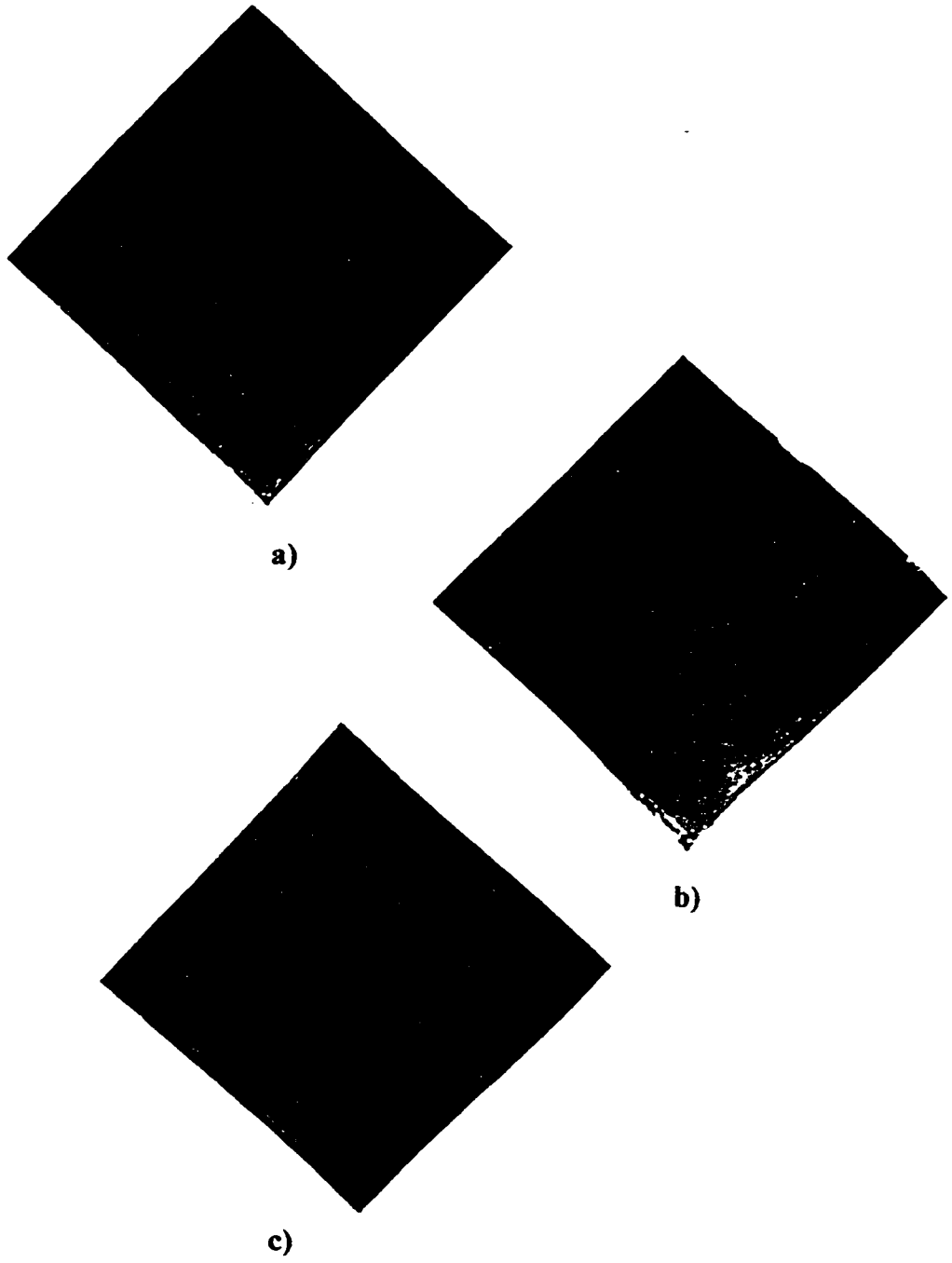

Figure 4.2.8 Upward displacement of neutral oil by water at 200 cm^3/h flow rate

a) at 0.24 PV; b) at 0.47 PV; c) at 59 PV (breakthrough)

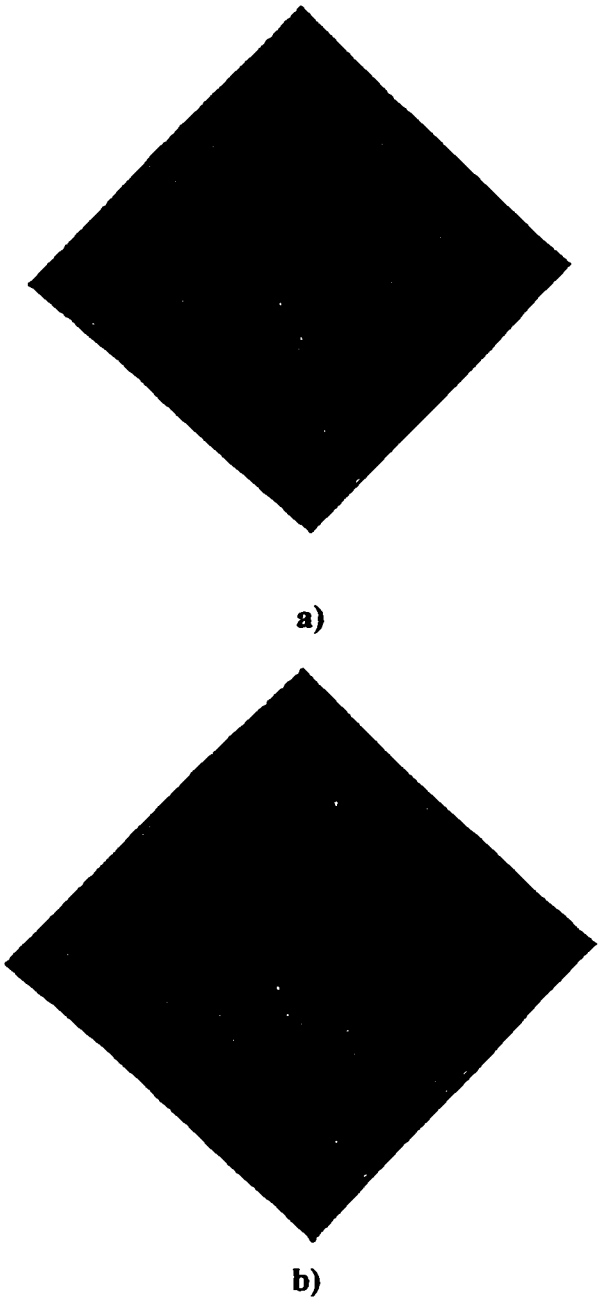

Figure 4.2.9 Upward displacement of neutral oil by distilled water at 300 cm^3/h flow rate: a) at 0.19 PV; b) at 0.39 PV (breakthrough).

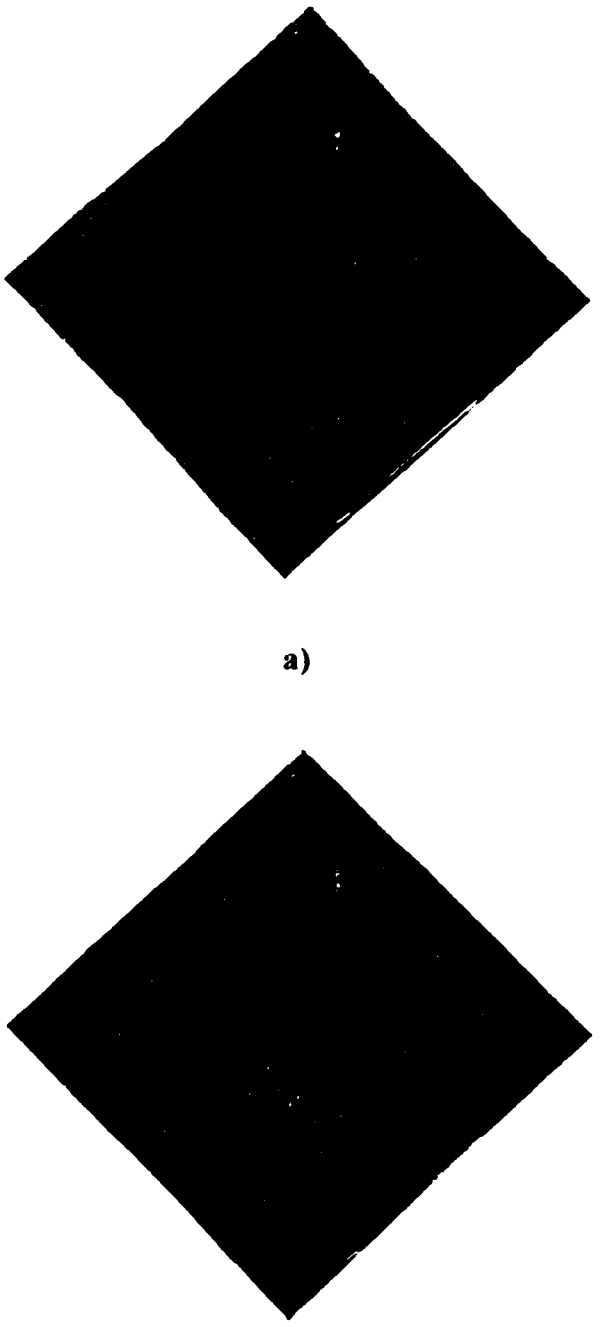

Figure 4.2.10 Upward displacement of neutral oil by water at 353 cm^3/h flow rate a) at 0.18 PV; b) at 0.38 PV.

4.3 Upward displacement of acidic oil by water.

The next set of experiments consisted of displacements of acidic oil by distilled water, in an upwards direction. In this set of experiments displacements have been carried out using a solution of 10mM of linoleic acid in paraffin oil (see table 3.1.1).

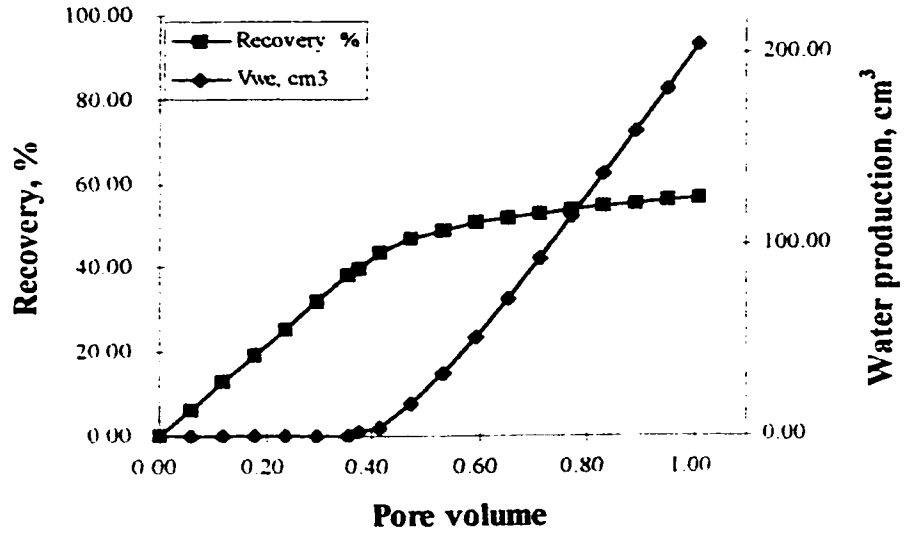

Figure 4.3.1 Upward displacements of acidic oil by distilled water at 122 cm^3/h flow rate.

The first displacement of acidic oil by water produced a breakthrough recovery of about 39%, lower for the corresponding recovery in the case of neutral oil displacement.

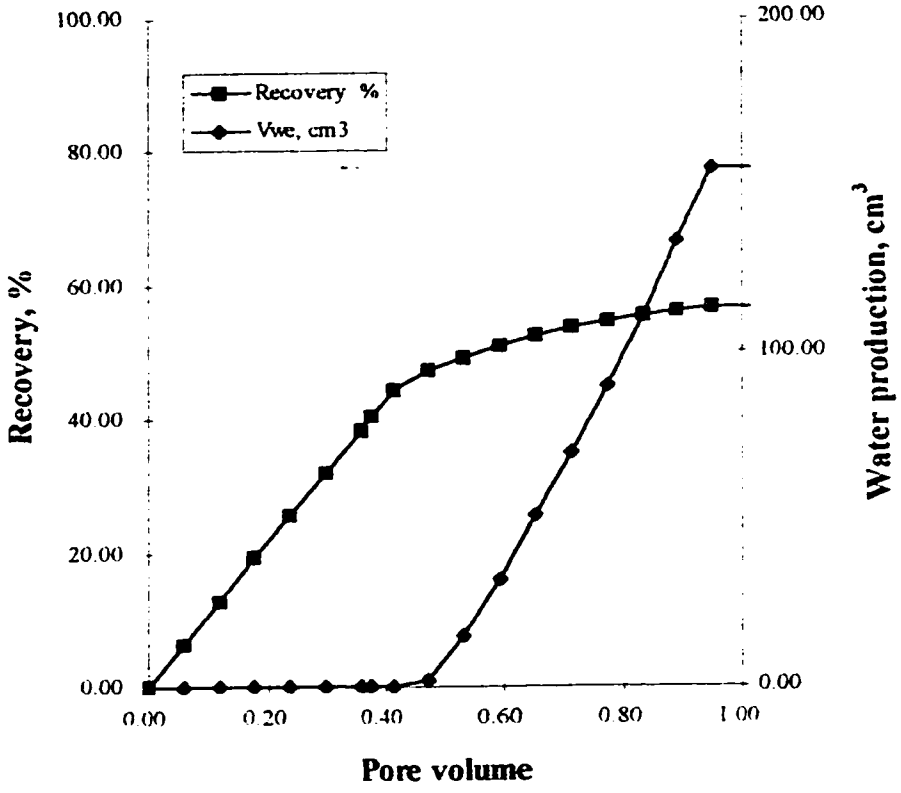

Figure 4.3.2 Upward displacements of acidic oil by distilled water at 147 cm^3/h flow rate.

The breakthrough recovery was about 38% for this displacement, showing the same trend, i.e. the decrease of breakthrough recovery with the increase of flow rate.

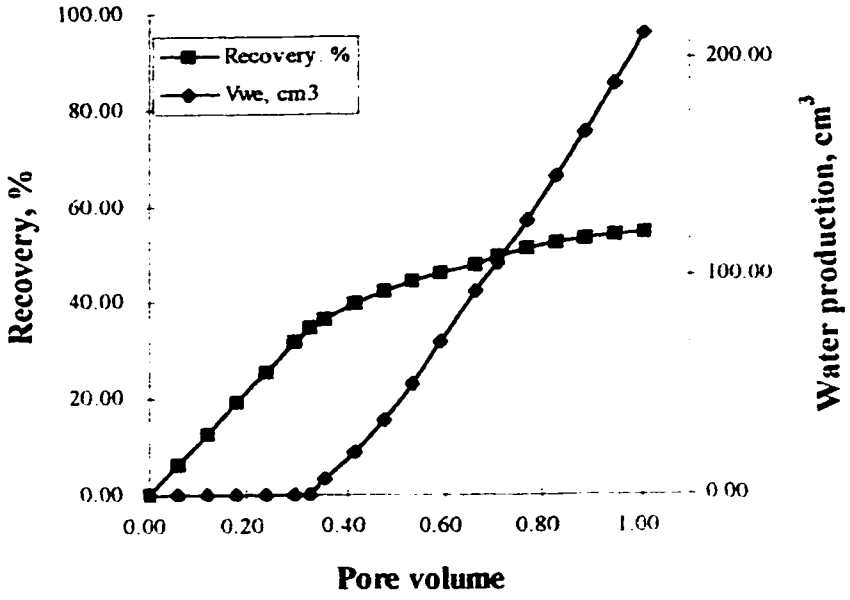

Figure 4.3.3 Upward displacements of acidic oil by distilled water at 178 cm^3/h flow rate.

The displacement **at** 178 cm^3/h flow rate gave a breakthrough recovery of 34.5 %.

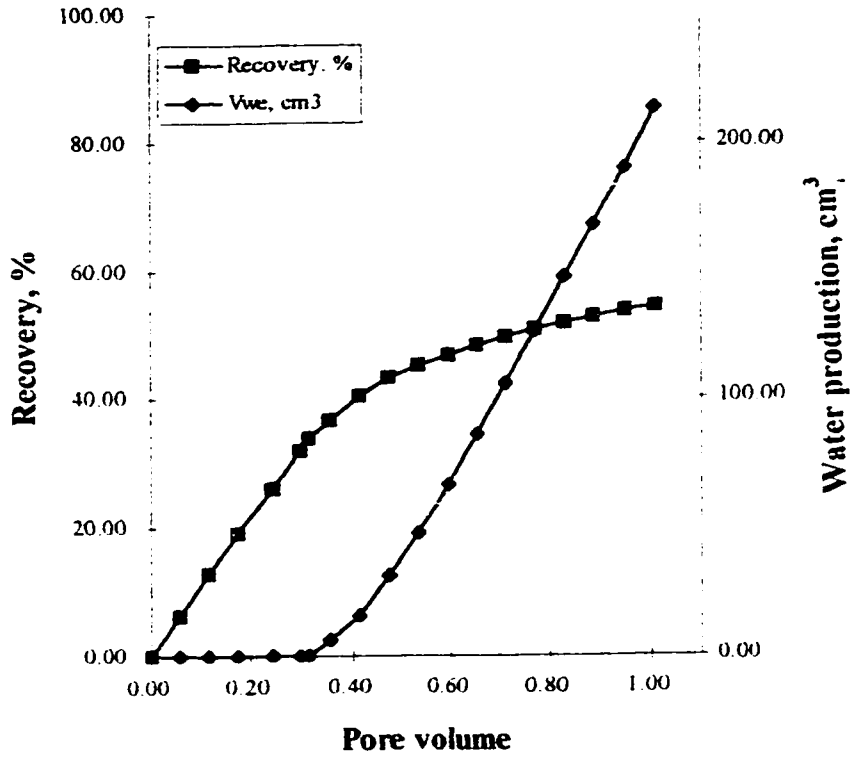

Figure 4.3.4 Upward displacements of acidic oil by distilled water at 201 cm^3/h flow rate.

This displacement produced a breakthrough recovery of 34%.

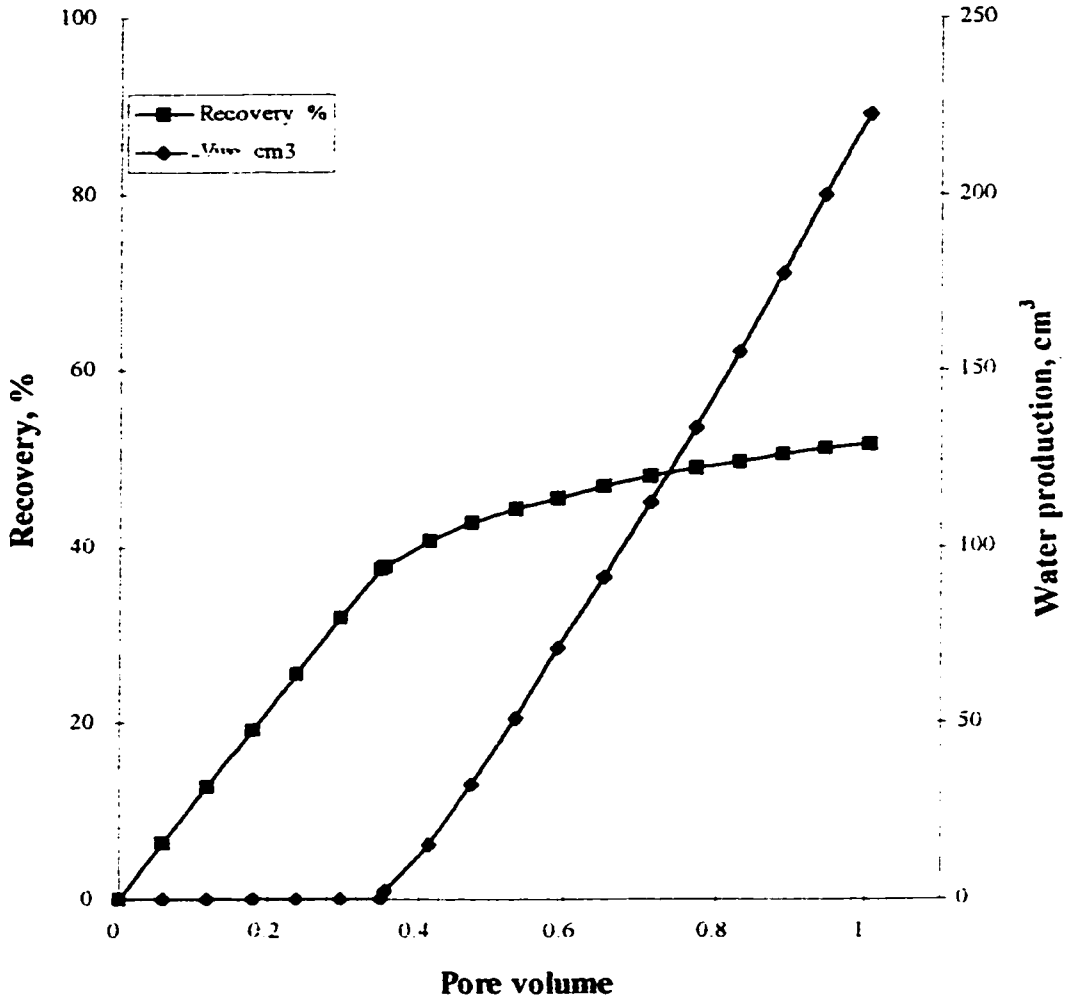

Figure 4.3.5 Upward displacements of acidic oil by distilled water at 252 cm^3/h flow rate.

The breakthrough recovery was 30% in this case.

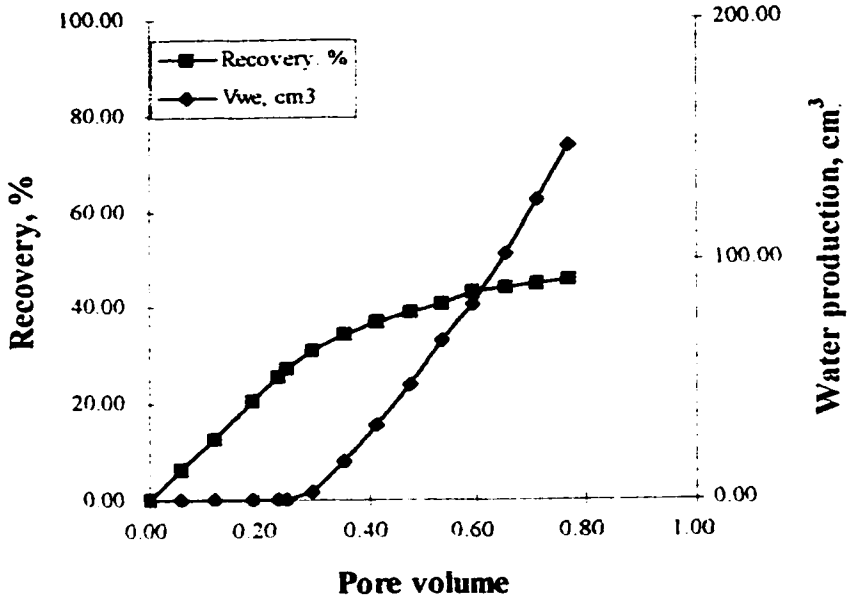

Figure 4.3.6 Upward displacements of acidic oil by distilled water at 300 cm^3/h flow rate.

The breakthrough recovery for the last displacement of this set was 27%.

4.4 Downward displacement of acidic oil by water.

The results of the downward displacements are presented in the following figures. These displacements showed the smallest breakthrough recoveries from all the displacements that were carried out throughout this work.

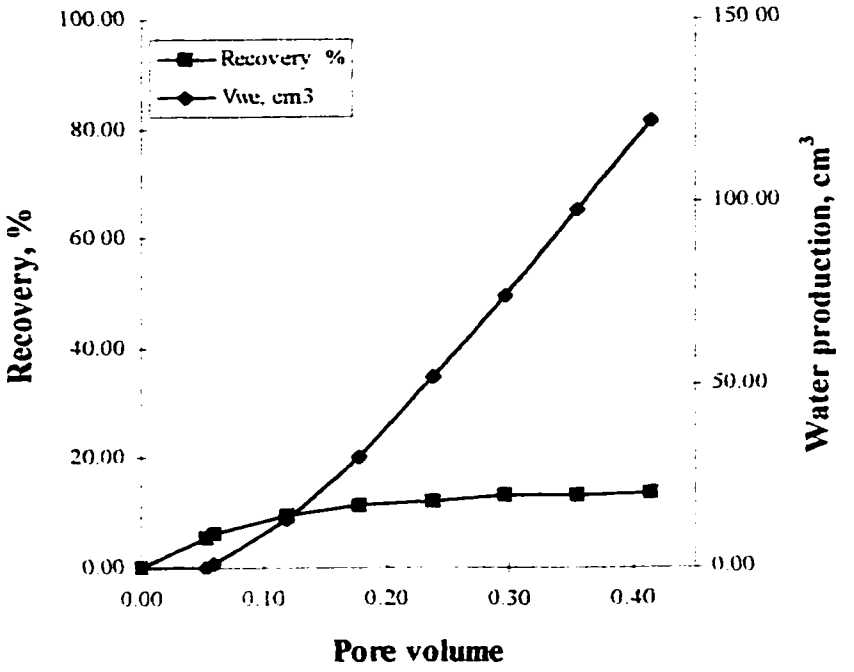

Figure 4.4.1 Downward displacements of acidic oil by distilled water at 113 cm^3/h flow rate.

A breakthrough recovery of 15% was obtained for this first displacement of the acidic oil in downward direction.

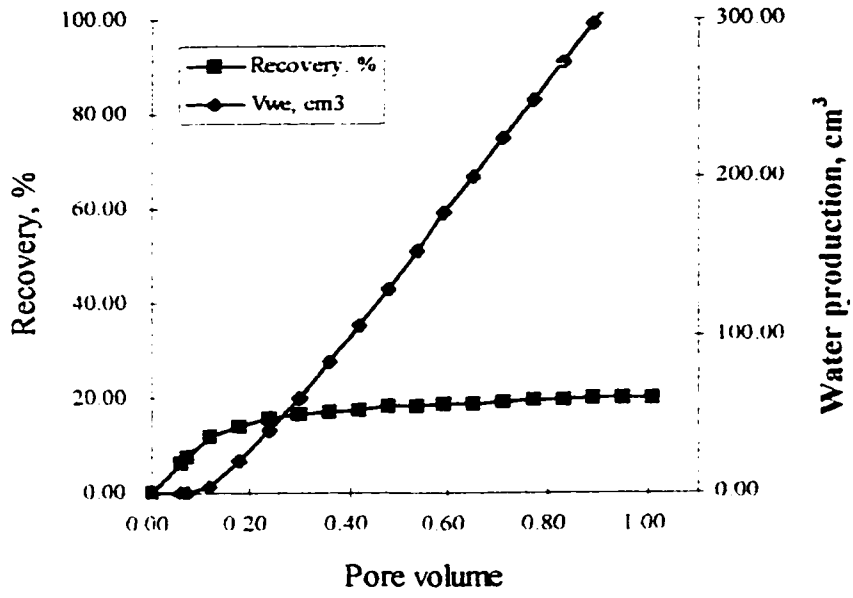

Figure 4.4.2 Downward displacements of acidic oil by distilled water at 197 cm^3/h flow rate.

This displacement gave a breakthrough recovery of 7.5%, very small compared to previous displacements.

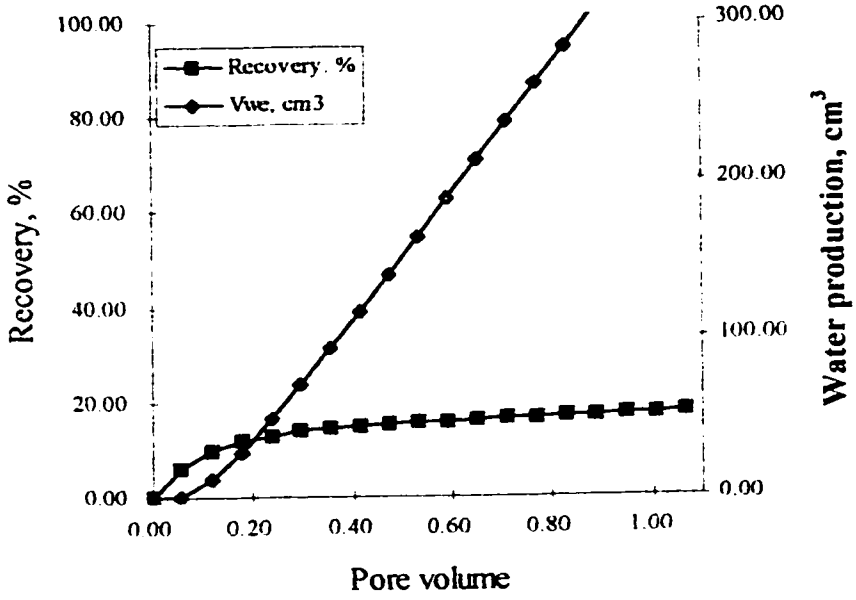

Figure 4.4.3 Downward displacements of acidic oil by distilled water at 248 cm^3/h flow rate.

The obtained breakthrough recovery was the smallest of all – about 6%.

The relationship between breakthrough recovery and flow rate for the upward displacements of acidic oil can be seen in figure 4.4.4 and the similar plot for downward displacements is shown in figure 4.4.5.

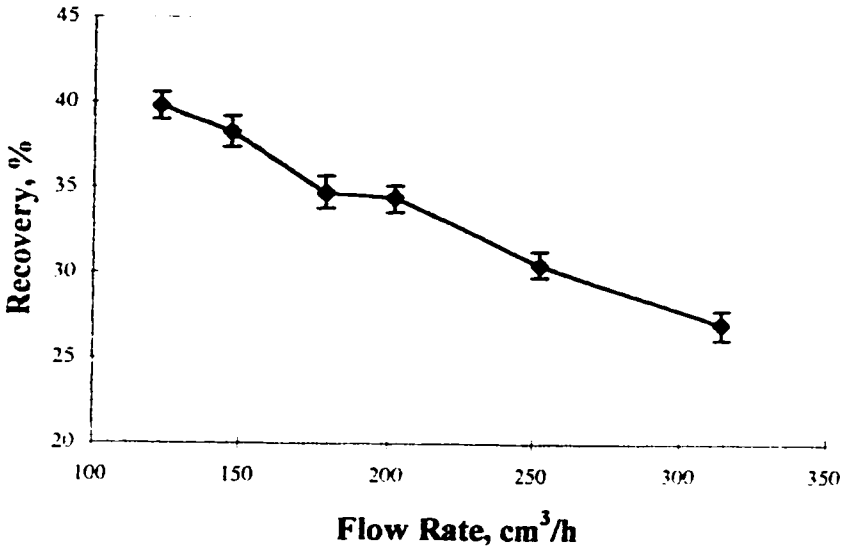

Figure 4.4.4 Breakthrough recovery versus flow rate the for upward displacements of acidic oil.

From the figure 4.4.4, one observes that, unlike the neutral oil displacements, which exhibited a maximum value curve, in the case of acidic oil displacements, the trend is a continuous decrease of breakthrough recovery with the increase of flow rate. The same holds true for downward displacements of acidic oil.

Like the displacements of neutral oil the figures 4.4.4 and 4.4.5 show the error bars associated with the replicated experiments.

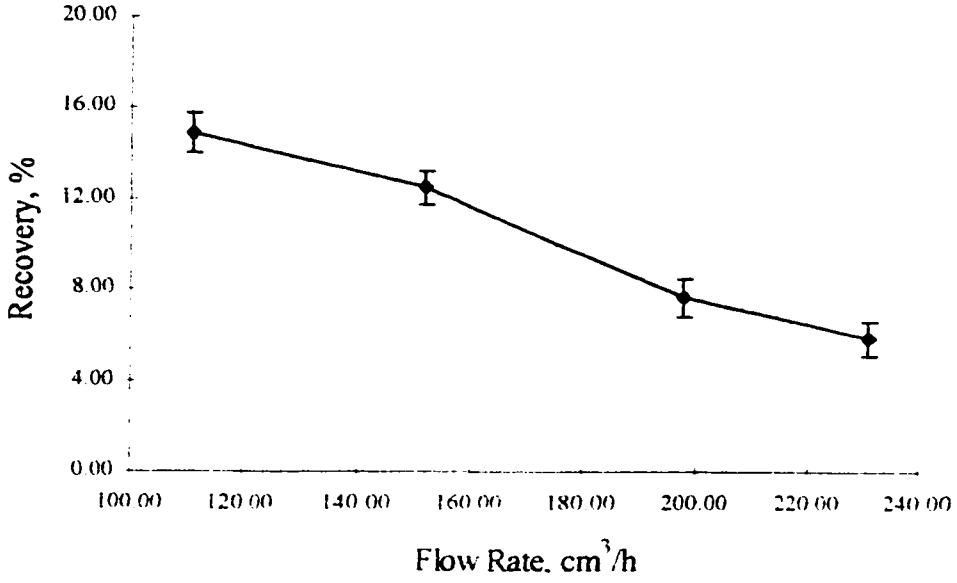

Figure 4.4.5 Breakthrough recovery versus flow rate the for downward displacements of acidic oil by distilled water.

Figures 4.4.6 and 4.4.8 show the photographs taken at 0.15 PV, and at breakthrough for the upward displacements run at the following flow rates: 122, 144, and 178 cm^3/h, respectively. The contour of the interface between the two fluids is a little more precise than in the case of neutral oil displacements, still the fingers do not appear very clearly.

As was the case with neutral oil displaced by water, the downward displacements exhibited lower breakthrough recoveries than upward displacements. This behavior can be explained if Equation 2.3.5.2 of fractional flow is considered. If the permeability is assumed to be constant, then four other variables can influence the value of f_1, during the displacement.

An increase of velocity of the fluid inside the porous medium, v, causes the second term in parenthesis to become smaller, which in turn, causes a decrease of recovery by increasing the fractional flow of water (viscous forces are important). If the flow is horizontal ($\sin \alpha = 0$), or $\Delta\rho = 0$ (fluids of equal density), the fraction in parenthesis becomes zero and again, fl increases. In the case of downward flow, the angle $\alpha = -\pi/2$ and $\sin \alpha = -1$, which increases the value of f_l to a higher value than in previous cases, causing a higher water saturation and the decrease of recovery in any particular region of the cell.

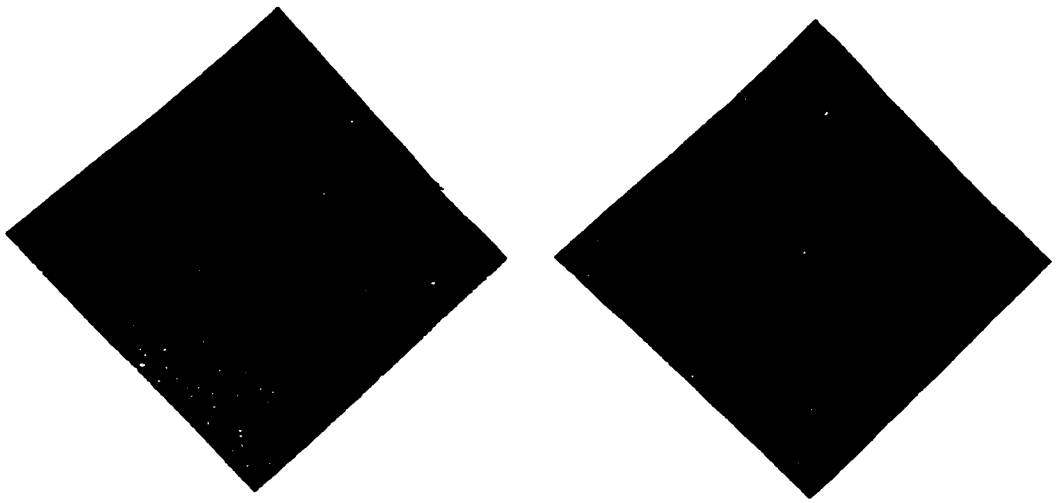

a) at 0.12 PV

b) at 0.18 PV

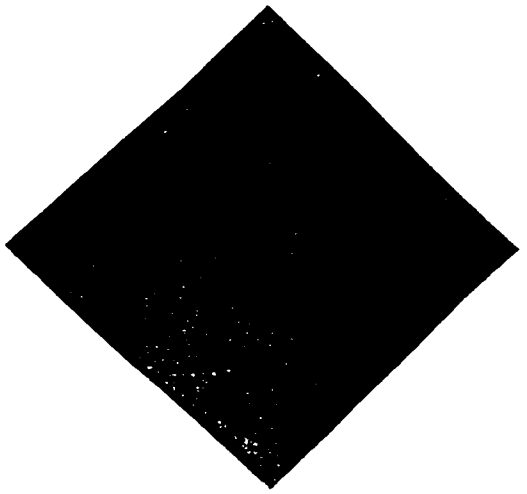

c) at 0.24 PV

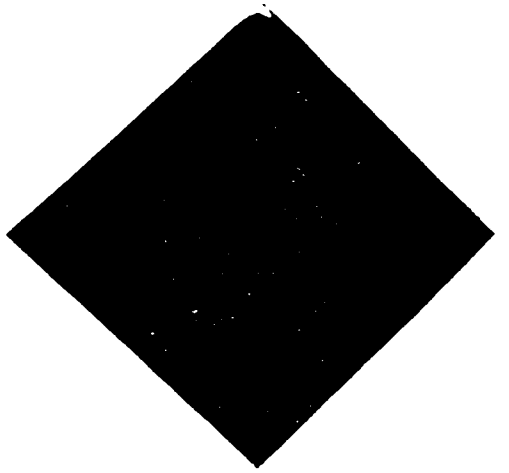

d) at 0.39 PV (breakthrough)

Fig 4.4.6 Upward displacement of the acidic oil by distilled water at 122 cm^3/h flow rate

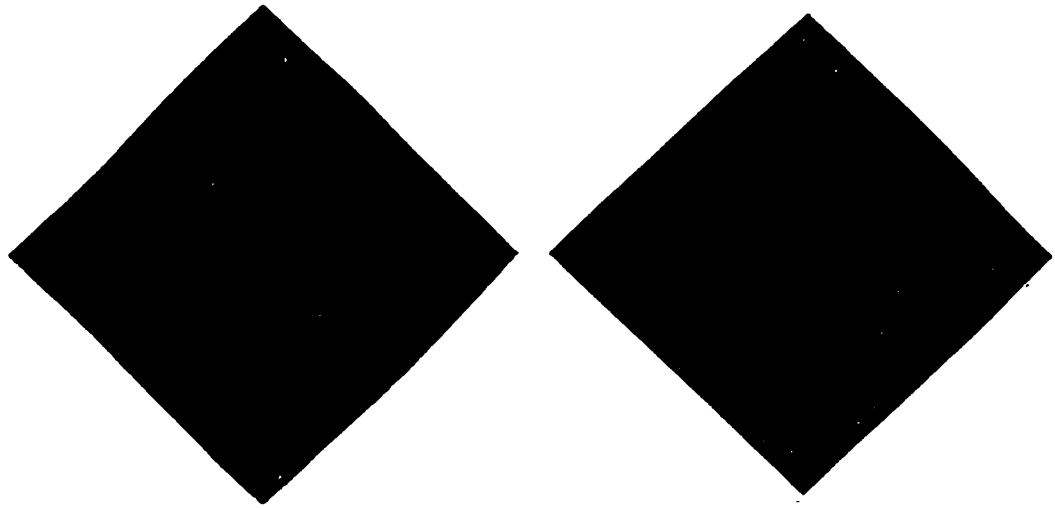

a) at 0.12 PV **b) at 0,20 PV**

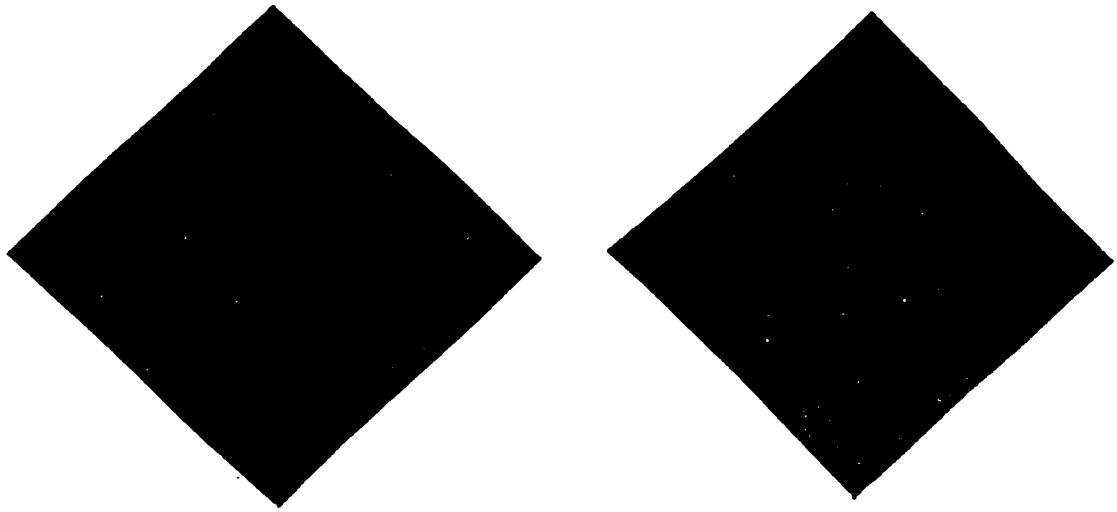

c) at 0.36 PV **d) at 0.38 PV (breakthrough)**

Fig 4.4.7 Upward displacement of the acidic oil by distilled water at 144 cm^3/h flow rate.

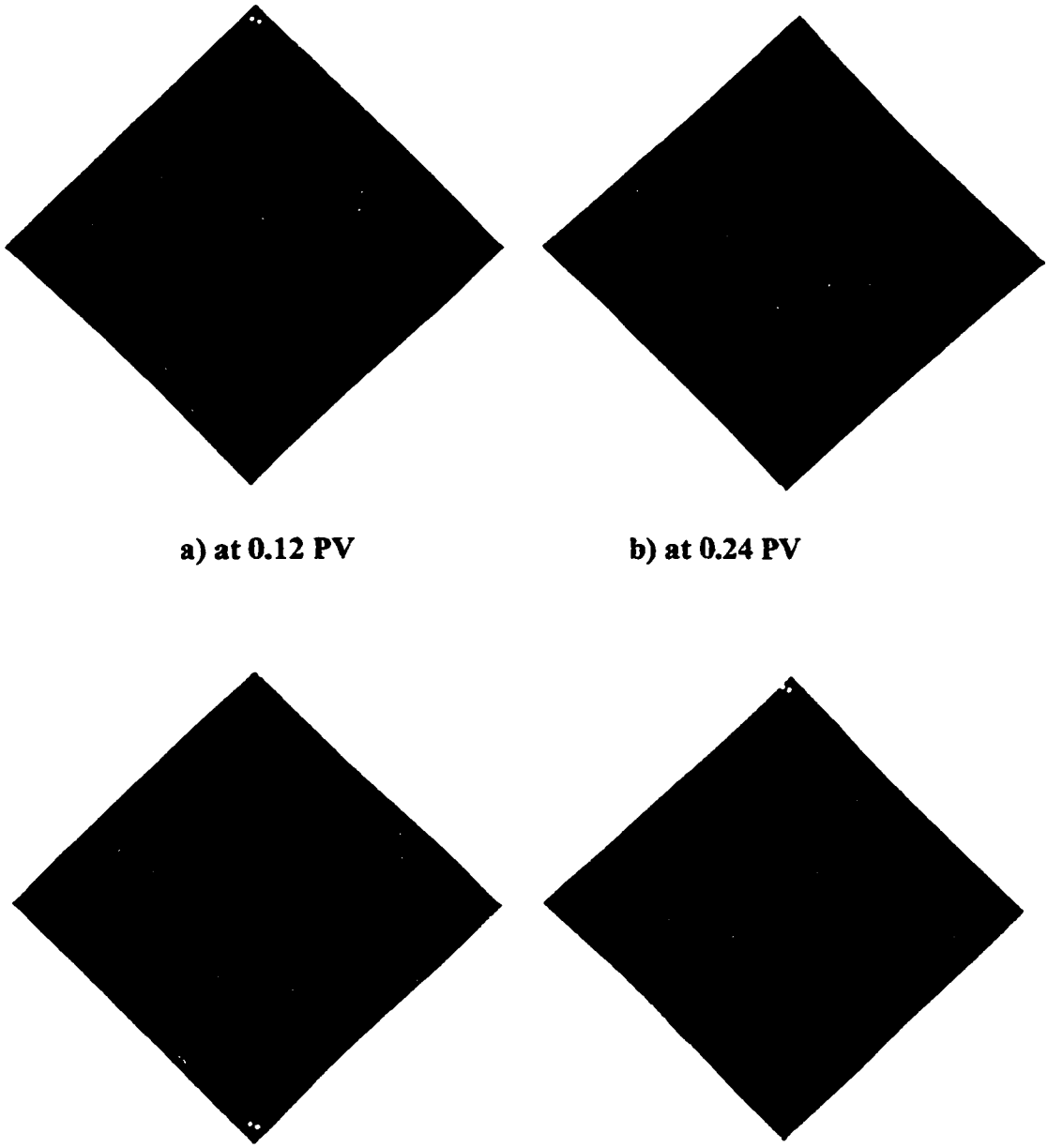

a) at 0.12 PV **b) at 0.24 PV**

c) at 0.28 PV **d) at 0.32 PV (breakthrough)**

Fig 4.4.8 Upward displacement of the acidic oil by distilled water at 178 cm^3/h flow rate.

4.5 Upward displacements of acidic oil by alkaline solutions.

The last set of experiments consisted of acidic oil displacements by alkaline solutions. A sodium hydroxide solution with a concentration of 25 mM was used in these experiments, the composition of acidic oil being kept the same as in acidic oil displacements by pure water. These experiments were carried out at the end of the experimental program because of the known problems regarding the strong influence played by the surfactant species formed in situ during the process by the reaction of organic acid with the alkali solution, leading to important changes in the wettability of the cell. A breakthrough recovery of about 75% - the highest in all sets of experiments - was obtained in the first alkaline displacement. However, in the subsequent experiments, the breakthrough recoveries were smaller than in the case of acidic oil displaced by water.

In the mean time the cell was partially blocked by a emulsion of oil water and surfactant (formed in situ) that was almost impossible to break, by washing with water or even with an organic solvent (acetone). This cleaning method was tried at the end of the experiments to avoid an additional contamination of the cell. Consequently the pressure drop across the cell has increased to dangerous levels, a fact that prohibited attempts to carry out downward displacements. In Appendix 1, photographs are shown to reveal the fact that blockage of the corners of the cell was so effective that they were out of the reach of the displacing solution. The only method that allowed the cell to be cleaned was the following

after an alkaline displacement was finished, the cell was subjected to a vacuum of about 10 -15 torr, for an extended period of time, usually between eight and ten hours. This operation removed most of the water and oil present inside the cell. Next, water was injected in the cell for periods of about ten hours to ensure a good cleaning. After the injection of water was ended, the cell was filled with acidic oil and thus, prepared for another run. If, in the process, the air accidentally entered the cell, an additional vacuum treatment was required to remove it from inside the cell.

Figures 4.5.1 through 4.5.4 present the results of the alkaline displacements

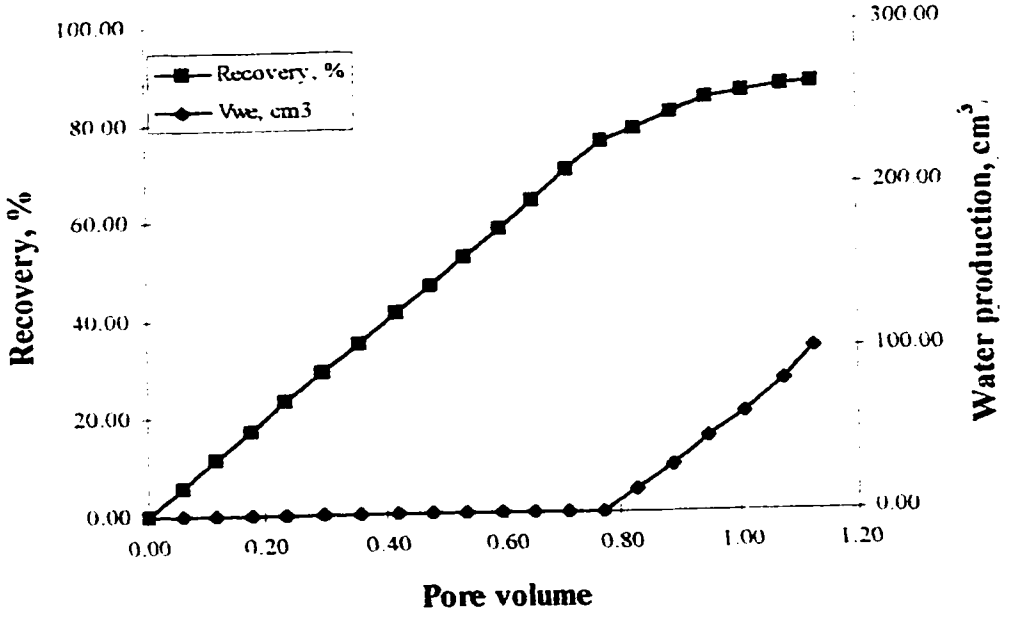

Figure 4.5.1 Upward displacement of acidic oil by alkaline solution at 110 cm^3/h flow rate.

A breakthrough recovery of 75.6% was obtained in this first experiment.

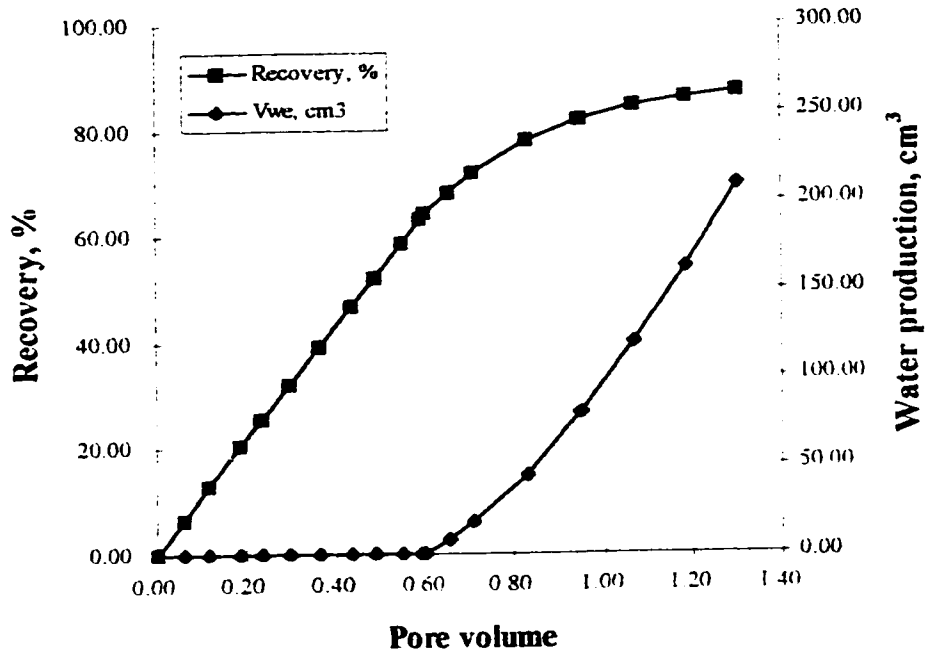

Figure 4.5.2 Upward displacement of acidic oil by alkaline solution at 172 cm^3/h flow rate.

The breakthrough recovery was 64% for the second displacement, still high compared to recoveries obtained for neutral and acid oil displacement by distilled water.

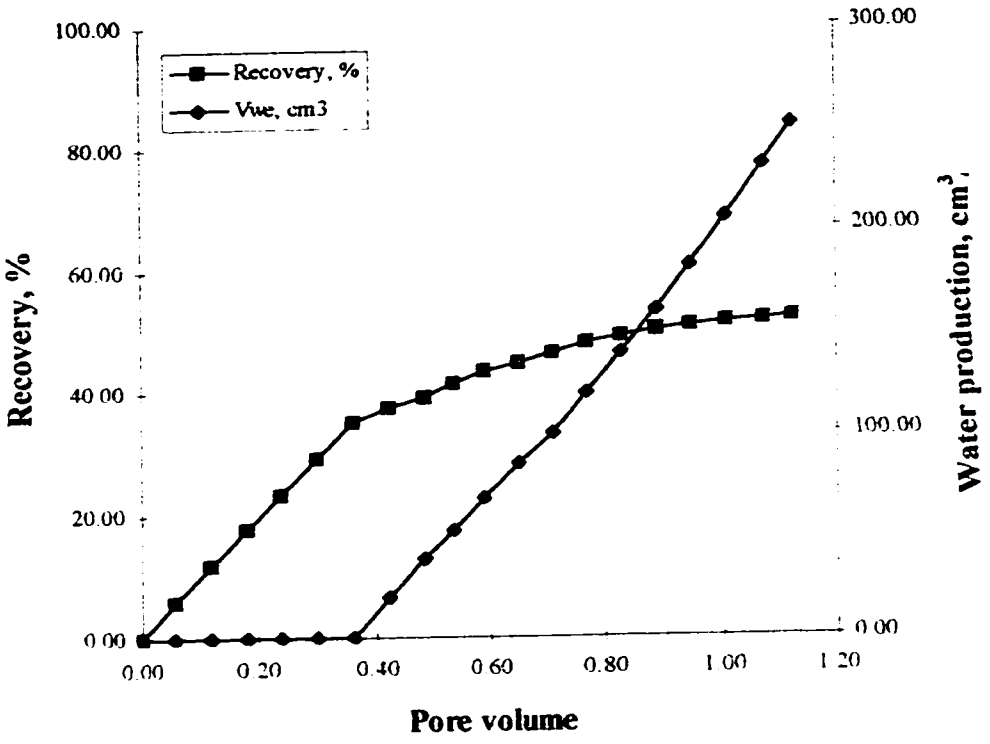

Figure 4.5.3 Upward displacement of acidic oil by alkaline solution at 238 cm^3/h flow rate.

The breakthrough recovery at this flow rate was 35%, much smaller than the one at the flow rate of 110 cm^3/h

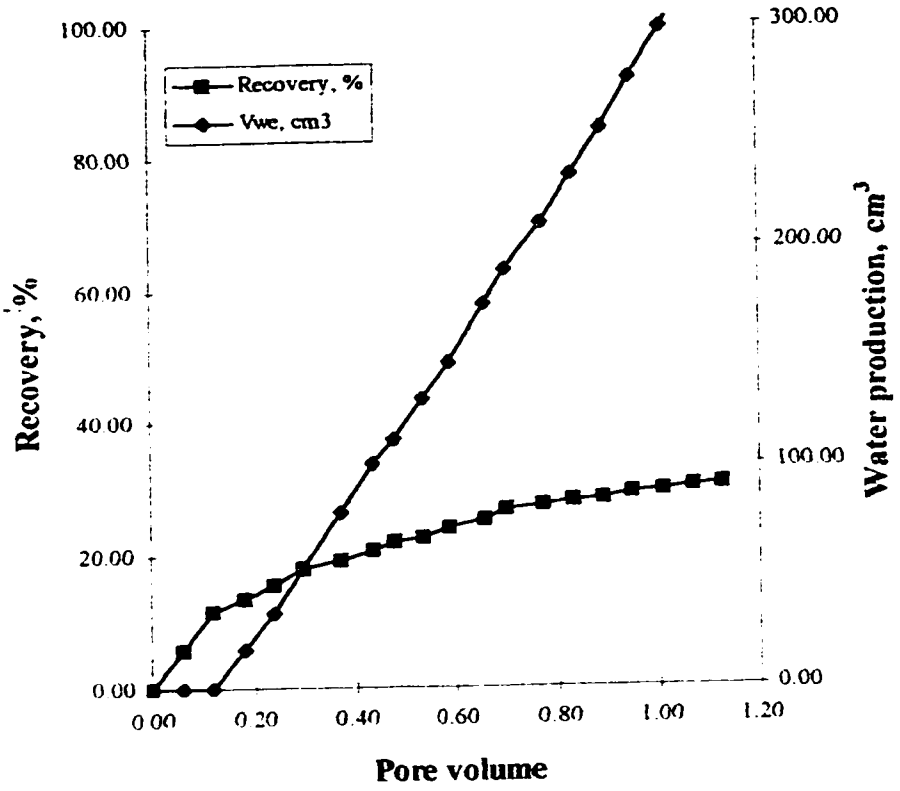

Figure 4.5.4 Upward displacement of acidic oil by alkaline solution at 330 cm^3/h flow rate.

For the flow rate of 330 cm^3/h, a very small breakthrough recovery (11.63%) was obtained.

The plot in figure 4.5.5 summarizes the results obtained in the alkaline displacements. The shape of the curve is similar to the previous case of acidic oil displacements by water, except that the decrease of breakthrough recovery with the increase of flow rate is sharper.

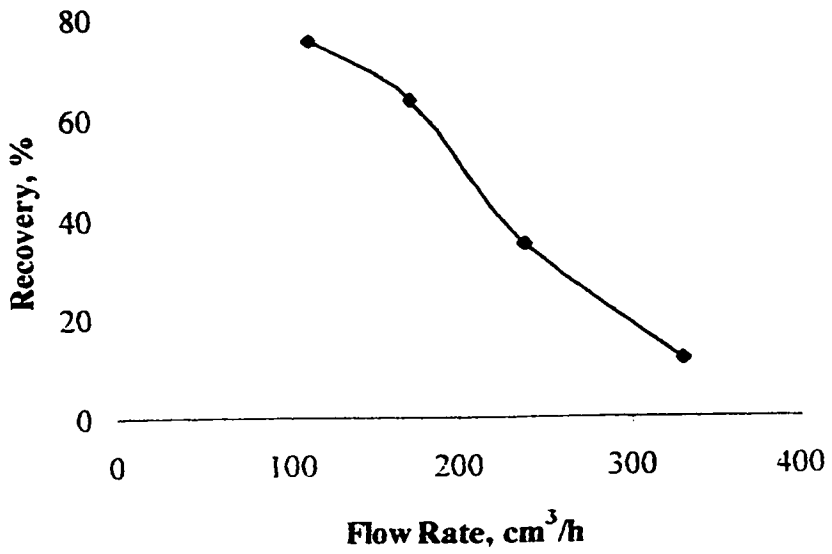

Figure 4.5.5 Breakthrough recovery versus flow rate for the upward displacements of acidic oil by alkaline solution

The sharp decrease of the breakthrough recovery is due to the fact that two effects superimpose:

i) the general tendency of the breakthrough to decrease with the increase of the flow rate. and

ii) the change in vettability that occurs during the first one or two alkaline displacements as it was already pointed out.

Figure 4.5.6 compares all the displacements carried out throughout this work.

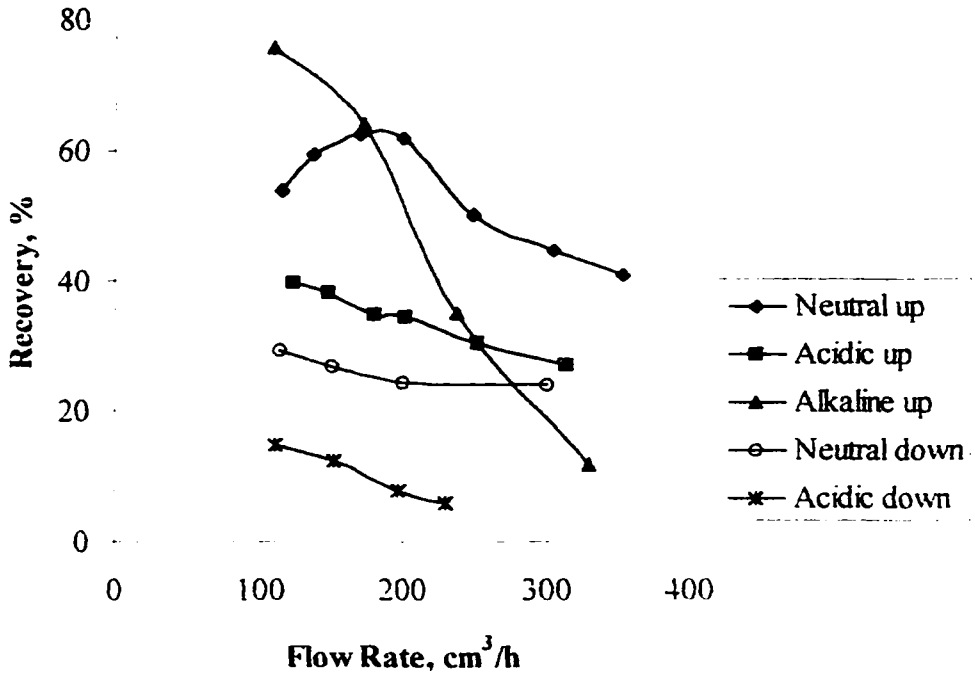

Figure 4.5.6 Summary of all five sets of experiments performed.

Figure 4.5.7 presents the photographs taken during the alkaline displacement at the flow rate of 110 cm^3/h. It was first experiment in the set of alkaline displacements, and, as it was already mentioned, it gave the highest breakthrough recovery. One observes the three well-shaped fingers, narrow at first, and then becoming wider as they approach the producer well.

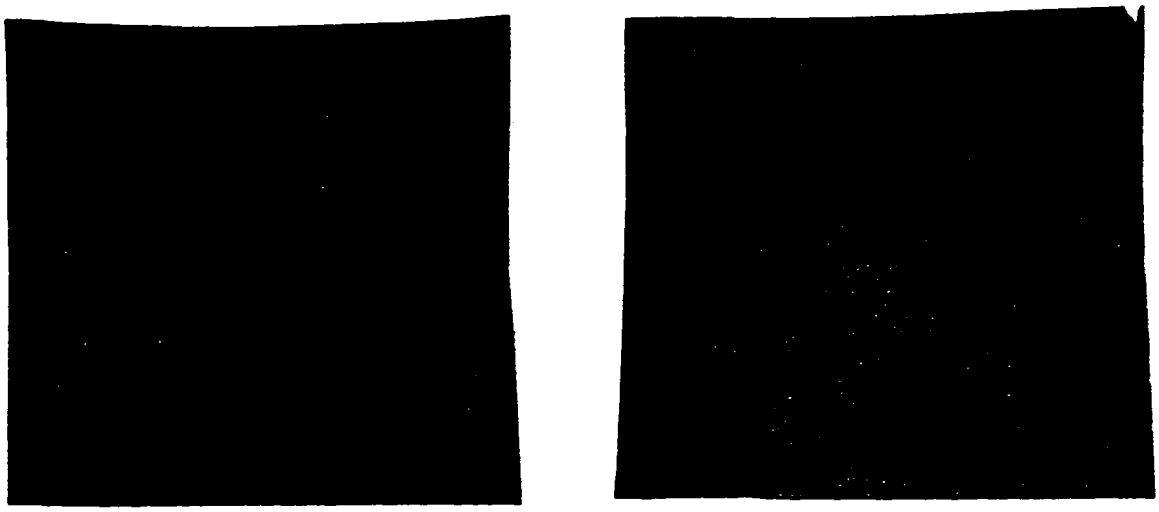

a) at 0.12 PV **b) at 0.36 PV**

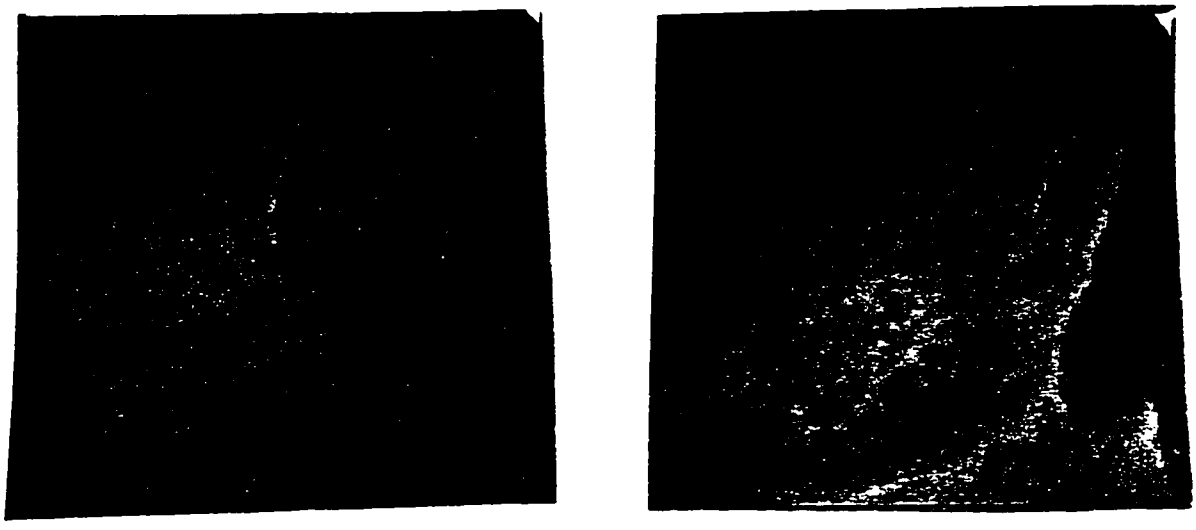

c) at 0.53 PV **d) at 0.77 PV (breakthrough)**

Figure 4.5.7 Alkaline displacement of the acidic oil at the 110 cm^3/h flow rate

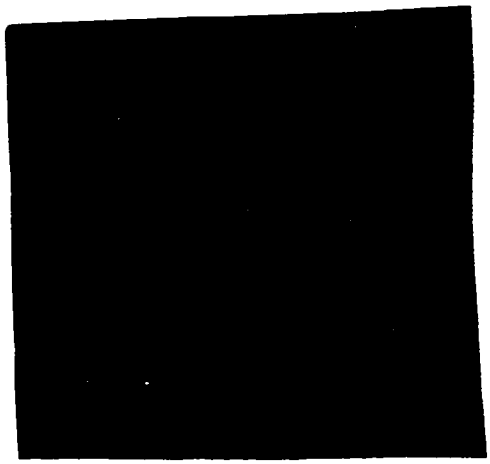

a) at 0.06 PV

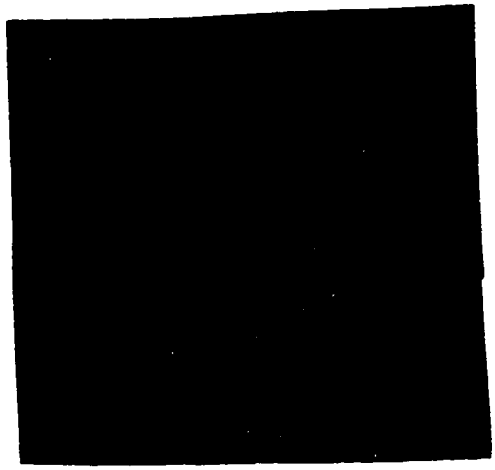

b) at 0.1 PV

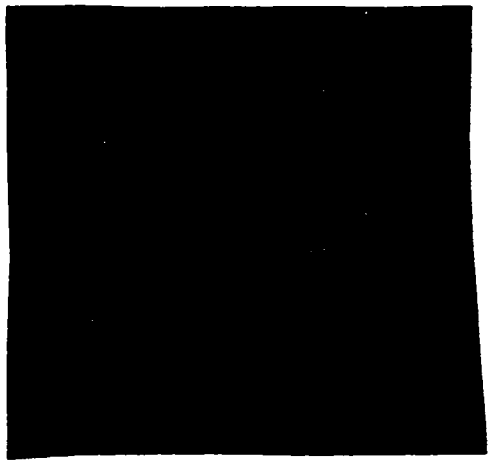

c) at 0.15 PV

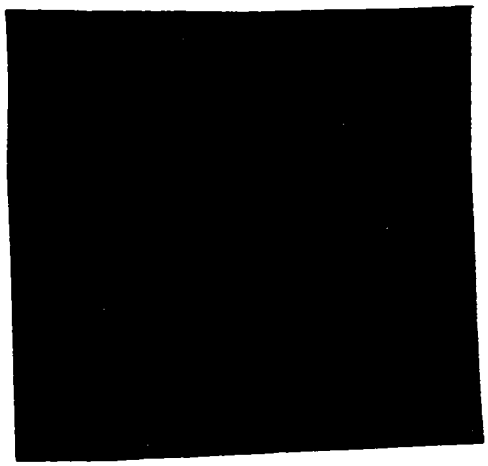

d) at 0.18 PV(beakthrough)

Figure 4.5.8 7 Alkaline displacement of the acidic oil at 238 cm^3/h flow rate

The sand behind the moving front is clean, only a few islands of oil are left behind. In the next displacement - Figure 4.5.8 - which was run at the flow rate of 238 cm^3/h, much more oil was left behind, and consequently, the recovery was much lower. The photographs in Appendix 1 show an attempt to run the third alkaline displacement, after the one depicted in figure 4.5.8. One can see the left and right corners of the cell completely blocked after the first displacement, preventing the displacing fluid to reach these areas in the cell. This is the reason that made these displacements very difficult to run.

4.6 Statistical manipulation of experimental data.

A randomized complete block design using data from the neutral oil, acidic oil and alkaline displacements analysis has been performed using MINITAB statistical package. Blocking is a technique used to increase the precision of an experiment. A block is a portion of the experimental material, set, etc. that should be more homogeneous than the entire material or set (Montgomery, 1997). Treatments performed on the experimental units have a certain degree of heterogeneity, and such, could negatively affect the results of a completely randomized design or a factorial design. The randomized block design requires that the blocks and treatments must be independent variables. The three major sets of experiments (i.e. neutral oil, acidic oil by water and acidic oil by alkaline solutions displacements) are considered as blocks, and the flow rates as treatments, (four experiments at four flow rates in each block). After coding the blocks (sets) as: 1 = neutral oil displacement, 2 = acidic oil displacement, 3 =

alkaline displacement, and flow rates as: 1 = 115 cm3/h, 2 = 170 cm3/h, 3 = 250 cm3/h, and 4 = 330 cm3/h, a two way analysis of variance for the randomized complete block design was performed on these data. The table 4.6.1 presents the input values along with the computed residuals and the fitted values, $\hat{y}$. For the hypothesis testing consider the null hypothesis: H_o = there is no difference in the block means, and the alternative hypothesis: H_a = a difference in the block means exists. Using the data from the Appendix 2 - the output of the analysis of variance, these hypotheses can be checked.

Table 4.6.1 The analysis of variance for the randomized complete block design.

Recovery	Coded Flow Rate	Coded set	Residuals	Fitted value $\hat{y}$
54	1	1	-10.0833	64.0833
62	2	1	-1.0833	63.0833
50	3	1	3.9167	46.0833
42	4	1	7.2500	34.7500
40	1	2	-4.8333	44.8333
34	2	2	-9.8333	43.8333
30	3	2	3.1667	26.8333
27	4	2	11.5000	15.5000
75	1	3	14.9167	60.0833
64	2	3	10.9167	59.0833
35	3	3	-7.0833	42.0833
12	4	3	-18.7500	30.7500

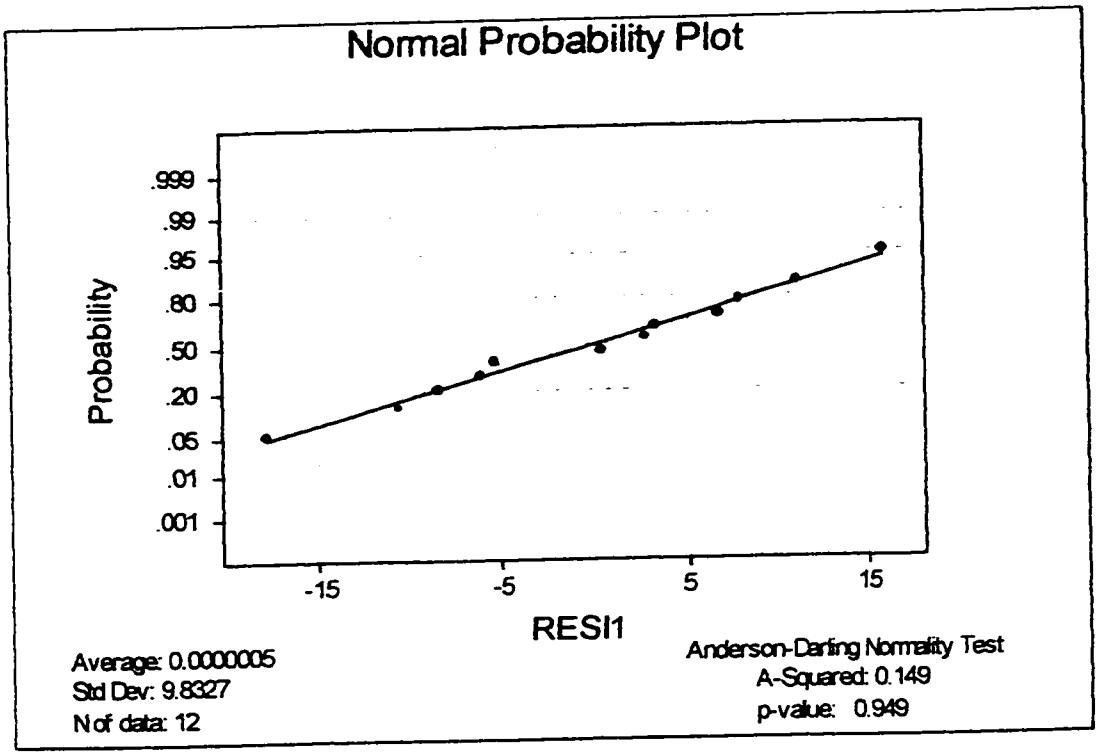

Figure 4.6.1 Normal probability plot for the residuals.

The normal probability plot for the residuals computed by the ANOVA program is a test for the equal-variance and normality assumptions (Montgomery, 1997), required by the block design. One can observe the co-linearity of the residuals proving the fact that these requirements are fulfilled. From the ANOVA output (Appendix 2), the F test statistic for the blocks (sets) has a value of 2.1. From F tables , for the blocks' degrees of freedom ($\nu_1 = 2$), error's degrees of freedom ($\nu_2 = 6$), and for the level of significance $\alpha = 0.05$, one finds a value of $F = 5.14$. The computed value for F (2.10) being less than this critical value, one draws the conclusion that there is no reason to reject the null hypothesis, i.e. no difference in block means, so the completely randomized design could be applied.

Next, using the data from the displacements of neutral oil by water upward, a multiple linear regression was performed. The breakthrough recovery was selected as dependent variable (y), while flow rate (F.R.), Reynolds (Re) number and capillary number (N_{Ca}) were selected as independent variables. The obtained regression equation is: Rec = 70.4 - 0.122 F.R. + 339106 Re. The third variable (N_{Ca}) was dropped, because it was highly correlated with other variables (see regression output in Appendix 3). The scatter plots of breakthrough recovery versus flow rate and Reynolds number are presented in figures 4.6.2 and 4.6.3, respectively. They look very much alike.

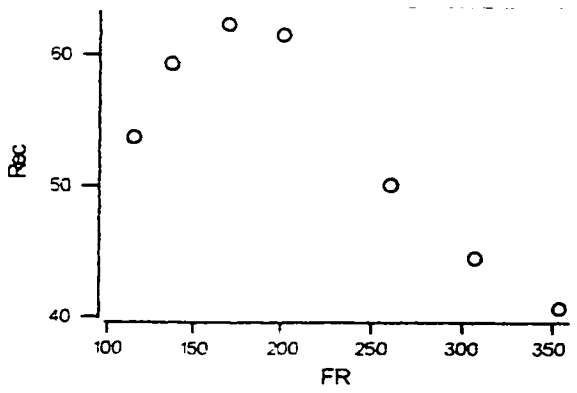

Figure 4.6.2 Scatter plot of breakthrough recovery versus flow rate.

for the upward displacements of neutral oil.

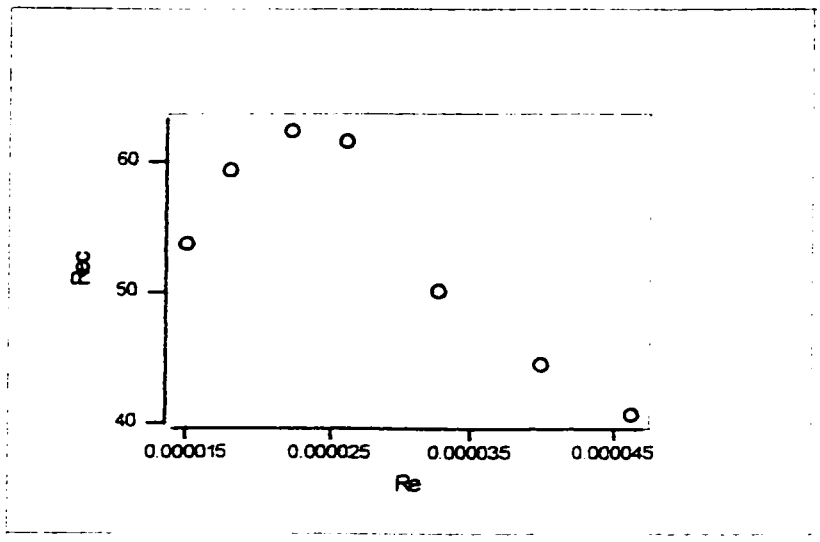

Figure 4.6.3 Scatter plot of breakthrough recovery versus Re, for the upward displacements of neutral oil.

According to the results of this first regression analysis, the fit of the data was rather poor, with a correlation coefficient of 51.3% (see Appendix 3). Another non-linear regression was performed, introducing as another variable the square of flow rate. This time, the fit was almost perfect - correlation coefficient given by the regression analysis was 99.9% (see Appendix 4).

A linearar regression was performed on the data from the upward displacements of acidic oil. In figure 4.6.4 the initial scatter plot is presented, while in figure 4.6.5 the plot of the fitted values can be seen.

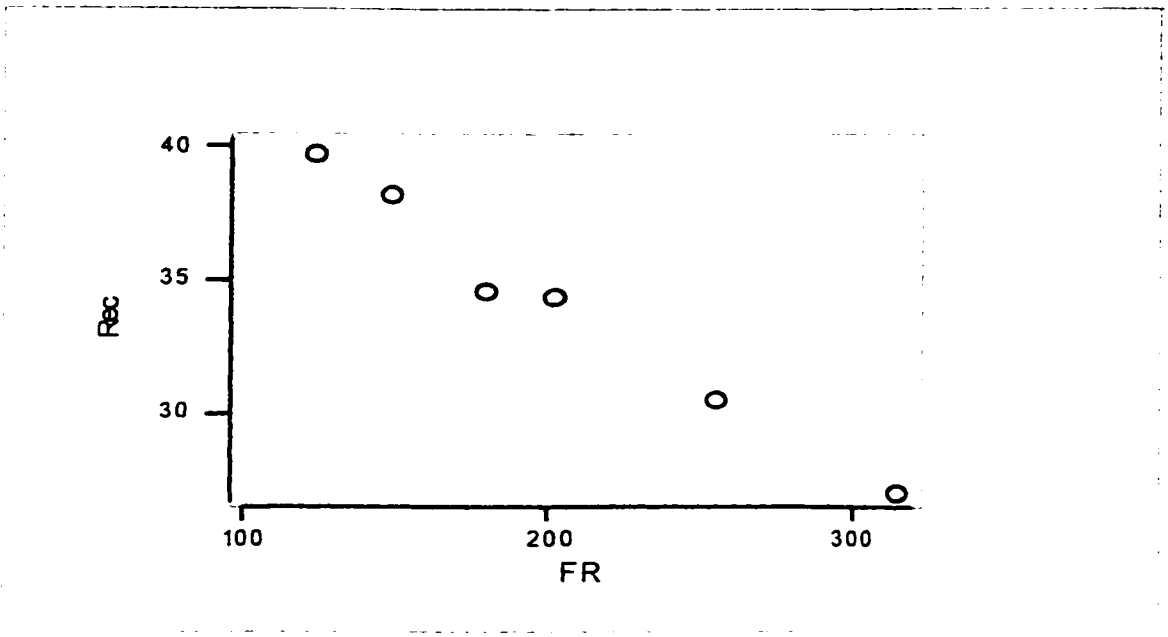

Figure 4.6.4 The initial scatter plot for the upward displacements of acidic oil

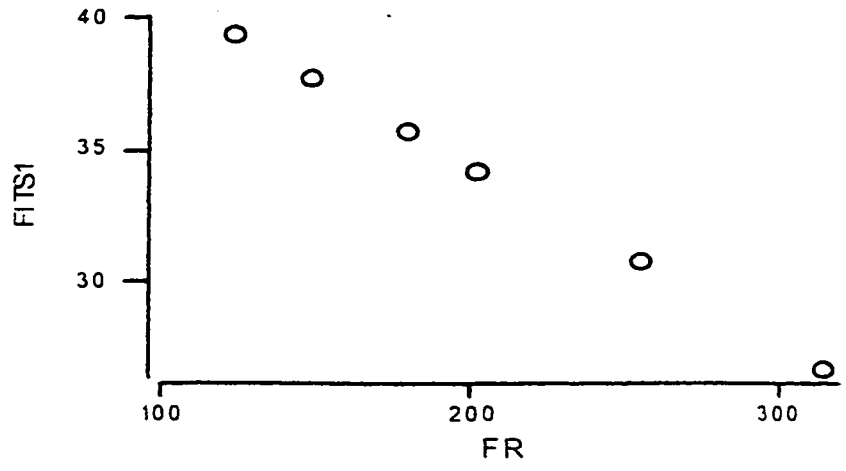

Figure 4.6.5 The fitted values plot for the upward displacements of the acidic oil.

5. CONCLUSIONS

1. The wet packing of the sand in the cell provided a more homogeneous sand pack.
2. The characteristics of the cell imposed limitations as far as the range of flow rates used in experiments is concerned. Particularly the superior limit was 400 cm^3/h.
3. The sand pack was characterized by determining its absolute permeability, as well as the ratio of relative permeabilities of water and oil.
4. The breakthrough recovery obtained with the three systems decreased in order: water - neutral oil, water - acidic oil, and alkaline solution - acidic oil displacements.
5. In the case of alkaline displacements, the first experiment at the flow rate of 110 cm3/h gave a high breakthrough recovery, followed by a sharp decrease of recovery for the subsequent displacements, as a result of wettability change – from water wet to oil wet.
6. A similar order of variation of breakthrough recovery versus the type of the system was found as in previously published data: (Nasr-El-Din et al., 1990), (Hornof et al., 1994)
7. However, unlike the later work, (Hornof et al., 1994) the displacements carried out in this work did not produce an increase of recovery after the breakthrough even though several pore volumes of NaOH solution were injected because of the blockage of the cell by what appears to be an emulsion.
8. The combination of three factors: silica sand, linoleic acid and sodium hydroxide led to unfavorable results as far as recovery is concerned. The modification of the wettability of the sand pack, or of the type/concentration of alkaline solution used, would probably give different results, if the emulsion formed in situ would have a lower viscosity. In this case,

the formed emulsion could have a beneficial effect on the displacement of oil by improving the mobility ratio of the two fluids.

9. Using the results of the multiple regression, a very good fit of data was obtained by correlating the breakthrough recovery with flow rate, Reynolds and capillary numbers.

6. RECOMMENDATIONS

1. The design of the cell can be slightly altered by providing two additional tubes to its corners on the horizontal diagonal, to allow a better cleaning of the cell.
2. A relief valve should be provided to the outlet of the cell, to prevent its breakage during a possible pressure build-up.
3. The ideal preparation of the cell between the alkaline displacements is to wash it with organic solvents to remove the oil entirely, followed by drying the sand pack by airflow. However, this approach has major disadvantages: very large amounts of the solvents required by the washing of the cell, great amount of time required to remove the solvents (once the oil has been washed away) by flow of air through the cell, and the extreme difficulty of air removal from the cell after it has been filled with oil.
4. A better characterization of the cell (more precise permeability measurements, oil and water saturations measurements) would be desirable.
5. An improvement of the method for filling the cell with sand would be desirable in order to decrease the amount of time required by this operation.

REFERENCES

Acheson, J. "Elementary Fluid Dynamics", Clarendon Press - Oxford, 1990.

Barenblatt, G.I., :Theory of Fluid Flows Through Natural Rocks", Kleuwer Academic Publishers, Dordrecht, 1990.

Barton, C.C., and La Pointe, P.R., "Fractals in Petroleum Geology and Earth Processes, Plennum Press, N.J., 1995.

Bear, J., Corapcioglu, M.Y, "Advances in Transport Phenomena in Porous Media", Martinus Nijhoff Publishers, Amsterdam, 1987.

Benham, A.L., Olson, R.W. "A model study of viscous fingering ", Society Petroleum Engineers Journal, June (1963).

Bentsen, R.G., "A new Approach to Instability Theory in Porous Media", Soc. Petr. Eng. J., 765, October, (1985).

Burk, J. H., "Comparison of Sodium Carbonate, Sodium Hydroxide, Sodium Orthosilicate, for Enhanced Oil Recovery, SPE Reservoir Engineering, 9-19, February, (1987).

Campbell, T.C., "The role of Alkaline Chemicals for the Recovery of Low Gravity Crude Oils", Journal of Petroleum Technology, November (1982).

Chapman, R.E.., "Petroleum Geology", Elsevier, Amsterdam, 1983.

Chen, T., "Flow Visualization of Immiscible Oil - Water Displacement in Unconsolidated Porous Media", B.A..Sc. Thesis, University of Ottawa, Chemical Engineering Department, (1992).

Cheremisinoff, N.P., Gupta, R., "Handbook of Fluids in Motion", Ann Arbor Science, The Butterworth Group, 1983.

Chiwetelu, C. I., Hornof, V. and Neale, G. H., "A dynamic model for the interaction of caustic reagent and acidic oils", Am. Inst. Chem. Eng. J., **36**, 233 - 241 (1990).

Chiwetelu, C. I., Neale, G. H., and Hornof, V. "Interfacial Activity of Linoleic Acid/Caustic Systems", Journal of Surface and Technology, No 4, 305 - 315 (1990).

Chuoke, R.L., van Meurs, P., and van der Poel, C., "The instability of slow, Immiscible, Viscous Liquid-Liquid Displacements in Permeable Media", Trans AIME, 216, 188 (1959).

Collins, R.E., "Flow of Fluids Through Porous Materials", Reinhold Publishing Corporation, New York (1961).

Constantinescu, V.N., "Laminar Viscous Flow", Springer, Berlin, 1995.

Cumberland, D.J., Crawford, R.J., "The Packing of Particles", Elsevier, Amsterdam-Oxford-New York-Tokyo, 1987.

Dake, L.P., "Fundamentals of Reservoir Engineering", Elsevier, Amsterdam, 1978.

Donaldson, E. C., Chilingarian, G. V. and Yen, T. E, "Enhanced Oil Recovery, II, Processes and Operations", Elsevier, Amsterdam, New York, (1985).

Dullien, F.A., "Porous Media Fluid Transport and Pore Structure ", Academic Press, New York (1979).

Dullien, F.A., "Porous Media Fluid Transport and Pore Structure", Academic Press, New York (1992).

Earnshaw, R.A., and Watson, D., "Animation and Scientific Visualization Tools and Applications, Academic Press, London, 1993.

Feder, J., "Fractals", Plenum Press, New York, 1988.

Flock, D.L., et al, "The influence Of Frontal Instabilities During Viscous Oil Displacement", Oil Sands, 380-385, (1977).

Gerhart, P. M., Gross, R. J., Hochstein, J. I, "Fundamentals of fluid mechanics", Addison-Wesley Publishing Company, New York, 1992.

Hele-Shaw, H. S., "The flow of water", Nature, **58**, 34 - 36 (1898) .

Homsy, G. M., "Viscous fingering in porous media", Ann. Rev. Fluid Mech., **19**, 271 275 (1987).

Hornof, V. and Bemard, C., "Effect of interfacial reaction on immiscible displacement in Hele-Shaw cells", Experiments in Fluids, **12**, 425 - 426 (1992).

Hornof, V., Neale, G.H., and Yu, A., "Effect of flooding sequence on the displacement of acidic oil by alkaline solutions.", Journal of Petroleum Science and Engineering, **10**, 291-297, (1994.

Howes B. J. "Enhanced oil recovery in Canada: success in progress", The Journal of Canadian Petroleum Technology, Nov.- Dec. 1988, v **27** No 6, 80-88.

Koederitz, L.F., "Introduction to Petroleum Reservoir Analysis", Gulf Publishing Co., Houston, 1989.

Lake, L. W., "Enhanced Oil Recovery", Prentice - Hall, Englewood Cliffs, New Jersey, 1989.

Latil, M., "Enhanced Oil Recovery", Gulf Publishing Co., Houston, 1980.

Lee, K.S., Claridge, E.L. "Areal Sweep efficiency of pseudoplastic fluids in a five-spot Hele-Shaw model", Society of Petroleum Engineers Journal, March (1963).

Lenormand. R., Zarcone, C., "Two-phase flow experiments in a two dimensional permeable medium." Physico-Chemical Hydrodynamics 6, 497-506, (1985).

Marle, C.M., "Multiphase Flow In Porous Media", Editions Technip, Paris (1981).

Melrose, J. C. and Brandauer, C. E, "Role of capillary forces in determining macroscopic displacement efficiency for oil recovery", J. Can. Pet. Tech., **14**, 56 - 62 (1974).

Montgomery, D.C., "Design and Analysis of experiments", John Wiley & Sons, New York, 1997.

Morrow, N.P., "Interplay of Capillary, Viscous and Buoyancy Forces in the Mobilization of Residual Oil". The Journal of Canadian Petroleum Technology 35-46, July-September (1979).

Nasr-El-Din, H. A., Khulbe, K. C., Hornof, V. and Neale, G. H., "Effects of interfacial reaction on the radial displacement of oil by alkaline solution", Revue de L'institut Français du Petrole, **45**, No 2, 231-244 mars-avril (1990).

Nasr-El-Din, H., Hornof V., and Neale, G. "Radial fingering in a water wet porous medium", Revue de l'institut français du petrole, Vol.**42**, No. 6, nov-dec. (1987).

Ni, L.W., Hornof, V. and Neale, G., "Radial Fingering in a porous medium", Revue de l'institut français du petrole, Vol.**41**, No. 2, mars-avril (1986).

Park, C. W. and Homsy, G. M., "The instability of long fingers in Hele-Shaw cell", Phys. Fluidsl **28**, 1583 - 1585 (1985).

Pavone, D., "Observations and Correlations for Immiscible Viscous - Fingering Experiments", SPE Reservoir Engineering, May (1992).

Polikar, M., et al, "Preparation of Synthetic Oil - Sand Cores", Journal of Petroleum Science and Engineering, **1**, 263-270 (1988).

Saffman, P. G. and Taylor, G. I., "The penetration of a fluid into a porous medium or Hele-Shaw cell containing a more viscous liquid", Proc. R. Soc. Lond. **A 245**, 312 - 329 (1958).

Sahimi, M., "Flow and Transport in Porous Media and Fractured Rock", VCH, Weinheim, 1995.

Scheidegger, A. E., "The physics of flow through porous media" University of Toronto Press, 1960.

Selley, E. "Petroleum Geology", Gulf Publishing Co., Houston, 1985.

Sherman, F.S., "Viscous Flow", McGraw Hill Publishing Company, New York, 1990.

Stalkup, F..I, "Miscible Displacement.", Dallas: Soc. Pet. Eng., AIME, (1984).

Taber, J. J., "Research on Enhanced Oil Recovery: past, present and future", Pure & Appl. Chem., Vol. **52**, pp. 1323-1347 (1980).

Taber, J.J. and Martin, F.D., "Polymers in Enhanced Oil Recovery - A General Introduction". Polymer Preprints. 22(2). 10-14. August(1981).

Vicsek, T., "Fractal Growth Phenomena.", World Scientific, New Jersey, 1989.

Wygal, R.J., "Construction of Models that Simulate Oil Reservoirs", Society of Petroleum Engineers Journal, 281-286, December (1963).

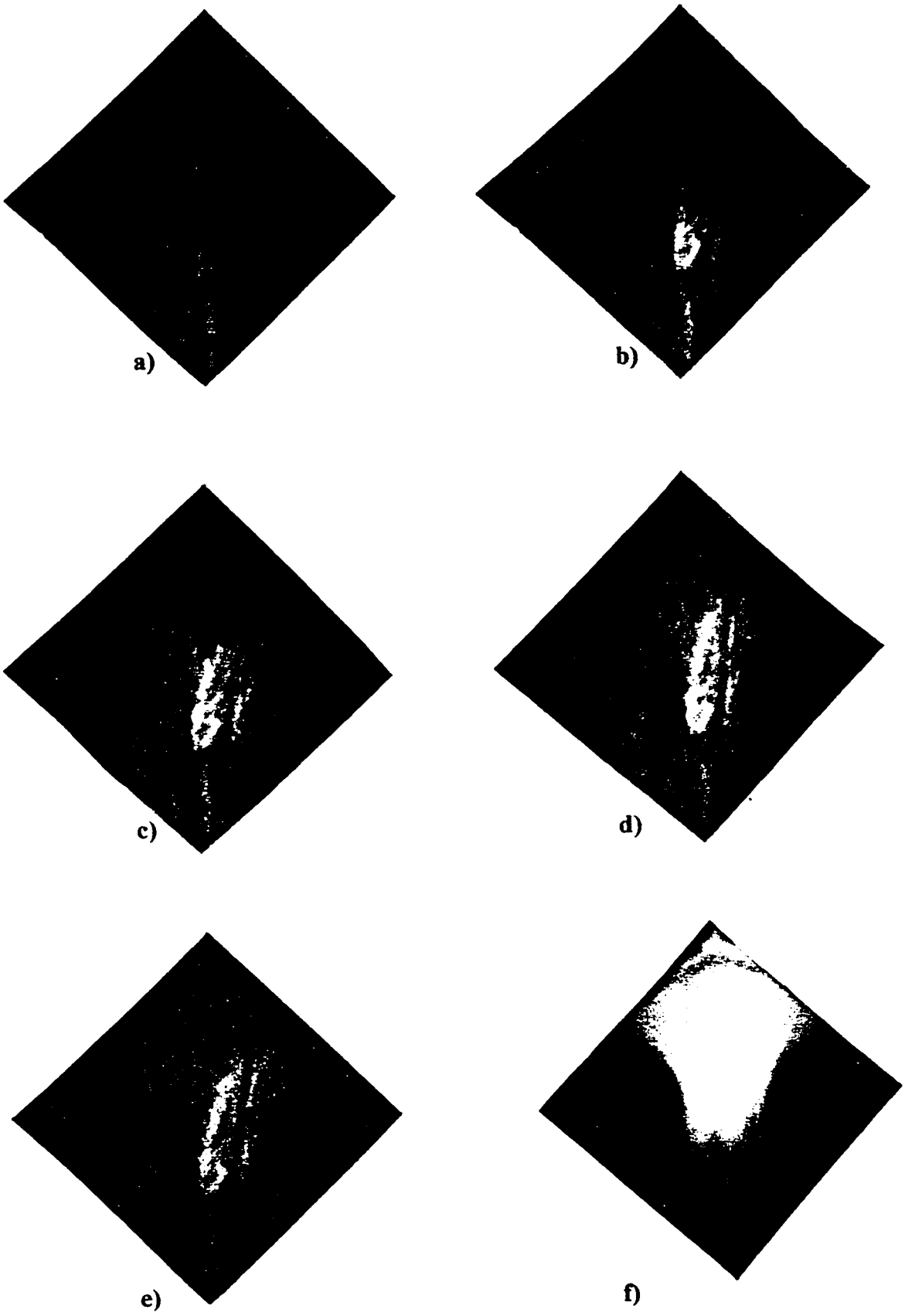

Appendix 1. Alkaline displacement of acidic oil at 220 cm^3/h flow rate.

Appendix 2

Worksheet size: 3500 cells

MTB > Name c4 = 'RESI1' c5 = 'FITS1'

MTB > Twoway 'recov' 'fr' 'set' 'RESI1' 'FITS1';

SUBC> Additive.

ANALYSIS OF VARIANCE recov

SOURCE	DF	SS	MS
fr	3	1680	560
set	2	786	393
ERROR	6	1064	177
TOTAL	11	3530	

MTB > %NormPlot 'RESI1'.

Executing from file: C:\STAT\MTBSEW\MACROS\NormPlot.MAC

Macro is running ... please wait

Appendix 3

Worksheet size: 3500 cells

```
MTB > Save 'C:\STAT\MTBSEW\EXERCISE\EXP_REG1.MTW';
SUBC>  Replace.
Saving worksheet in file: C:\STAT\MTBSEW\EXERCISE\EXP_REG1.MTW
MTB > regress y in c2 using 4 predictors in c1, c3-c5

MTB > regress y in c7 using 4 predictors in c8-c11

*     C9 is highly correlated with other X variables
*     C9 has been removed from the equation

The regression equation is
C7 = 61.4 - 1.07 C8 + 266810 C10 + 3100149 C11

Predictor      Coef     Stdev   t-ratio      p
Constant     61.392     9.936      6.18  0.009
C8          -1.0702    0.9079     -1.18  0.323
C10          266810    259520      1.03  0.380
C11         3100150   2850529      1.09  0.356

s = 5.612      R-sq = 77.9%     R-sq(adj) = 55.7%

Analysis of Variance

SOURCE       DF      SS       MS      F      p
Regression    3   332.11   110.70   3.51  0.165
Error         3    94.49    31.50
Total         6   426.59

SOURCE       DF   SEQ SS
C8            1   290.20
C10           1     4.65
C11           1    37.25

Unusual Observations
Obs.     C8      C7      Fit  Stdev.Fit  Residual  St.Resid
 6      305   44.64    44.63       5.61      0.01     0.68 X
 7      353   40.82    40.64       5.61      0.18     0.68 X

X denotes an obs. whose X value gives it large influence.
```

Appendix 4

MTB > regress y in c1 using 5 predictors in c2-c6

* Velocity is highly correlated with other X variables
* Velocity has been removed from the equation

* NOTE * F.R. is highly correlated with other predictor variables
* NOTE * F.R.sq is highly correlated with other predictor variables

The regression equation is
Recovery = - 9.60 + 1.05 F.R. - 0.00233 F.R.sq - 568766 Re - 486778 Ca

Predictor	Coef	Stdev	t-ratio	p
Constant	-9.596	3.707	-2.59	0.122
F.R.	1.05428	0.05780	18.24	0.003
F.R.sq	-0.0023287	0.0001167	-19.96	0.003
Re	-568766	47077	-12.08	0.007
Ca	-486778	31413	-15.50	0.004

s = 0.4964 R-sq = 99.9% R-sq(adj) = 99.7%

Analysis of Variance

SOURCE	DF	SS	MS	F	p
Regression	4	426.10	106.53	432.22	0.002
Error	2	0.49	0.25		
Total	6	426.59			

SOURCE	DF	SEQ SS
F.R.	1	290.20
F.R.sq	1	65.62
Re	1	11.10
Ca	1	59.18

Unusual Observations

Obs.	F.R.	Recov.	Fit	Stdev.Fit	Residual	St.Resid
6	305	44.640	44.639	0.496	0.001	1.34 X
7	353	40.820	40.818	0.496	0.002	1.37 X

X denotes an obs. whose X value gives it large influence.

IMAGE EVALUATION
TEST TARGET (QA-3)

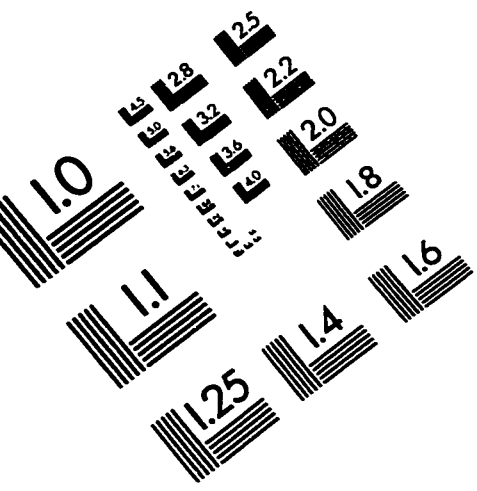

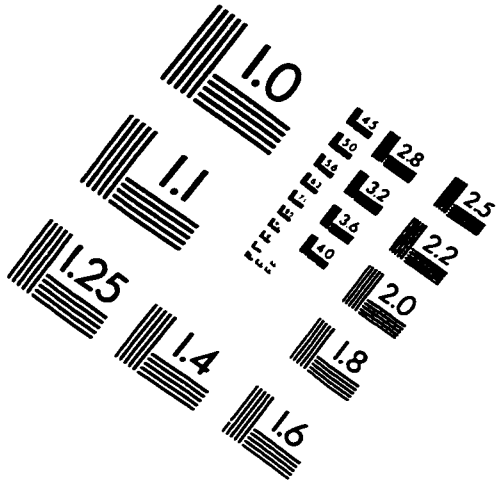

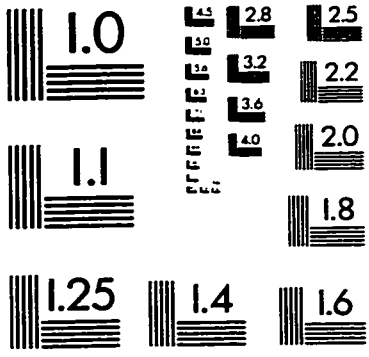

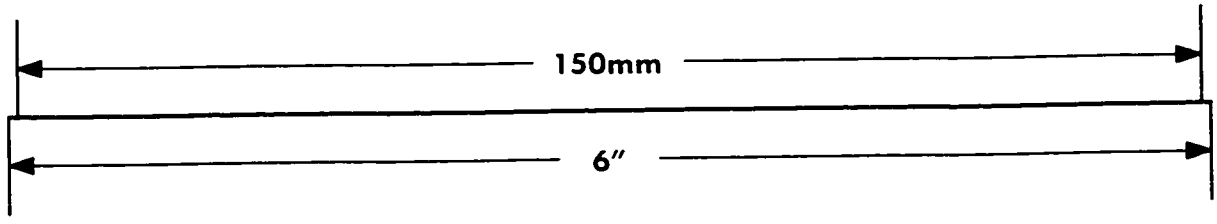

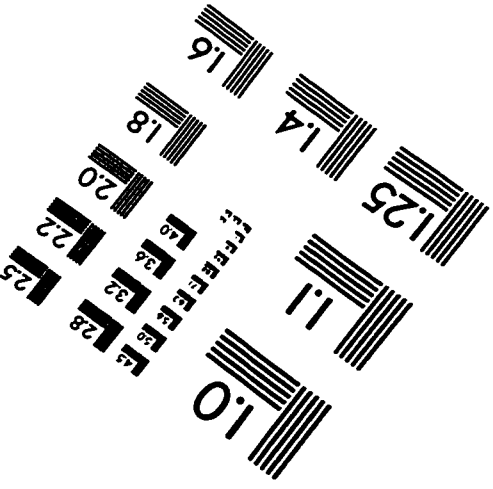

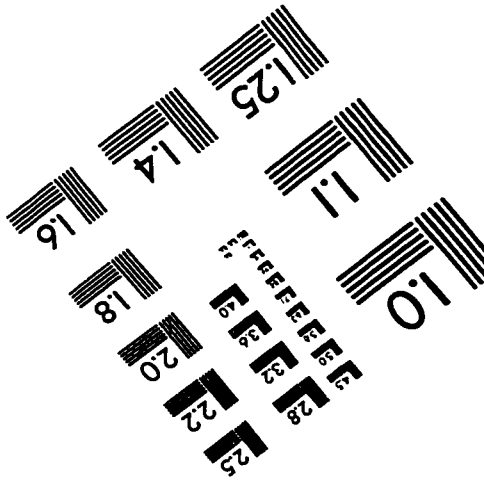

APPLIED IMAGE . Inc
1653 East Main Street
Rochester, NY 14609 USA
Phone: 716/482-0300
Fax: 716/288-5989